

Development of acellular conduits for peripheral nerve repair and regeneration

&

In-vitro neuromodulation targeting microglia activity

Inauguraldissertation

zur

Erlangung der Würde eines Doktors der Philosophie

vorgelegt der

Philosophisch-Naturwissenschaftlichen Fakultät

der Universität Basel

von

Alois Conradin Hopf

aus Binningen, Basel-Land

Basel, 2023

Originaldokument gespeichert auf dem Dokumentenserver der Universität Basel edoc.unibas.ch

Genehmigt von der Philosophisch-Naturwissenschaftlichen Fakultät

auf Antrag von

Erstbetreuer: Prof. Dr. Raphael Guzman, Zweitbetreuer: Prof. Dr. Verdon Taylor,
externer Experte: Prof. Dr. Morten Meyer

Basel, den 20.09.2022

Prof. Dr. Marcel Mayor
Dekan

During the time of this thesis two separate projects were followed in the area of regenerative neuroscience. The first project focused on the development of an acellular nerve graft for peripheral nerve repair and replacement. During this project, protocols were established for the decellularization of pig nerves. Most research regarding the production of acellular nerve grafts is conducted using rodent models. However, due to size and modality mismatch of rodent and human peripheral nerves, a suitable large animal donor is required for clinical application. This project was enabled by the EUROSTAR grant to PD Dr. Srinivas Madduri, the Department of Biomedicine, University of Basel and the Department of Neurosurgery, University Hospital Basel.

During the second part of this thesis, I focused on the impact of neuromodulation protocols on microglia activity and how to modulate their inflammatory response via targeted stimulation *in-vitro*. Neuromodulation therapies are investigated in various diseases and conditions, experimentally, such as in Alzheimer's Disease but also clinically as in chronic pain. The beneficial outcomes of electric stimuli are mainly attributed to direct effect on neuronal cells. However, long lasting improvement following neuromodulation cannot be explained by immediate effects on neuronal excitability only. Newer developments indicate a direct impact of electric fields on glia cells. Therefore, the direct impact on glia activity was further investigated during this project. This project was enabled by the Gerbert Rűf Foundation grant to Dr. Bekim Osmani, the Department of Biomedicine, University of Basel and the Department of Neurosurgery, University Hospital Basel and Bottneuro AG.

Even though these projects are of different origins, potential future combinations are possible. First, the *in-vitro* electrical stimulation device, developed during the second project can be used for mesenchymal stem cell differentiation into Schwann cell-like cells used for recellularization of acellular grafts as described in the review written during the first project¹.

Second, a recent study has shown enhanced peripheral nerve regeneration by providing electric pulses to the regenerating nerves². Optimal electrical stimulation parameters for axonal elongation and nerve regeneration can be established using the *in-vitro* electrical stimulation device developed during this thesis. Further, during this thesis a patent was filled for soft neuronal implants on cellulose basis³. By wrapping the developed acellular grafts with these neuronal implants, electrical stimulation protocols can be applied to enhance nerve regeneration even further.

Third, to mimic the natural microenvironment present during neuroinflammation *in-vivo*, acellular grafts loaded with inflammatory molecules such as cytokines, growth factors and enzymes can be used as a model of neuroinflammation *in-vitro*. Using such a 3D system, the impact of electric fields on microglia activity can be analyzed in a system more closely resembling natural conditions without the potential paracrine effects of simultaneous stimulation of neural cells. An ongoing collaboration with Prof. Bert Müller from the department of Biomedical Engineering investigates microglia modulation in an artificial 3D scaffold made from electrospun cellulose scaffolds.

Acknowledgment

This dissertation would not have been completed without the help and support of many different people from family to friends and colleagues to scientific supervisors and mentors. Without their continuous intellectual and emotional support this thesis could not have been written. I'm grateful for the support I received and the lessons I've learned during this, at least partially difficult time.

First of all, I want to thank for all the scientific help in and around the lab during this time. My gratitude goes to Prof. Raphael Guzman for the scientific guidance during the last years. I feel honoured that I could have been part of his research group and contribute to these interesting research fields. During the time in the group Brain Ischemia and Regeneration I've learned a lot about scientific work and the scientific world. Another thank is therefore directed to all the group members for their feedback, experimental help, discussions, and the good company within the last years. Special thanks to Dr. Catherine Brégère for the continuous support in designing and conducting experiments and to MSc. Pia Bustos for the repeated help in conducting experiments and keeping the lab running.

I would also like to thank my direct supervisors of the two different projects. Dr. Bekim Osmani and PD Dr. Srinivas Madduri for providing the opportunity to work on these interesting topics.

Thanks to Dr. Miriam Weisskopf from the Experimental Animal OR facilities from the university hospital Zurich for providing me help with the required porcine tissue harvest and documentation. For providing help with the electrical stimulation device design and 3D printing I would like to express my appreciation towards Beat Degen from the Laboratories technical facilities.

At this point, I would also like to thank Dr. Catherine Brégère which helped me writing and especially proofreading this thesis.

Finally, I want to express my gratitude towards my Ph.D. advisory committee: Prof. Dr. Verdon Taylor, Prof. Dr. Morten Meyer and Prof. Dr. Raphael Guzman for the annual feedback, critics and inputs and the final approval of my thesis.

These projects were funded by EUROSTAR (PD Dr. Srinivas Madduri), Gerbert Rűf Foundation (Dr. Bekim Osmani), the Department of Biomedicine, the Department of Neurosurgery and Bottneuro AG. Thanks for the financial support.

Next, I would like to thank all the people from Bottneuro. First of all, to Dr. Bekim Osmani, CEO and great colleague making the transition from academia to industry possible. Thanks to his entrepreneurial spirit I'm looking forward towards a great time and even greater achievements with Bottneuro. I'm convinced that with such an inspiring team and dedicated people we can bring sustainable benefits to the patients.

Last but not least, I want to express my gratitude towards my family and friends. They provided me with all the needed support and stood by my side whenever needed. They were a source of motivation and pushed me to move forward when I was struggling. My parents and brothers supported me during all my decision and influenced me to become the best version of myself.

Finally, thanks to all my friends, 4102 Kingz and Queenz for supporting me throughout the years and helping me to find my path. Without you, all of this would be pointless.

Thank you all!

Table of Contents

<i>Acknowledgment</i>	1
<i>List of Patents, Papers and Incorporation</i>	5
Publications	5
Patents	5
Incorporation	5
<i>First Project: Development of acellular conduits for peripheral nerve repair and regeneration</i>	7
Abstract	9
Introduction	11
The Peripheral Nervous System and Peripheral Nerves	11
Peripheral Nerve Injuries and current therapeutic strategies.....	12
Decellularized nerve conduits.....	12
Aim of the project	15
Results	16
Publication: „Optimized Decellularization Protocol for Large Peripheral Nerve Segments: Towards Personalized Nerve Bioengineering”	17
Outlook	35
Review paper: „Schwann Cell-Like Cells: Origin and Usability for Repair and Regeneration of the Peripheral and Central Nervous System”	37
<i>Second Project: In-vitro neuromodulation targeting microglia activity</i>	69
Abstract	71
Introduction	73
Microglia.....	73
Microglia and Chronic Pain	74
Microglia modulation in chronic pain	75
Microglia and Alzheimer’s Disease	76
Microglia modulation in AD.....	77
Aim of the project	79
Bottneuro AG	80
Methods & Material	81
BV-2 cells culture.....	81
Animals.....	81

Primary murine microglia isolation and culture.....	81
Experimental setup.....	82
3D printed electrical stimulation device.....	83
Cytokine analysis.....	83
Results.....	87
LPS dose-dependent release of cytokines.....	87
Direct current stimulation reduces cell proliferation	88
40 Hz Alternate current stimulation suppresses BV-2 cell activity.....	89
40 Hz Alternate current stimulation suppresses primary murine microglia activity	90
Applied current depends on frequency and applied voltage.....	91
Discussion.....	93
Development of a new electrical stimulation device.....	93
LPS-stimulated production of pro-inflammatory cytokines as an <i>in vitro</i> model of neuroinflammation	94
Biphasic stimulation of glia cells has a neuroprotective effect	94
Oscillating transmembrane potential may mimic healthy brain state.....	96
Relevance of <i>in-vitro</i> results for future neuromodulation strategies	98
Conclusion/Outlook.....	99
<i>Reference list</i>	101
<i>Curriculum Vitae</i>	117

List of Patents, Papers and Incorporation

During this thesis, significant contributions to following papers, patents and incorporations were made:

Publications:

1. **Schwann Cell-Like Cells: Origin and Usability for Repair and Regeneration of the Peripheral and Central Nervous System**¹
Alois Hopf, Dirk J Schaefer, Daniel F Kalbermatten, Raphael Guzman, Srinivas Madduri
Published August 2020 in „Cells”
2. **Toward optoacoustic sciatic nerve detection using an all-fiber interferometric-based sensor for endoscopic smart laser surgery**⁴
Hervé Nguendon Kenhagho, Ferda Canbaz, Alois Hopf, Raphael Guzman, Philippe Cattin, Azhar Zam
Published February 2022 in „Lasers in Surgery and Medicine”
3. **Optimized Decellularization Protocol for Large Peripheral Nerve Segments: Towards Personalized Nerve Bioengineering**⁵
Alois Hopf, Lina Al-Bayati, Dirk J Schaefer, Daniel F Kalbermatten, Raphael Guzman, Srinivas Madduri
Published August 2022 in „Bioengineering”

Patents:

1. **Tissue regeneration patch and corresponding fabrication process**⁶
Inventors: Bekim Osmani, Raphael Guzman, Tino Töpfer, Bert Müller, Carina Luchsinger Salinas, Alois Hopf, Mahyar Joodaki
Submitted to the European Patent Office (07. May 2021), Application No.: EP21172804.3
2. **Neural implant based on a cellulose thin film and corresponding fabrication process**³
Inventors: Bekim Osmani, Raphael Guzman, Tino Töpfer, Bert Müller, Carina Luchsinger Salinas, Alois Hopf, Mahyar Joodaki
Submitted to the European Patent Office (07. May 2021), Application No.: EP21172809.2

Incorporation:

1. **Bottneuro AG** - Incorporation: 20. January 2021
Founders: Bekim Osmani, Tino Töpfer, Bert Müller, Pascal Brenneisen, Rolf Wildermuth, Alois Hopf, Raphael Guzman, Cornelia Gut-Villa, Guido Sigron, Magnus Kristiansen

First project:

Development of acellular conduits for peripheral nerve repair and regeneration

Alois Conradin Hopf

Supervisor: PD Dr. Srinivas Madduri

Publications:

Schwann Cell-Like Cells: Origin and Usability for Repair and Regeneration of the Peripheral and Central Nervous System¹

Alois Hopf, Dirk J Schaefer, Daniel F Kalbermatten, Raphael Guzman, Srinivas Madduri

Published August 2020 in „Cells”

Toward optoacoustic sciatic nerve detection using an all-fiber interferometric-based sensor for endoscopic smart laser surgery⁴

Hervé Nguendon Kenhagho, Ferda Canbaz, **Alois Hopf**, Raphael Guzman, Philippe Cattin,

Azhar Zam

Published February 2022 in „Lasers in Surgery and Medicine”

Optimized Decellularization Protocol for Large Peripheral Nerve Segments: Towards Personalized Nerve Bioengineering⁵

Alois Hopf, Lina Al-Bayati, Dirk J. Schaefer, Daniel Kalbermatten, Raphael Guzman, Srinivas

Madduri

Published August 2022 in „Bioengineering”

Abstract

Following complete nerve transection, the gold standard for repair and regeneration is an autologous nerve transplant. However, this involves a second surgery at the donor-site followed by sensory loss and the risk of neuroma formation. Further requirements in length and diameter of the donor nerve limits the number of potential autografts, especially for large gap transplantations. Therefore, decellularized nerve allografts are of great interest for long gap peripheral nerve repair. In this work, different decellularization (DC) techniques are combined for removal of immunogenic material and to eliminate remaining cellular debris while preserving the extracellular matrix and the nerve ultrastructure which is essential for efficient axonal regeneration. An optimized DC protocol, based on different chemical detergents in combination with enzymatic treatment was developed for pig nerves. The use of pig nerves gives a constant source of nerves in all sizes suitable for human transplantation with low variability regarding, age, sex and health of the donor. However, functional benefit of such acellular nerve grafts decreases with increasing gap size. Therefore, combining optimized acellular grafts with cell-based therapies is a good strategy for longer nerve gap repair. Transplantation of Mesenchymal Stem cells (MSC) has shown enhanced peripheral nerve regeneration in animal models as well as in human trials. In this study we can show long term (>53 day) survival and engrafting of human adipose derived MSCs into the previously decellularized grafts. For satisfying clinical outcome following severe Peripheral Nerve Injuries (PNI), biological cues are required additionally to the provided scaffold. Schwann Cells (SC) transplantation into the peripheral nervous system (PNS) and central nervous system (CNS) were successful in promoting axonal elongation and functional recovery. Within this project, a systematic review was written describing the use of SCs and especially the induction of a SC-like phenotype from various cell types for clinical application in the PNS and CNS.

Introduction

The Peripheral Nervous System and Peripheral Nerves

The nervous system is divided into the CNS and the PNS. Whereas the brain and the spinal cord are part of the CNS, peripheral nerves and ganglia which are connecting the various organs and extremities to the CNS are part of the PNS. The peripheral nerves are responsible for transmitting impulses from the periphery to the CNS for processing information and transmission of the signal from the CNS to the periphery for inducing processes such as locomotion. Signal transmission depends on neuronal depolarization and subsequent repolarization. This process is crucial for physiological of the nervous system, thus the ionic gradients, solutes and macromolecules which can potentially influence neuronal de- an re-polarization needs to be tightly controlled⁷. The PNS is subdivided into the autonomic nervous system and the somatic nervous system. In brief, the autonomic nervous system regulates involuntary physiological processes such as the heart rate, respiration, and digestion. The somatic nervous system on the other hand is responsible for conscious, voluntary processes and controls the body movement via skeletal muscles⁸. Each nerve of the PNS such as the sciatic nerve, focus of this study, consists of multiple somatic and autonomic axons enclosed in a sheath of connective tissue. Peripheral nerves are organized in a multi-layered structure with an anastomosis of blood vessels providing each layer with required nutrients and oxygen. The innermost layer, the endoneurium consist of a thin layer of collagen surrounding each individual axon. The next outer layer, the perineurium bundles together several of nerve fibers in what is called fascicles. Several fascicles are embedded within the outermost layer, the epineurium, which covers the entire nerve⁹. Single nerve fibers, consisting of the axons and its surrounding endoneurium vary significantly in diameter which effect signal transmission velocity. However, the major factor influencing signal transmission speed is the myelin sheaths. Nerve fibers can either be myelinated, therefore fast transmitting or unmyelinated and slow transmitting¹⁰. SC are the specific cells for myelination in the PNS, whereas in the CNS oligodendrocytes are the myelinating cell type. There are two major phenotypes of SC. Myelinating SC, responsible for axonal myelination and non-myelinating SC, called remak SC responsible to bundle non-myelinated axons, including many sensory and autonomous axons in so called remak bundles^{11,12}. Myelin sheaths are rich in laminin and their main role is electrical insulation of the axons to increase impulse propagation and signal conduction speed. SC are responsible for production of various factors such as proteoglycans, fibronectin and collagen forming the basal

lamina tube¹³. In case of PNS injuries, SC are critical responders and provide the required factors for mitigating the damage and inducing axonal regeneration¹⁴.

Peripheral Nerve Injuries and current therapeutic strategies

PNI are of clinical importance and are still a major social and economic burden. The estimation goes up to one million new incidences per year worldwide¹⁵. Lesions in the peripheral nerve result in partial or total loss of sensory, motor, and autonomic function in the affected part of the body. Due to missing contact with axonal-derived factors and invading macrophages into the injury site, SC distal to the injury site undergo significant changes in their signalling environment¹⁶. In brief, SC, distal to the injury site converse to a repair SC phenotype which provide the required factors for neuronal survival and axonal regeneration and to myelin clearance¹⁷. Further, SC undergo cellular elongation and branching to form cellular tracks, so-called bungner bands which are providing the axons with the required structural support for regeneration and target innervation¹⁸. Due to the missing structural support for the elongating axons, functional recovery is often rare and unsatisfying, especially after neurotmesis, a complete nerve transection. Although it was recognized more than a century ago that peripheral nerves are able to regenerate, clinical outcome of therapies are often unsatisfactory especially in severe injuries¹⁹. It can be shown that peripheral axons have the ability to regenerate when given a conduit or pathway to the target of reinnervation. For clinical satisfying recovery after neurotmesis, tension-free nerve reconstruction is required. Therefore, direct end-to end suturing of the proximal to the distal stump is promising for injuries without substantial tissue loss only which i.e. result from sharp cuts^{20,21}. However, larger injuries including substantial loss of nerve tissue can lead to neuroma and scar tissue formation which inhibits nerve regeneration if no scaffold for axonal elongation is provided. Even though SC at the site of injury support axonal growth from the proximal to the distal stump, PNI remain clinically challenging. Nowadays, autologous nerve transplantation is the gold standard for large gap injuries although only around 50% of patients receiving autografts regain useful function^{22,23}. Additionally, the autologous transplantation comes with significant limitations such as limited supply, donor-site morbidity, sensory loss, and an additional surgery needed to harvest donor nerve tissue which carries risks by itself. Therefore, there is a need to find new innovative therapies^{24,25}.

Decellularized nerve conduits

Over decades of research, a wide variety of available transplants were developed from synthetic biocompatible conduits i.e., hollow fibers, hydrogels, chitosan, collagen conduits, to

autologous non-nervous tissue grafts such as vein or muscles to processed allografts and autografts^{20,26}. While synthetic nerve conduits are successful in shorter gap injuries (<3cm) to provide a pathway, they fail in longer and larger diameter gaps due to the lack of a laminin scaffold and growth factors secreted by SC. For enhanced nerve regeneration, neurotrophic factors expressed by SC during regeneration are thought to play a crucial role²⁷. Human cadaveric nerve allografts overcome some critical limitations like donor-site morbidity and supply limitations, however there are significant costs and complexity by transplanting such tissue which require the use of immunosuppressant drugs until the nerve graft is repopulated by host SC^{28,29}. The requirement of the patient to receive systematic immunosuppression for up to 18 months may result in opportunistic infections or even tumour formation^{30,31}. Therefore, processing nerve allografts to remove cellular material and reduce immunogenicity by simultaneous preservation of the regenerative capacity of the natural tissue is of great interest. Multiple methods were developed to prepare decellularized nerve grafts such as mechanical disruption like freeze-thawing, mainly at beginning of the process to disrupt cell membranes and lyse the cells. More recently, decellularization of peripheral nerves was accomplished using additional ultrasonication steps for improved debris removal; chemical detergents (ionic, non-ionic, zwitterionic), acid and alkaline treatments, hypo- and hypertonic solution and chelating agents to lyse cells and solubilize cellular proteins; enzymatic degradation for specific removal of inhibiting factors and additional removal of cellular components and irradiation to disrupt proteins^{25,32-35}. Various common decellularization methods and agents were reviewed by Gilpin and Yang in 2017³⁶. The common goals of all these techniques are first to reduce graft immunogenicity by removing host DNA, myelin and axons. Second, to preserve the extracellular matrix and basal lamina which support nerve regeneration³⁷. Third, to remove inhibitory factors like myelin and proteoglycan present in the native nerve^{38,39}.

The Hudson method for peripheral nerves was shown to effectively and reliably remove myelin and cellular compartments³⁷. The major difference to other decellularization protocols was the superior preservation of laminin and the basal lamina architecture. The Hudson method utilizes repeated washes in buffered solutions, anionic detergent Triton X-200, zwitterionic detergent sulfobetaine (SB)-10 and SC-16. The tube-like structure of the basal lamina that run the entire nerve is of great importance for peripheral nerve repair after injury^{37,40}. The Hudson method was used commercially for producing human decellularized nerve segments for peripheral nerve repair since 2007⁴¹. These conduits were clinically successful and reported meaningful recovery rates of 75%-100% even in long gap repair of up to 50 mm^{42,43}. Unfortunately, Triton X-200 a key detergent in the Hudson protocol is no longer manufactured and cannot be synthesized locally in sufficient

quantities. A suitable one to one replacement has not been found yet⁴⁴. This highlights the need to identify and describe a range of decellularization detergents to develop protocols suitable for clinical application.

Aim of the project

The goal of the present publication: „Optimized Decellularization Protocol for Large Peripheral Nerve Segments: Towards Personalized Nerve Bioengineering” was to address the drawbacks (i.e., donor-site morbidity, limited supply, second surgery and loss of sensory function) associated with the current gold standard in peripheral nerve repair. The project involves the production of an optimized acellular nerve graft (ANG). The ANG was analysed regarding the removal efficiency of myelin, DNA and axonal material. Further, the ANG was used as 3D scaffold for MSC culture to analyse its biocompatibility. The ultimate goal of this project was to develop a biologically functional nerve allograft for long-gap nerve repair in humans.

The first aim of this project was to produce an acellular, non-immunogenic nerve allograft from a controllable source towards clinical settings. Most DC protocols were developed for rodents. However, decellularized rodent nerves are not suitable for human nerve repair due to size and modality mismatch. Therefore, a constant source, low in variability regarding axonal myelination, length and diameter is required to produce standardized nerve grafts for clinical application. Pigs were found to be a suitable source for nerve grafts. Constant supply with low variability regarding age, myelination and health status from the donor is possible compared to human donor post-mortem. Immunogenicity must be reduced while maintaining the extracellular matrix to provide an environment similar to autologous nerve transplants. By combining different approaches for decellularization by chemical detergents and enzymatic treatment, efficient removal of host myelin, axons and DNA was accomplished. Such processed scaffolds should be suitable for xenotransplantation without immunosuppressants. Due to optimization of incubation time and reducing concentration of certain chemicals, especially of Sodium Deoxycholate, the native structure of the nerve was well preserved. By including enzymatic treatment like Chondroitinase ABC and elastase, specific degradation of inhibitory factors was improved and removal of cellular debris was achieved.

Second, the decellularized pig graft was used as a 3D scaffold for cell studies. Optimal conditions for long-term survival and proliferation of human mesenchymal Stem/stromal Cells (MSC) in these decellularized grafts were investigated for potential clinical translation. Namely, culture condition was changed to an animal serum free system to reduce potential harmful effect later in clinical settings. Therefore, Fetal Calf Serum (FCS) was replaced by human Platelet Lysate which could be produced patient specifically. It was shown that human MSC proliferation in the 3D acellular graft was improved in media supplemented with human platelet lysate compared to

FCS supplements. And that this effect is specific to the 3D system provided by the developed grafts⁵.

Results

A paper including the results of this project was published in „Bioengineering” at the 24th of august 2022. The authors are Alois Hopf, Lina Al-Bayati, Dirk Schaefer, Daniel Kalbermatten, Raphael Guzman and Srinivas Madduri. The publication is included in the present thesis.

Article

Optimized Decellularization Protocol for Large Peripheral Nerve Segments: Towards Personalized Nerve Bioengineering

Alois Hopf^{1,2}, Lina Al-Bayati^{1,2}, Dirk J. Schaefer^{1,3}, Daniel F. Kalbermatten^{1,3,4,5}, Raphael Guzman^{2,6} and Srinivas Madduri^{1,3,4,5,*}

- ¹ Department of Biomedical Engineering, University of Basel, Gewerbestrasse 14, 4123 Allschwil, Switzerland
 - ² Department of Biomedicine, University Hospital Basel, Hebelstrasse 20, 4031 Basel, Switzerland
 - ³ Department of Plastic, Reconstructive, Aesthetic and Hand Surgery, University Hospital Basel, University of Basel, Spitalstrasse 21, 4031 Basel, Switzerland
 - ⁴ Plastic, Reconstructive and Aesthetic Surgery, Department of Surgery, Geneva University Hospitals, University of Geneva, 1211 Geneva, Switzerland
 - ⁵ Bioengineering & Neuroregeneration, Department of Surgery, Geneva University Hospitals, University of Geneva, Rue Michel-Servet 1, 1211 Geneva, Switzerland
 - ⁶ Department of Neurosurgery, University Hospital Basel, Spitalstrasse 21, 4031 Basel, Switzerland
- * Correspondence: srinivas.madduri@unige.ch; Tel.: +41-61-556-5049

Abstract: Nerve injuries remain clinically challenging, and allografts showed great promise. Decellularized nerve allografts possess excellent biocompatibility and biological activity. However, the vast majority of decellularization protocols were established for small-size rodent nerves and are not suitable for clinical application. We aimed at developing a new method of decellularizing large-diameter nerves suitable for human transplantation. Repeated rounds of optimization to remove immunogenic material and preserve the extracellular structure were applied to the porcine sciatic nerve. Following optimization, extensive *in vitro* analysis of the acellular grafts via immunocytochemistry, immunohistology, proteomics and cell transplantation studies were performed. Large segments (up to 8 cm) of the porcine sciatic nerve were efficiently decellularized and histology, microscopy and proteomics analysis showed sufficient preservation of the extracellular matrix, with simultaneous consistent removal of immunogenic material such as myelin, DNA and axons, and axonal growth inhibitory molecules. Cell studies also demonstrated the suitability of these acellular grafts for 3D cell culture studies and translation to future large animal studies and clinical trials. By using non-human donors for peripheral nerve transplantation, significant drawbacks associated with the gold standard can be eliminated while simultaneously preserving the beneficial features of the extracellular matrix.

Keywords: decellularization; acellular allograft; large-gap repair; neurotmesis; peripheral nerve injuries; porcine sciatic nerve



Citation: Hopf, A.; Al-Bayati, L.; Schaefer, D.J.; Kalbermatten, D.F.; Guzman, R.; Madduri, S. Optimized Decellularization Protocol for Large Peripheral Nerve Segments: Towards Personalized Nerve Bioengineering. *Bioengineering* **2022**, *9*, 412. <https://doi.org/10.3390/bioengineering9090412>

Academic Editor: Hae-Won Kim

Received: 2 August 2022

Accepted: 18 August 2022

Published: 24 August 2022

Publisher's Note: MDPI stays neutral with regard to jurisdictional claims in published maps and institutional affiliations.



Copyright: © 2022 by the authors. Licensee MDPI, Basel, Switzerland. This article is an open access article distributed under the terms and conditions of the Creative Commons Attribution (CC BY) license (<https://creativecommons.org/licenses/by/4.0/>).

1. Introduction

Peripheral nerve injuries are of clinical importance, with an estimated global incidence of one million cases each year [1]. Lesions in the peripheral nerve result in a decreased or complete loss of sensory and motor functions. Although it was recognized more than a century ago that peripheral nerves possess a regenerative capacity, clinical outcomes of therapies are often unsatisfactory, especially in severe injuries [2]. Direct suturing is promising for small injuries, but only because satisfactory recovery requires tension-free nerve reconstruction [3,4]. Following injuries with extensive damage, including a substantial loss of nerve tissue, autologous nerve transplantation is the current gold standard [5]. However, only around 50% of patients who receive autografts regain normal function [6] due to its limitations, such as a limited supply, donor-site morbidity, and size-modality mismatch. Thus, there is a need to find new innovative therapies [7,8]. Over decades of research, a wide variety of available transplants have been developed and range from synthetic

biocompatible conduits to autologous non-nervous tissue grafts, such as veins or muscles, to processed allografts and autografts [3,9]. One promising alternative to the current gold standard is processed allografts.

Allografts have the advantage of mitigating donor-site morbidity and are unlimited in supply and size. Furthermore, based on their extracellular matrix (ECM) composition, they are bioactive and biodegradable. By processing, allografts can be decellularized and therefore the immunogenic material, such as cells, cellular components and other regeneration inhibitors, can be removed from the tissue, with only the ECM scaffold remaining, preferably in its native structure and composition. By this method, the bioactive and mechanical properties of the scaffold remain, which was shown to induce cell adhesion, migration, proliferation, differentiation and angiogenesis [10]. However, the optimal balance between the structural integrity of the basal lamina and the ECM and the removal of cellular components and inhibitors remains to be defined.

Multiple methods have been developed for preparing decellularized nerve grafts such as mechanical disruption, e.g., freeze-thawing, mainly at the beginning of the process in order to disrupt cell membranes and lyse the cells. More recently, decellularization of nerve grafts was accomplished using additional ultrasonication steps for improved debris removal, chemical detergents (ionic, non-ionic, zwitterionic), acid and alkaline treatments, hypo- and hypertonic solutions and chelating agents to lyse cells and solubilize cellular proteins, enzymatic degradation for the specific removal of inhibiting factors, and additional removal of cellular components and irradiation to disrupt proteins [8,11–14]. Various common decellularization methods and agents were reviewed by Gilpin and Yang in 2017 [15].

The ultimate goal of all these techniques is first to reduce graft immunogenicity by removing host cells and cellular components, myelin and axons. Second, to preserve the extracellular matrix and basal lamina, which support nerve regeneration [16]. Third, to remove inhibitory factors such as myelin and proteoglycan present in the native nerve [17,18]. However, most protocols were established for small-scale rat and mouse sciatic nerves and are therefore not suitable for human-size nerve segments. Decellularization is generally performed on a rolling shaker to expose the tissue to the decellularization agent with uniform and consistent concentrations. Thus, the main mode of penetrating the tissue is diffusion. As observed in this study, decellularization protocols established for rodent sciatic nerves were not suitable for the decellularization of large-diameter pig nerves and require several adjustments in detergents, concentrations and duration of exposure.

The goal of this study was to develop and investigate a new method of decellularizing large-diameter nerves, which are suitable for human transplantation. By combining a mild chemical disruption of cellular components with enzymatic degradation, a large acellular nerve scaffold was produced that does not contain detectable amounts of myelin or axons and has a preserved ECM structure. Injecting primary, human adipose-derived MSC (hASC) and tracking their activity allowed us to conclude upon the biocompatibility of these scaffolds (Figure 1).

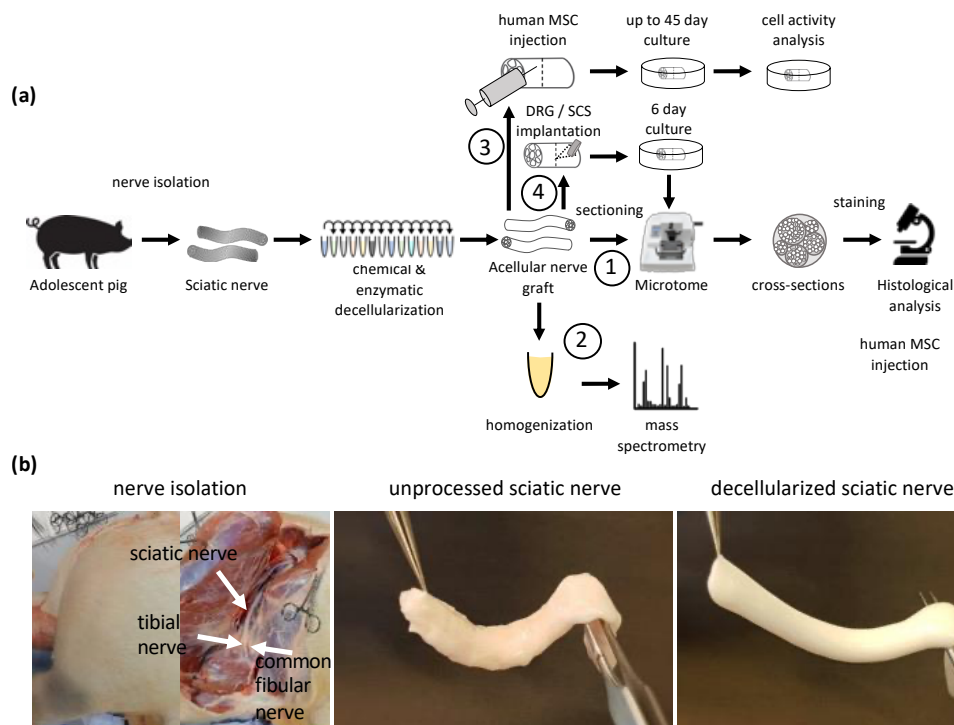


Figure 1. Experimental overview: (a) Illustration of the experimental setup. Sciatic and common fibular nerves of adolescent pigs were isolated. Following isolation, the nerves were treated with a series of various chemical and enzymatic detergents for decellularization. The resulting acellular nerve grafts were analyzed and tested in different ways. (1) Cross-sections via microtome were made from acellular graft and used for immunohistochemistry. (2) Proteomic analysis of the acellular graft to detect the number of removed peptides and known inhibitors of axonal regeneration due to the decellularization process. (3) Acellular grafts were used as 3D scaffolds for cell culture. Cells in the 3D scaffold were cultured for up to 45 days and cellular behavior was analyzed by measuring cellular metabolism via resazurin. (4) Dorsal root ganglion (DRG) and Spinal cord segments (SCS) were implanted in acellular grafts and cultured for 6 days prior to fixation, sectioning and histological analysis; (b) Representative images of nerve isolation from adolescent pigs. Unprocessed sciatic nerve with excessive fat and connective tissue and a reddish color, Decellularized sciatic nerve with removed excessive tissue and white appearance.

2. Materials and Methods

2.1. Sciatic and Common Fibular Nerve Isolation

Nerve tissue was carefully isolated from domestic pigs (*sus scrofa domesticus*; Schweizer Edelschwein), which were euthanized 2–4 h prior to isolation. Special attention was given not to damage (pull and/or quench) the nerve and therefore not to disrupt the structure. The isolated nerve was sectioned in length from 0.5 cm to 8 cm for decellularization and subsequent analysis and testing. Tissue was collected in Phosphate-Buffered saline without Ca^{2+} and Mg^{2+} ($\text{PBS}^{-/-}$) (Sigma-Aldrich, Buchs, Switzerland, Cat. No. D8537) on ice and delivered to the laboratory for experimentation. Unprocessed control tissue was placed immediately after isolation in 4% paraformaldehyde (PFA) (Carl Roth, Cat. No. 0335.2) in

PBS^{-/-} and placed on ice for delivery to the laboratory where it was placed at 4 °C for the remaining 24 h of tissue fixation.

No animals were raised or euthanized for the sole purpose of this study. For this study, biological waste was reused. Nerve tissue was isolated from 11 pigs post-mortem at the Center for Surgical Research & Central Biological Laboratory, University of Zurich. Animals were euthanized either by 100 mg/kg potassium chloride or by bleeding out under full anaesthesia. The animal housing and experimental protocols were approved by the Cantonal Veterinary Office, Zurich, Switzerland, under License ZH 115/2018, 084/2017, ZH 047/2020, ZH 052/2020, ZH 132/2017, ZH 213/2019 and ZH 219/2016.

2.2. Decellularization

Decellularization (DC) protocols were optimized based on previously published protocols for the decellularization of rodent nerves [7,16,19,20]. Protocol 1 was initially optimized for the decellularization of Sprague-Dawley rat sciatic nerves and subsequently applied to the nerves isolated from domestic pigs of 30 to 110 kg. Quantification experiments were performed using nerve segments of 4 cm and 8 cm, respectively. For cell transplantation studies, decellularization was performed on about 8 cm-long common fibular nerves, which were segmented in a size range of 4 mm after decellularization. All decellularization steps were performed at room temperature (RT) on an rs-tr05 roller mixer (Carl Roth, Karlsruhe, Germany) at 20 RPM unless otherwise stated. Segments were submerged in an excessive volume of detergents unless otherwise stated. After decellularization, each segment was washed 3 times to remove residual detergents in PBS^{-/-}, each for 5 min. For the decellularization process, osmotic pressure, chemical disruption, solubilization and enzymatic degradation were applied for the removal of cells, cell debris, DNA, lipids, other immunogenic material and growth inhibitory molecules as described in more detail in the Section 4.

In brief, the initial protocol (protocol 1) was as follows: nerve segments were placed in ddH₂O for 7 h, followed by 1 M NaCl (Sigma-Aldrich, Cat. No. S7653) for 15 h. After rinsing nerve segments with ddH₂O, segments were placed in 2.5 mM of non-ionic Span20 (Sigma-Aldrich, Cat. No. S6635) in PBS^{-/-} for 24 h. Span20 removal was performed by washing the segments in PBS^{-/-} for 15 min. Segments were then placed in ddH₂O for 7 h, followed by 1 M NaCl for 15 h, and then rinsed in ddH₂O. Next, segments were placed in 100 mM of zwitterionic CHAPS (Sigma-Aldrich, Cat. No. C3023) in PBS^{-/-} for 24 h.

Protocol 2 followed the same procedure as protocol 1. However, at the end, nerve segments were placed in 1 mL/cm of segment length of 0.2 U/mL chondroitinase ABC (Merck, Tomoguro, Tokyo, Cat. No. C2905) in chondroitinase buffer (50 mM TRIS, 60 mM sodium acetate pH 8, 0.02% bovine serum albumin [BSA] (Sigma-Aldrich, Cat. No. A3294)) at 37 °C for 24 h. Segments were then rinsed in PBS^{-/-} and placed in 0.05 U/mL elastase (Merck, Cat. No. E7885) in PBS^{-/-} for a further 24 h.

Protocol 3 was based on protocol 2, but incubation times for non-ionic Span20 and zwitterionic CHAPS were doubled from 24 h to 48 h. All other incubation times remained the same and detergents and their order of applications were unchanged.

Protocol 4 was based on protocol 3. However, after initial decellularization steps in ddH₂O for 7 h and 1 M NaCl for 15 h, segments were placed in 4% sodium deoxycholate (Sigma-Aldrich, Cat. No. D6750) in ddH₂O for 24 h.

Protocol 5, which was further used in the detailed analysis, was based on protocol 4, with the difference that sodium deoxycholate concentrations were reduced from 4% to 0.001%.

2.3. Neurospecimen Preparation

Decellularization protocol optimization was performed on 1 cm-long segments of sciatic nerves. Quantification of remaining myelin, DNA, axonal debris and laminin was performed on 4 cm and 8 cm-long segments of decellularized sciatic nerve tissue. hASC were transplanted in 4 mm-long segments of decellularized common fibular nerves. Dorsal

root ganglion (DRG) and spinal cord segment (SCS) were transplanted into 8 mm-long segments of decellularized sciatic nerves. Following decellularization, acellular grafts were either fixed immediately or stored at 4 °C in PBS^{-/-} overnight for cell transplantation. For proteomics studies, unprocessed tissue was stored at 4 °C in PBS^{-/-} for 11 days until the decellularization procedure of the experimental condition was completed. For the structural analysis, samples were fixed in 4% PFA at 4 °C for 24 h. The fixed segments were sequentially dehydrated in increasing EtOH concentrations and xylene and embedded in paraffin using a TPC 15 DUO (MEDITE GmbH, Dietikon, Switzerland). The 5 µm-thin cross- and longitudinal sections were made by a rotary microtome (Microm HM 340E; Thermo Fisher Scientific, Waltham, MA, USA).

2.4. Immunohistochemistry

Antigen retrieval by proteinase K (Sigma-Aldrich, Cat. No. 03115836001) for 10 min at 37 °C was performed prior to immunohistochemistry for polyclonal laminin staining. Sections were blocked for 1 h at RT in a blocking buffer consisting of 1% BSA and 0.1% TritonX-100 in PBS^{-/-}. Primary antibodies, namely laminin (Merck, Cat. No. L9393), myelin basic protein (MBP) (Bio-Rad, Hercules, CA, USA: Cat. No. MCA409S) and β-tubulin III (Abcam, Chuo-ku, Tokyo, Cat. No. ab18207), were incubated overnight at 4 °C in the blocking buffer. Sections were then washed in PBS^{-/-} 3 times for 10 min before the addition of secondary antibodies (goat anti-rabbit IgG-a488; Thermo Fisher Scientific, Cat. No. A-11008; goat anti-rat IgG-a647; Thermo Fisher Scientific, Cat. No. A-21247) and 4',6-diamidino-2-phenylindole (DAPI) (Sigma-Aldrich, Cat. No. 32670) in blocking buffer for 1 h at RT in the dark. After washing 3 times for 10 min with PBS^{-/-}, the slides were covered with mounting media and coverslips. For a general evaluation of successful decellularization, longitudinal and cross-sections were further dyed using standard Gill's hematoxylin and eosin protocol, staining acidic structures purple and basic structures pink. To verify cellular and myelin removal, segments were dyed using a standard Luxol fast blue assay with Cresyl violet counterstain. In brief, after deparaffination in Xylenes (Sigma-Aldrich, Cat. No. 247642) for 3 × 2 min, sections were rinsed in 96% ethanol and incubated in 0.1% Luxol Fast Blue solution (CliniSciences, Cat. No. 26056-10) at 56 °C for 20 h. After washing with 96% ethanol samples were differentiated in 0.05% lithium carbonate (Sigma-Aldrich, Cat. No. 62470) and stained with 0.1% cresyl violet acetate solution (Sigma-Aldrich, Cat. No. C5042) for 4 min. The samples were dehydrated and mounted with mounting media [21].

2.5. Decellularization Efficiency Analysis

Decellularized tissue was analyzed using immunohistochemistry images. Cross-sections were imaged and the most promising protocols were selected qualitatively. In the following experiments, the decellularization efficiency of selected protocols was confirmed and further optimized. Changes in the decellularization protocols which affected decellularization efficiency negatively were not repeated. However, improvements in the decellularization protocols were repeated and confirmed in the following experiments on nerve tissue from different pigs. This process was repeated for several rounds until one protocol was found that removed immunogenic material and preserved ECM structures. Images were taken using a Nikon Ti2 Eclipse microscope (Nikon, Chiyoda, Tokyo, Japan) and CFI Plan Apo Lambda objectives. Fluorescence images were acquired by a photometrics Prime95B camera using a 5-bandpass light filter. Color images were acquired by a Nikon DS-Ri2 camera.

2.6. Quantification of Cellular Components

The decellularization efficiency of the qualitatively selected optimized protocol was quantified. Regions of Interest (ROI) were defined via manual segmentation of fascicles using the NIS-elements software. All subsequent steps were based on the ROI. Autofluorescence of the tissue was subtracted using non-stained negative controls. The remaining

MBP, β -tubulin III and DAPI signal after decellularization were then plotted in relation to the signal of unprocessed tissue segments. Images were taken using a Nikon Ti2 Eclipse microscope (Nikon, Chiyoda, Tokio, Japan) and CFI Plan Apo Lambda objectives. Fluorescence images were acquired by a photometrics Prime95B camera using a 5-bandpass light filter. Color images were acquired by a Nikon DS-Ri2 camera.

2.7. Mass Spectrometry-Based Proteome Analysis

2.7.1. Sample Preparation

Three milligrams of sample were lysed in 150 μ L of lysis buffer (5% sodium dodecyl sulfate [SDS], 100 mM TEAB, pH = 8) using a PIXUL (Active Motif) sonication device (50 N Pulse, 1 kHz PRF, 20 Hz burst rate). Lysates were centrifuged at 15,000 RCF for 15 min and the protein concentration of the supernatant was assessed using a BCA assay (Thermo Fisher Scientific); 10 μ g of protein per sample were reduced by tris (2-carboxyethyl)phosphine at 95 $^{\circ}$ C for 10 min. Proteins were alkylated using 15 mM iodoacetamide at RT in the dark for 30 min and further processed using S-TRAP (Protify) microcartridges, according to the manufacturer's specifications. For digestion, trypsin was used (1/25 *w/w*, ratio trypsin/protein; Promega, Madison, WI, USA) at 47 $^{\circ}$ C for 1 h. After drying the samples under vacuum, peptides were stored at -20° C and dissolved in 0.1% aqueous formic acid solution at a concentration of 0.5 mg/mL upon use.

2.7.2. Mass Spectrometry-Based Analysis

For each sample, 0.25 μ g total peptides including 5 fmol/ μ g iRT peptides (Biognosys AG, Schlieren, Switzerland) were subjected to liquid chromatography-mass spectrometry analysis using an Exploris 480 mass spectrometer equipped with a nanoelectrospray ion source (both Thermo Fisher Scientific). Peptide separation was carried out using an Ultimate 3000 System (Thermo Fisher Scientific) equipped with a reverse phase-high performance liquid chromatography column (75 μ m \times 30 cm) packed in-house with C18 resin (ReproSil-Pur C18-AQ, 1.9 μ m resin; Dr. Maisch GmbH, Ammerbuch, Germany) and a custom-made column heater (60 $^{\circ}$ C). Peptides were separated using a linear gradient from 95% solvent A (0.1% formic acid, 99.9% water) and 5% solvent B (80% acetonitrile, 0.1% formic acid, 19.9% water) to 35% solvent B over 45 min, and further to 50% solvent B over 10 min at a flow rate of 300 nL/min.

For data-independent acquisition (DIA) analysis, each MS1 scan (120k resolution) covering 350 *m/z* to 1400 *m/z* was followed by high collision dissociation (HCD) scans (15k resolution, 22 ms injection time, 8 *m/z* isolation windows with 1 *m/z* overlap, 28 HCD collision energy, 300% automatic gain control) covering the mass range of 400 *m/z* to 900 *m/z*.

2.7.3. DIA Data Analysis

DIA data was analyzed using Spectronaut (V15.5). A *sus scrofa* (pig) FASTA was downloaded on 14 October 2021 (unreviewed, one entry per gene). Trypsin/P was set as enzymatic specificity and two missed cleavages were allowed. Oxidation and protein N-terminal acetylation were set as variable modifications, whereas carbamidomethylation (C) was set as a fixed modification. The protein Q value filter was set to 1% for global filtering and to 5% for runwise filtering. Q value filtering was activated, leading to an incomplete protein abundance matrix.

2.7.4. Data Availability

Raw Data of mass spectrometry experiments are accessible via MassIVE: <ftp://MSV000090072@massive.ucsd.edu> (accessed on 1 August 2022), username: "MSV000090072_reviewer", password: "Decellularized".

2.8. hASC Isolation, Characterization, Transplantation and Activity Measures

hASC were isolated and characterized as previously described [22]. Adipose tissue was obtained from healthy human donors undergoing elective liposuction. Informed consent was obtained from the patient prior to liposuction, in addition to approval by the institutional ethics committee of the Basel University Hospital.

In brief, to obtain hASC isolation, fat tissue was cleared from erythrocytes by rinsing with PBS and centrifugation, followed by enzymatic digestion using 0.1% (*w/v*) type I collagenase for 3 h at 37 °C and centrifugation at 4 °C for 5 min at 250 g. The resulting cell pellet was resuspended in growth medium (GM) containing Dulbecco's Modified Eagle's Medium (DMEM, Gibco-Fisher Scientific, Cat. No. 4196503), 10% fetal bovine serum (FBS), 1% penicillin/streptomycin and 5 ng/mL basic fibroblast growth factor (Peprotech, Rocky Hill, NJ, USA, Cat. No. 100-18B). Cells were cultured for 14 days at 5% CO₂ and 37 °C. GM was changed every 72 h and cells subdivided at 90% confluency using 0.25% trypsin-EDTA. For cell characterization via flow cytometry, the following fluorophore-conjugated antibodies were used: CD29⁺-PE (Biolegend, Cat. No. 303003), CD73⁺-APC (Biolegend, Bunkyo Ward, Tokyo, Cat. No. 344005), CD90⁺-PE/Cy7 (Biolegend, Cat. No. 328123) and CD105⁺-a488 (Biolegend, San Diego, CA, USA, Cat. No. 323209). Gates were set based on fluorophore-conjugated IgG1 isotype control, namely IgG1-PE (Biolegend, Cat. No. 400111), IgG1-APC (Biolegend, Cat. No. 400119), IgG1-PE/Cy7 (Biolegend, Cat. No. 400125), and IgG1-a488 (Biolegend, Cat. No. 400132). In total, 386,902 CD29⁺CD73⁺CD90⁺CD105⁺ cells were analyzed using a BD FACSAria III (BD Bioscience, Franklin Lakes, NJ, USA). Characterization via Immunocytochemistry was performed as follows. Cells were fixed with 4% PFA for 10 min, then washed with PBS^{-/-}. Membrane permeabilization was performed by 0.3% Triton X-100 in PBS^{-/-} for 20 min. Permeabilization solution was washed twice with PBS^{-/-}. After 1 h of blocking by 1% protease-free BSA in PBS^{-/-} primary antibodies were added in blocking buffer. Primary antibodies, namely CD105 (Abcam, Cat. No. ab44967), CD44 (Abcam, Cat. No. ab6124), CD90 (Abcam, Cat. No. ab23894) and CD29 (Abcam, Cat. No. ab134179) were incubated overnight at 4 °C in blocking buffer. The remaining primary antibodies were washed away by rinsing cells three times with PBS^{-/-} each time for 10 min. Secondary antibodies (goat anti-rabbit IgG-a546 (Thermo Fisher Scientific, Cat. No. A-11010) and goat anti-mouse IgG-a488 (Thermo Fisher Scientific, Cat. No. A-11029)) and DAPI were added in blocking buffer for 1 h at RT in the dark. Cells were rinsed with PBS^{-/-} and immediately imaged using a Nikon Ti2 Eclipse microscope as previously described (Figure S1).

Decellularized common fibular nerves were cut into 5 mm-long segments and 250k hASC were injected into the grafts using a 30G syringe in a total volume of 50 µL media. Grafts were submerged in GM for a constant supply of nutrients and placed in a 5% CO₂ incubator at 37 °C. GM contained either 10% FBS as previously described or 5% human platelet lysate (HPL) and 2 U/mL of heparin sodium salt as serum supplement. GM was changed every 48 h. Cell activity was measured by the reduction in resazurin whereby living cells turned from an oxidized blue dye to a pink resorufin product. Cell activity was measured on predefined days 1, 4, 7, 11, 14, 16, 18, 21, 23, 25, 31, 35, 39, 42, 46, 49 and day 53 by a microplate reader, Synergy H1 Hybrid Reader (BioTek, Winooski, VT, USA). Cell activity on day 1 was used for normalization.

2.9. Isolation of Embryonic Chicken DRG and SCS

Fertilized chicken eggs were purchased from Gepro Geflügelzucht AG (Flawil, Switzerland). The eggs were incubated for 10 days at 37.8 °C and 100% relative humidity (E10). Embryo collection and dissection were conducted under aseptic conditions in the laminar flow hood with sterile equipment and solutions. For the embryo dissection, a stereomicroscope was utilized. Dissection was performed using previously published protocols for DRG isolation [23,24]. Following DRG isolation, the spinal cord was isolated and segmented into 200 µm-long segments.

2.10. Transplantation of DRG and SCS into Acellular Graft

For cell implantation, all the decellularization steps were performed in a sterile environment and the decellularized tissue was treated with 100 U/mL of penicillin, 100 U/mL of streptomycin and 0.25 µg/mL of Gibco amphotericin B for at least 48 h to prevent bacterial and fungal contamination.

Small incisions at the middle of 8 mm-long segments of acellular graft were made using a sterile scalpel. DRG or SCS was implanted into the acellular graft using forceps and held in place using a carrier fibrin hydrogel [22]. The acellular grafts were then placed in a petri dish containing GM as previously described for the hASC culture. GM was replaced every other day. After 6 days, the acellular graft was fixed for 24 h with 4% PFA before embedding in paraffin. Embedded tissue was sectioned in 5 µm thin cross-sections. Implantation of SCS and DRG into the acellular graft was analyzed by staining for β-tubulin III (Figure S2).

3. Results

3.1. Stepwise Removal of Immunogenic Material from Large-Diameter Pig Nerves

Optimization of the decellularization protocol was performed on 1 cm long sciatic nerve segments. Protocol 1 was previously established for the decellularization of small-diameter rat nerves (data not shown). Applying it to large-diameter sciatic pig nerves resulted in no substantial removal of immunogenic material, such as myelin, axons and DNA. However, also no disruption of the endoneurial tubes was detected after treatment (Figure 2, column 2). Additional enzymatic degradation steps by elastase and chondroitinase ABC in protocol 2 removed axonal debris and DNA substantially, while preserving the extracellular structure as observed by laminin staining (Figure 2, column 3). Complete removal of axonal debris was achieved by doubling the incubation time of non-ionic Span20 and zwitter-ionic CHAPS from 24 h to 48 h (Figure 2, column 4), but no myelin removal was observed. An additional processing step comprising of the addition of 4% sodium deoxycholate completely removed myelin and any remaining debris. However, the ECM structure was highly disrupted (Figure 2, column 5). Reducing the applied sodium deoxycholate by a factor of 4000× led to the efficient removal of myelin, axons, and DNA, while the ECM structure remained mainly intact and only a minor disruption of the laminin structure was observed (Figure 2, column 6).

3.2. Optimized Decellularization Protocol Removes Immunogenic Material in Therapeutically Relevant Nerve Length While Preserving Extracellular Structure

Sciatic nerves of therapeutically relevant lengths of 4 cm and 8 cm were decellularized using the previously developed protocol 5. As shown in Figure 3a (upper row), immunogenic material can be removed throughout 8 cm-long segments and the intact endoneurial tubes show that the extracellular structure can be well preserved (Figure 3a, lower row). The quantification of the removal of immunogenic material in 4 cm- and 8 cm-long segments also showed a highly significant (adjusted *p*-values < 0.0001) removal of immunogenic material. In addition, no significant removal of laminin was observed (Figure 3b,c). For 4 cm-long segments, after 1 cm only 0.28 ± 0.37% of DAPI, 9.51 ± 5.89% of β-tubulin III and 2.89 ± 2.36% of MBP remained. After 2 cm, in the middle of the 4 cm-long segments, 2.53 ± 0.61% of DAPI, 26.07 ± 2.67% of β-tubulin III and 9.96 ± 1.41% of MBP remained (Figure 3b [left column],c). For 8 cm-long segments, after 1 cm only 1.5 ± 0.67% of DAPI, 4.01 ± 1.18% of β-tubulin III and 11.19 ± 6.12% of MBP remained. After 2 cm, 2.82 ± 1.13% of DAPI, 7.73 ± 1.69% of β-tubulin III and 13.88 ± 5.47% of MBP remained. After 3 cm, 4.56 ± 1.08% of DAPI, 6.07 ± 2.18% of β-tubulin III and 8.39 ± 2.76% of MBP remained. After 4 cm (middle of the 8 cm-long segments), 3.01 ± 1.13% of DAPI, 5.4 ± 3.03% of β-tubulin III and 13.76 ± 4.83% of MBP remained (Figure 3b [right column],c).

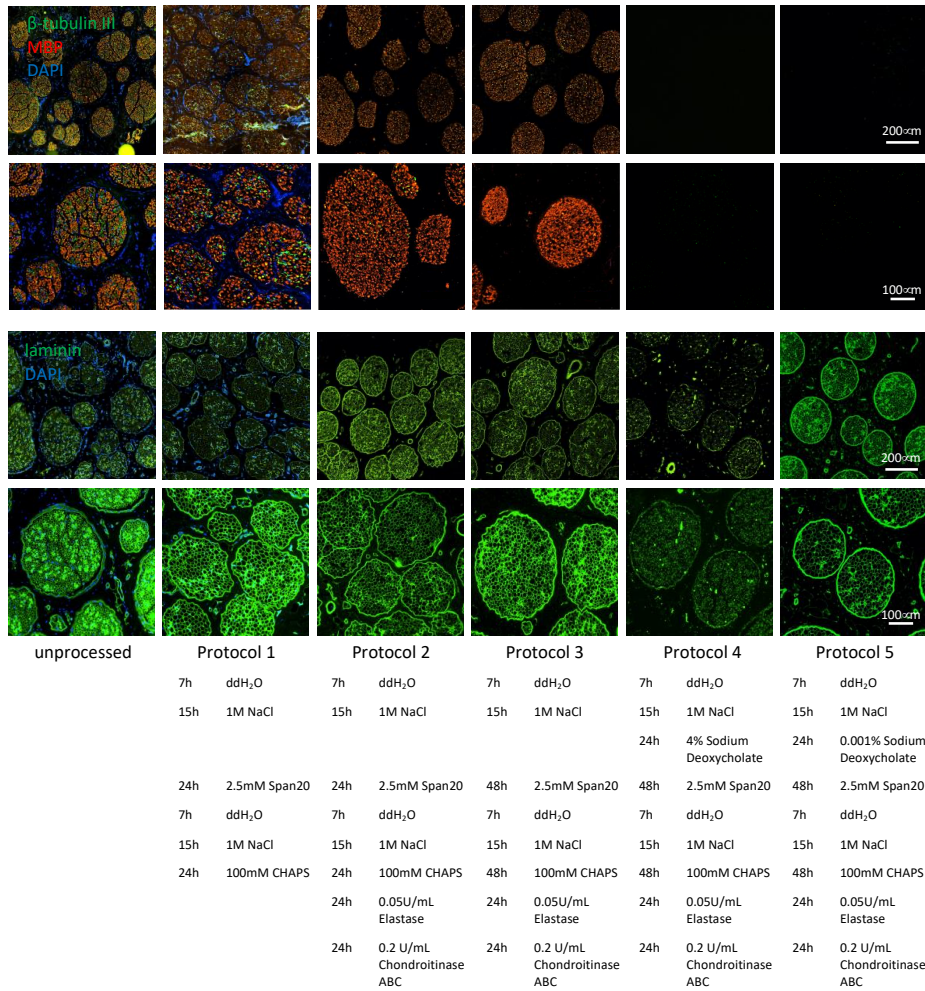


Figure 2. Removal of immunogenic material and ECM preservation by optimized protocols from large diameter pig nerves. First row: scale bar 200 μm , representative images of remaining axonal β -tubulin III, MBP and DAPI. Second row: scale bar 100 μm , zoomed-in representative images of remaining axonal β -tubulin III, MBP and DAPI. Third row: scale bar 200 μm , representative images of remaining ECM laminin structure and DAPI. Fourth row: scale bar 100 μm , zoomed-in representative images of remaining ECM laminin structure and DAPI. Each column shows a further optimization step towards protocol 5, an acellular graft with removed axonal β -tubulin III, MBP, DAPI and a conserved laminin structure signal. Protocol 5 was used for further analysis.

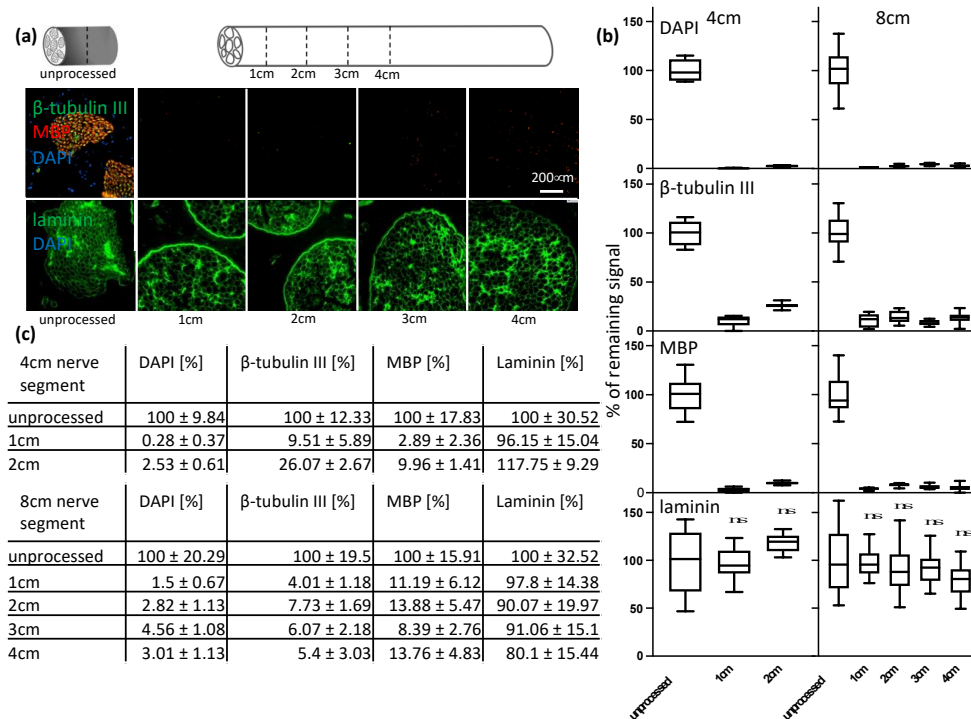


Figure 3. Quantification of remaining cellular components in longer nerve segments. (a) The remaining immunogenic material and laminin structure were analyzed every 1 cm up to the middle of an 8 cm-long pig sciatic nerve segment decellularized by protocol 5. Representative images: the remaining ECM laminin structure and DAPI are shown in the upper row, together with the remaining axonal β-tubulin III, MBP and DAPI signals in the bottom row (scale: 200 μm). (b) Graphic documentation: the remaining axonal β-tubulin III, MBP, DAPI and laminin signals were quantified. Fascicles were manually segmented and the remaining signals were normalized to signal unprocessed tissue. For statistical analysis, a one-way ANOVA was performed. Adjusted *p*-value: < 0.0001 = ****, ns: no significant differences. (c) Numerical documentation: percentage of the remaining axonal β-tubulin III, MBP, DAPI and laminin signals for 4 cm and 8 cm-long segments every 1 cm until the middle.

3.3. Decellularization Protocol 5 Leads to Preservation of ECM While Removing Lipids and Cellular Content

Efficient removal of lipids was confirmed by Luxol fast blue staining of the acellular grafts and showed that dark blue myelin structures within the fascicles were removed completely. Furthermore, it can be observed that the removal of myelin was consistent across the whole diameter and length of the decellularized tissue and no patches of remaining myelin were found. Consistent cell removal was confirmed by the removal of the Cresyl violet stain (purple) (Figure 4, top rows). Preservation of the ECM was shown by hematoxylin and eosin stain (Figure 4, bottom rows). The overall structure of the ECM was well preserved. Although an analysis of higher magnified images indicates a partial disruption of the endoneurial tubes, the ECM matrix was consistently present within the fascicles, but some ring-like structures could still be seen in higher magnified cross-section images of the acellular grafts. In longitudinal sections of hematoxylin and eosin-stained

slices, a fibrous structure can be observed in the acellular graft as in unprocessed ones, thus indicating a good cross- and longitudinal preservation of the ECM.

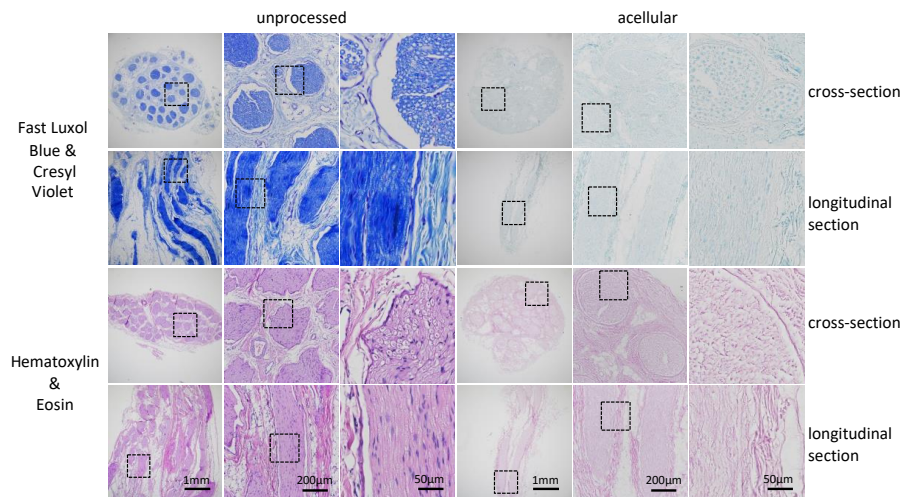


Figure 4. Histological analysis of the ECM and the remaining myelin structure of protocol 5. Luxol fast blue and Cresyl violet stain: myelin (blue) and nuclei (purple) (**top**). Hematoxylin and eosin stain: ECM (pink) and nuclei (purple) (**bottom**). The 5 µm thick cross-sections and longitudinal sections zoomed into framed segments. Scale: 1 mm, 200 µm, 50 µm.

3.4. Preservation of the Overall ECM Structure with Minor Disruption of the Endoneurial Tubes

Sciatic nerves of a therapeutically relevant length of 4 cm and 8 cm were decellularized using the newly developed protocol. Immunogenic material could be removed, and the laminin structure was well preserved throughout the large segments as shown previously (Figure 3). However, a minor disruption of the endoneurial tubes could be detected as seen best by hematoxylin and eosin stainings. The ring-like structure of the endoneurial tubes was clearly observable in the magnified hematoxylin and eosin images of the unprocessed tissue, whereas disruption and collapsing of this ring-like structure can be seen in the processed tissue. Additionally, some shrinkage of the tissue and cracks in formation can be observed in processed, but also in unprocessed, segments (Figure 4).

3.5. Decellularization Process Consistently Removes a Significant Proportion of Proteins

Using mass spectrometry, an average 4046 ± 10 proteins could be detected in unprocessed tissue, whereas in decellularized tissue, an average of 2424 ± 292 proteins were detected (Figure 5b). In total, 1078 proteins were no longer detectable in any of the acellular samples. This list of proteins no longer detectable after decellularization contain known inhibitors to axonal regeneration such as reticulon, also known as Nogo, and chondroitin sulfate proteoglycan 4, which was specifically enzymatically removed using chondroitinase ABC during the decellularization process (Table S1). By categorizing detected peptides into subcategories, it can be seen that several peptides from all chosen subcategories are no longer detectable in acellular grafts. Cytoskeleton-associated peptides were significantly reduced from 454 ± 2.7 in unprocessed grafts to 289 ± 28.7 in acellular grafts. The number of peptides associated with axons was significantly reduced from 93 ± 0.4 peptides in unprocessed grafts to 60.8 ± 8.3 in acellular grafts. The 4 ± 0 axon regeneration-associated peptides were detected in unprocessed grafts versus 2.5 ± 0.5 in acellular grafts. Regulation of neuron projection development-associated peptides were significantly reduced

from 68.3 ± 0.4 to 37 ± 5.1 . ECM-associated peptides were significantly reduced from 117.8 ± 0.4 to 85.5 ± 6.3 . Collagen-containing ECM-associated peptides were significantly reduced from 88.8 ± 0.4 to 69 ± 5.6 . Finally, 16 ± 0 peptides associated with the myelin sheath were above the detection limit in unprocessed grafts whereas 14.5 ± 0.5 were detectable after decellularization (Figure 5c).

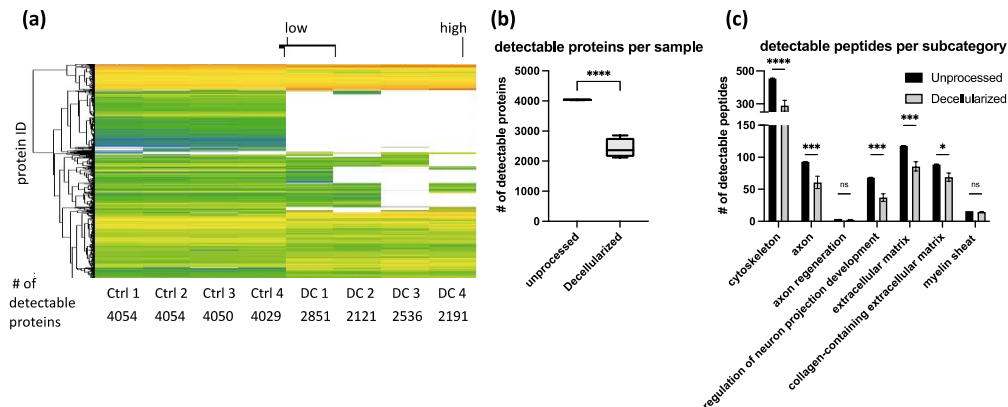


Figure 5. Peptide removal in acellular grafts. Each column represents the protein abundance of one replicate. Ctrl 1–4 are unprocessed samples. DC 1–4 are decellularized samples. (a) Heatmap. In total, 4054 proteins were measured. Each line represents one UniProt ID identifying one protein. green: high abundance of protein in the sample. White: low abundance of protein in the sample. (b) Total number of proteins above detection limit. (c) Number of peptides per subcategory. Subcategories defined by AmiGO2 GO class for *sus scrofa* and UniPort as contributor. The bar plot shows the number of detectable peptides in all replicates in chosen subcategories (cytoskeleton, axon-, axon regeneration, regulation of neuron projection development-, ECM-, collagen-containing ECM, myelin sheath associated peptides). For statistical analysis, Two-way ANOVA was performed. Adjusted p -value: $<0.0001 = ****$, $p < 0.001 = ***$, $p < 0.01 = **$, $p < 0.05 = *$ ns: no significant differences.

3.6. Decellularized Porcine Sciatic Nerves Suitable for Human Cell Transplantation

Isolated hASC were analyzed using flow cytometry; 81% of cells were CD29+CD73+CD90+CD105+ (Figure S1a). These findings were confirmed via immunocytochemistry. Additionally, expression of the MSC marker CD44 was shown via immunocytochemistry stainings (Figure S1b). hASC were injected into decellularized porcine sciatic nerves either in fetal calf serum (FCS) or HPL-supplemented GM. Heparin was added in the latter case to avoid clogging. Cell activity increased within the first 11 days in standard 2D culture and remained constantly high, regardless of the used media. An increase in cellular activity could be observed along 14 days post-transplantation into the graft using HPL-containing media only. In media containing FCS, cellular activity remained constant over the course of the experiment and did not increase or vanish, thus indicating cell survival, but lack of proliferation. The absolute cellular activity of cells cultured in the nerve scaffolds remained below the cellular activity of 2D-cultured cells, regardless of the chosen media (Figure 6a). However, comparing cell activity in 2D- vs. A 3D culture is error-prone due to different growth area/volumes in which cells can grow. Comparing the effect of FCS- versus HPL-containing media did not show any relative difference when cells were cultured in a 2D system. However, when comparing HPL- to FCS-containing media in the nerve scaffolds, a 2.2-fold increase in relative cell activity could be observed within the first 14 days and remained constant until termination of the experiment at day 53 (Figure 6b). Further, acellular grafts can be used as a 3D culture system for embryonic chicken tissue explants as

seen by DRGs and SCS which were cultured for up to 6 days in the acellular grafts. DRGs and SCS can be detected over a distance up to 500 μm by axonal staining (Figure S2).

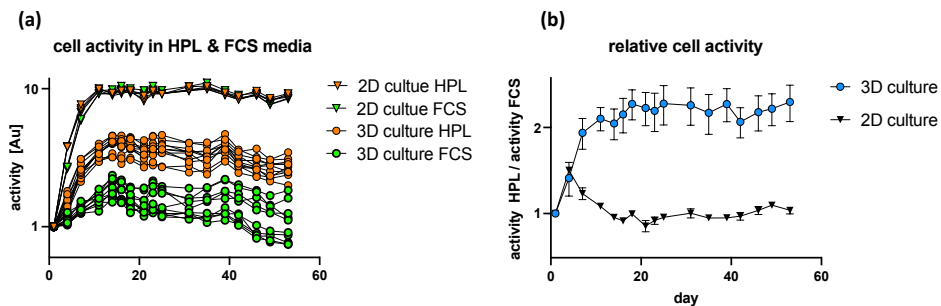


Figure 6. Decellularized nerve as 3D-scaffold for hASC culture. (a) 250k hASC were injected per 3D acellular graft (dots), 10k hASC seeded in 2D-culture well as a control (triangles). Cellular activity was analyzed using resazurin every 3–5 days in media supplemented by 10% FCS (green) or 5% HPL and 2 U/mL heparin (orange). Cell activity normalized to cell activity at day 1 post-transplantation. Triangles represent cell activity in 2D-culture plates and dots represent cell activity in 3D-culture. (b) cell activity regarding FCS- and HPL-supplemented media. Relative cellular activity of hASC cultured in HPL-supplemented media normalized to relative cellular activity of hASC cultured in FCS-supplemented media. Black triangles represent normalized cell activity in 2D culture and blue dots represent normalized cell activity in 3D.

4. Discussion

The objective of this study was to develop and establish a protocol for the efficient removal of immunogenic material from large diameter/longer peripheral nerve segments with only a simultaneous minimal impact on the ECM structure of the nerve. For potential future clinical applications, domestic pigs were chosen as the donor source due to their comparable size to humans. Our study shows that these objectives were achieved by combining various zwitterionic, non-ionic and ionic detergents together with enzymatic treatments. Furthermore, it could be demonstrated that after the decellularization process, the grafts did not show cytotoxicity as demonstrated by human cell studies.

Adapting the protocol previously used for the decellularization of rat sciatic nerve, i.e., 24 h of zwitterionic CHAPS treatment as described by Hudson in 2004, followed by 24 h of treatment using the non-ionic surfactant Span20 required several optimization steps as shown in Figure 2 [16]. Due to the large size and increased amount of connective tissue of porcine sciatic nerves compared to adult rat sciatic nerves, the previous protocol was not efficient in removing immunogenic material such as DNA, axons and myelin (Figure 2, protocol 1). As previously described by Hundepool et al. in 2017, adding enzymatic treatment, such as elastase, helped to remove axons and Schwann cells while preserving the ECM structure [20]. In addition, to improve nerve regeneration, chondroitin sulfate proteoglycans, which inhibit axonal regeneration, were enzymatically degraded using chondroitinase ABC as described by Im et al. in 2019 [25]. Chondroitin sulfate proteoglycan 4 is the only detectable chondroitin sulfate proteoglycan in the unprocessed samples and is completely removed in all four DC samples (Table S1). These enzymatic treatments allowed us to remove the vast majority of axonal debris and DNA without disrupting the ECM structure (Figure 2, protocol 2). To remove the last parts of axonal debris and DNA, the incubation times for CHAPS and Span20 were doubled from 24 h to 48 h to allow the detergents to disperse throughout the several-fold larger segments of pig nerve. By this, axons and DNA were removed entirely from the tissue, but myelin removal was not accomplished with this protocol (Figure 2, protocol 3).

As described in 1983 [26], sodium deoxycholate can be used for the solubilization and extraction of myelin from nerve tissue. As recently reported, sodium deoxycholate has also been used in decellularization [27]. Nevertheless, due to the relatively large size of the tissue and to allow complete perfusion of the detergents, we did not want to reduce treatment duration. With a concentration described previously for the solubilization of myelin and decellularization, myelin removal was highly efficient, and it was no longer detectable after 24 h of treatment. However, the protein denaturing capacities of the anionic sodium deoxycholate disrupted the extracellular structure as indicated by disruption of the laminin structure. After treatment with 4% sodium deoxycholate, the laminin structure found in unprocessed tissue of the endo- pero- and epi-neurium was highly segmented (Figure 2, protocol 4). To reduce the impact on the extracellular structure while maintaining efficient myelin removal, sodium deoxycholate was titrated down from an initial concentration of 40 g/L to a final concentration of 10 mg/L. In this way, myelin removal was still achieved, and undesired ECM damage was significantly reduced (Figure 2, protocol 5).

Thus, the goal of this study was to develop a decellularization protocol for a clinically relevant size of nerve segments. Once an efficient decellularization protocol was established for 1 cm-long segments of the porcine sciatic nerve without any disruption of the ECM structure; further, longer segments of 4 cm and 8 cm were decellularized. It was assumed that given the increased size of the tissue, the active agents would need more time to penetrate the tissue and wash out debris. However, we were able to show that the efficient removal of immunogenic material was successful throughout longer segments. Following signal quantification, we observed residual signal of axonal and myelin signals, but little for DNA (Figure 3). We concluded that the consequence of the further removal of immunogenic material would result in a major disruption of the ECM structure. To confirm our findings, we analyzed the tissue by immunohistochemistry. A previous analysis conducted using antibody staining led to uncertainty. If no positive signal can be detected any longer, we cannot be certain if the extensive decellularization process has led to a removal of the whole protein as targeted or to a disruption of the epitope only. Therefore, by using immunohistochemistry, namely hematoxylin and eosin, as well as Luxol fast blue and Creyl violet staining, we were able to confirm what we observed using immunocytochemistry (Figure 4). Additionally, by the broad staining of the histological stains, we can exclude that the newly developed decellularization protocol acts on single proteins only and that an overall removal of cytoplasmic proteins, nuclei and lipids can be achieved, as well as a preservation of the overall ECM structure and not only laminin. However, it can be observed by laminin staining of the processed tissue that the multilayered perineurium structure is loosened. We hypothesize that this effect is the result of the enzymatic degradation of the elastin within the perineurium by elastase, which is necessary to achieve efficient axonal removal (Figure 3). As tissue shrinkage and crack formation was observed in processed and in unprocessed tissue, we conclude that this arises due to the standard dehydration steps required for paraffin embedding of the tissue and not due to the decellularization process itself (Figure 4). In general, we conclude that the remaining nerve structure should be sufficiently well preserved to act as a guiding structure for elongating axons, blood vessels and cell distribution across the grafts as it resembles the native ECM structure in much greater detail than any of the artificial biological and non-biological nerve guiding conduits used for nerve regeneration applications [28–32].

Peptide removal among repeated decellularization experiments was consistent as evidenced by proteomics analysis (Figure 5). In our optimized protocol, around 1500 proteins were reduced below the detection limit. Categorizing them into clusters of interest showed that peptide removal was not specific to certain categories. Peptides were considered as removed when each of the four decellularized replicates was below the technical detection limit. Proteins that are strongly removed, but still detectable, were not listed as removed (Table S1). Quantitative conclusions about the amount of remaining protein are limited due to the lack of appropriate controls for tissue loss during the decellularization process. The strong impact of the decellularization process on protein content renders impossible a

normalization approach to directly compare the number of single proteins to each other in unprocessed and acellular grafts (Figure 5). For proteomics analysis, only 3 mg of tissue was used per sample. To lower the variability among the samples, complete acellular grafts should be homogenized. By this, artifacts in sample collection could be reduced and variability lowered.

As expected, proteomics analysis revealed partial removal of ECM-associated peptides. However, IHC images confirm the preservation of the overall ECM structure as previously discussed which is crucial as a guiding structure for regenerating axons. Using IHC, laminin was analyzed specifically due to its biological relevance. It has been shown that laminin is crucial for nerve regeneration and remyelination by Schwann cells [33]. Therefore, it is of greatest importance to preserve the laminin structure during decellularization as shown by IHC. Even though direct proof of successful nerve regeneration using our acellular conduits is lacking, efficient nerve reinnervation due to the observed *in vitro* results can be expected.

Based on previous studies, it could be shown that HPL-supplemented media significantly improved the neurotrophic potency of hASC as shown by robust axonal outgrowth *in vitro* [34]. Interestingly we could show that serum supplements have a different impact on cells being cultured in 2D culture or in 3D acellular nerve scaffolds. Whereas cellular activity increased in a comparable manner in 2D culture, regardless of the chosen media composition, HPL-supplemented media had a positive impact on cellular activity in 3D nerve scaffolds, whereas FCS-supplemented media did not induce a rise in cellular activity. We conclude that the experimental design is not sensitive enough at beginning of the experiments for the 2D culture system. Based on the literature, we expected a positive effect of HPL on cell activity in a 2D culture system as well [35]. To increase experimental sensitivity, the starting cell density has to be lowered and cell activity measured more regularly. Combining these findings with the improved neurotrophic potency of hASC by HPL-supplemented media gives us a viable system for future studies of axonal outgrowth and nerve regeneration both *in vitro*, as well as *in vivo*. Additionally, the first proof of biocompatibility was shown by the implantation of human tissue-derived mesenchymal stem cells. Therefore, we can conclude that potentially harmful factors of the decellularization process were sufficiently removed and that the graft could be used for *in vivo* nerve regeneration studies (Figure 6). According to the 3R principle of animal experimentation, we were able to show that by extensive *in vitro* analysis of the remaining factors and structural integrity by immunocytochemistry, immunohistochemistry, proteomics analysis, and biocompatibility by primary human cell implantation, new functional decellularization protocols can be established without the need of animal studies.

During this study, primary experiments were conducted for the implantation of DRG and SCS of chicken embryos to study axonal outgrowth in the acellular graft and to examine the usability of the grafts as a 3D culture system. For this, transplants were placed in a small incision in the graft and held in place by a fibrin hydrogel carrier. Following incubation, fixation, paraffin embedding and sectioning, immunocytochemistry images were taken as described previously in the methods. Based on that, it was expected to detect axonal elongation and compare the axonal elongation rate as an *in vitro* model of axonal regeneration. DAPI and β -tubulin III signaling was clearly detectable at the place of implantation. However, the achieved resolution and the uncertainty of the exact graft implantation site did not allow any conclusion about the axonal signal outside the implant or about axonal elongation. Therefore, no conclusion about the axonal elongation rate can be made (Figure S2). Nevertheless, we can conclude that DRG and SCS implantation can be performed using this experimental setup and that they can survive for several days within the acellular grafts. Of note, quantification of the amount of axonal elongation and an improved analysis adapted to a 3D system is necessary. By this, we expect that the acellular 3D grafts can be used to study axonal outgrowth as previously shown in a 2D *in vitro* setup [34].

We are aware that the lack of *in vivo* animal studies is a limitation of our work and would allow a more direct conclusion about biocompatibility, particularly axonal outgrowth

and the regain of motor and sensory function and behavior outcome. However, the need for large animals required for large nerve gap studies with human nerve-sized implants and the resulting costs and ethical concerns makes it even more important for newly developed decellularization protocols to be improved and tested extensively in vitro before translating to in vivo studies.

5. Conclusions

Our study reports a protocol for efficient decellularization of larger segments of porcine peripheral nerves. It was shown that DC protocols established in a rodent model require substantial adaptations for being efficient in large segments of porcine nerves. Based on extended in vitro optimization and testing, a protocol was developed which allows immunogenic material removal while preserving the overall nerve structure. Proteomic analysis and cell culture experiments indicate biocompatibility of the acellular graft and suitability for application in transplantation studies. Furthermore, recellularization of acellular porcine nerve grafts with autologous hASC and autologous HPL may open a new option for in vitro generation of a functional, non-immunogenic personalized nerve graft circumventing the major drawbacks associated with autologous nerve grafting.

Supplementary Materials: The following supporting information can be downloaded at: <https://www.mdpi.com/article/10.3390/bioengineering9090412/s1>, Figure S1: hASC characterization; Figure S2: chicken Spinal Cord Segment and Dorsal Root Ganglion transplantation; Table S1: proteins removed below detection limit by decellularization in all replicates.

Author Contributions: S.M. designed the research, acquired the funding and supervised the project; A.H. and L.A.-B., conducted the experiments; S.M., D.J.S., D.F.K., R.G., L.A.-B. and A.H., organized the materials and database; A.H. collected the data, performed the statistical analysis and wrote the first draft of the manuscript; S.M. revised the manuscript. All authors have read and agreed to the published version of the manuscript.

Funding: This research was funded by EUROSTARS, grant number E!10668 to Madduri Srinivas.

Informed Consent Statement: Informed consent was obtained from the subjects undergoing elective liposuction for isolation and purification of hASC.

Data Availability Statement: Raw Data of mass spectrometry experiments are accessible via MassIVE: <ftp://MSV000090072@massive.ucsd.edu> (accessed on 1 August 2022), username: "MSV000090072_reviewer", password: "Decellularized".

Acknowledgments: We thank the Center for Surgical Research, University of Zurich for kind help and support for collecting the peripheral nerves from post mortem pigs. Further, we thank Michael Abanto and Loic Sauter of the DBM Microscopy Core Facility, University of Basel, for their kind help and excellent technical support. Additionally, we thank Klemens Fröhlich from the Proteomics Core Facility, University of Basel, for the proteomics analysis.

Conflicts of Interest: The authors declare no conflict of interest.

References

1. Daly, W.T.; Yao, L.; Abu-rub, M.T.; O'Connell, C.; Zeugolis, D.I.; Windebank, A.J.; Pandit, A.S. The Effect of Intraluminal Contact Mediated Guidance Signals on Axonal Mismatch during Peripheral Nerve Repair. *Biomaterials* **2012**, *33*, 6660–6671. [\[CrossRef\]](#) [\[PubMed\]](#)
2. Navarro, X.; Vivó, M.; Valero-Cabré, A. Neural Plasticity after Peripheral Nerve Injury and Regeneration. *Prog. Neurobiol.* **2007**, *82*, 163–201. [\[CrossRef\]](#)
3. Griffin, J.W.; Hogan, M.V.; Chhabra, A.B.; Deal, D.N. Peripheral Nerve Repair and Reconstruction. *J. Bone Jt. Surg.* **2013**, *95*, 2144–2151. [\[CrossRef\]](#)
4. Sunderland, S. Factors Influencing the Course of Regeneration and the Quality of the Recovery after Nerve Suture. *Brain* **1952**, *75*, 19–54. [\[CrossRef\]](#)
5. Pfister, B.J.; Gordon, T.; Loverde, J.R.; Kochar, A.S.; Mackinnon, S.E.; Cullen, D.K. Biomedical Engineering Strategies for Peripheral Nerve Repair: Surgical Applications, State of the Art, and Future Challenges. *Crit. Rev. Biomed. Eng.* **2011**, *39*, 81–124. [\[CrossRef\]](#)
6. Lee, S.K.; Wolfe, S.W. Peripheral Nerve Injury and Repair. *J. Am. Acad. Orthop. Surg.* **2000**, *8*, 243–252. [\[CrossRef\]](#)

7. Moore, A.M.; MacEwan, M.; Santosa, K.B.; Chenard, K.E.; Ray, W.Z.; Hunter, D.A.; Mackinnon, S.E.; Johnson, P.J. Acellular Nerve Allografts in Peripheral Nerve Regeneration: A Comparative Study. *Muscle Nerve* **2011**, *44*, 221–234. [\[CrossRef\]](#)
8. Ray, W.Z.; Mackinnon, S.E. Management of Nerve Gaps: Autografts, Allografts, Nerve Transfers, and End-to-Side Neuroorrhaphy. *Exp. Neurol.* **2010**, *223*, 77–85. [\[CrossRef\]](#)
9. Houdek, M.T.; Shin, A.Y. Management and Complications of Traumatic Peripheral Nerve Injuries. *Hand Clin.* **2015**, *31*, 151–163. [\[CrossRef\]](#)
10. Zhang, X.; Chen, X.; Hong, H.; Hu, R.; Liu, J.; Liu, C. Decellularized Extracellular Matrix Scaffolds: Recent Trends and Emerging Strategies in Tissue Engineering. *Bioact. Mater.* **2021**, *10*, 15–31. [\[CrossRef\]](#)
11. Hiles, R.W. Freeze Dried Irradiated Nerve Homograft: A Preliminary Report. *Hand* **1972**, *4*, 79–84. [\[CrossRef\]](#)
12. Sondell, M.; Lundborg, G.; Kanje, M. Regeneration of the Rat Sciatic Nerve into Allografts Made Acellular through Chemical Extraction. *Brain Res.* **1998**, *795*, 44–54. [\[CrossRef\]](#)
13. Crapo, P.M.; Gilbert, T.W.; Badylak, S.F. An Overview of Tissue and Whole Organ Decellularization Processes. *Biomaterials* **2011**, *32*, 3233–3243. [\[CrossRef\]](#)
14. Gilbert, T.W.; Sellaro, T.L.; Badylak, S.F. Decellularization of Tissues and Organs. *Biomaterials* **2006**, *27*, 3675–3683. [\[CrossRef\]](#) [\[PubMed\]](#)
15. Gilpin, A.; Yang, Y. Decellularization Strategies for Regenerative Medicine: From Processing Techniques to Applications. *BioMed Res. Int.* **2017**, *2017*, 9831534. [\[CrossRef\]](#) [\[PubMed\]](#)
16. Hudson, T.W.T.; Zawko, S.; Deister, C.; Lundy, S.; Hu, C.C.Y.; Lee, K.; Schmidt, C.E.C. Optimized Acellular Nerve Graft Is Immunologically Tolerated and Supports Regeneration. *Tissue Eng.* **2004**, *10*, 1641–1651. [\[CrossRef\]](#) [\[PubMed\]](#)
17. Graham, J.B.; Muir, D. Chondroitinase C Selectively Degrades Chondroitin Sulfate Glycosaminoglycans That Inhibit Axonal Growth within the Endoneurium of Peripheral Nerve. *PLoS ONE* **2016**, *11*, e0167682. [\[CrossRef\]](#)
18. McKerracher, L.; Rosen, K.M. MAG, Myelin and Overcoming Growth Inhibition in the CNS. *Front. Mol. Neurosci.* **2015**, *8*, 51. [\[CrossRef\]](#)
19. Kim, J.K.; Koh, Y.-D.; Kim, J.O.; Seo, D.H. Development of a Decellularization Method to Produce Nerve Allografts Using Less Invasive Detergents and Hyper/Hypotonic Solutions. *J. Plast. Reconstr. Aesthet. Surg.* **2016**, *69*, 1690–1696. [\[CrossRef\]](#)
20. Hundepool, C.A.; Nijhuis, T.H.J.; Kotsougiani, D.; Friedrich, P.F.; Bishop, A.T.; Shin, A.Y. Optimizing Decellularization Techniques to Create a New Nerve Allograft: An in Vitro Study Using Rodent Nerve Segments. *Neurosurg. Focus* **2017**, *42*, E4. [\[CrossRef\]](#)
21. Bae, J.Y.; Park, S.Y.; Shin, Y.H.; Choi, S.W.; Kim, J.K. Preparation of Human Decellularized Peripheral Nerve Allograft Using Amphoteric Detergent and Nuclease. *Neural Regen. Res.* **2021**, *16*, 1890–1896. [\[CrossRef\]](#) [\[PubMed\]](#)
22. Prautsch, K.M.; Degrugillier, L.; Schaefer, D.J.; Guzman, R.; Kalbermatten, D.F.; Madduri, S. Ex-Vivo Stimulation of Adipose Stem Cells by Growth Factors and Fibrin-Hydrogel Assisted Delivery Strategies for Treating Nerve Gap-Injuries. *Bioengineering* **2020**, *7*, 42. [\[CrossRef\]](#) [\[PubMed\]](#)
23. Powell, S.; Vinod, A.; Lemons, M.L. Isolation and Culture of Dissociated Sensory Neurons from Chick Embryos. *J. Vis. Exp.* **2014**, *91*, e51991. [\[CrossRef\]](#) [\[PubMed\]](#)
24. Prautsch, K.M.; Schmidt, A.; Paradiso, V.; Schaefer, D.J.; Guzman, R.; Kalbermatten, D.F.; Madduri, S. Modulation of Human Adipose Stem Cells' Neurotrophic Capacity Using a Variety of Growth Factors for Neural Tissue Engineering Applications: Axonal Growth, Transcriptional, and Phosphoproteomic Analyses In Vitro. *Cells* **2020**, *9*, 1939. [\[CrossRef\]](#)
25. Im, J.H.; Lee, J.Y.; Lee, S.; Lee, M.G.; Chung, Y.G.; Kim, K.W. Comparison of the Regeneration Induced by Acellular Nerve Allografts Processed with or without Chondroitinase in a Rat Model. *Cell Tissue Bank* **2019**, *20*, 307–319. [\[CrossRef\]](#)
26. Riccio, P.; Simone, S.M.; Cibelli, G.; De Santis, A.; Bobba, A.; Livrea, P.; Quagliariello, E. Solubilization of Myelin Proteins By Detergents. *Struct. Funct. Membr. Proteins* **1983**, *11*, 361–364. [\[CrossRef\]](#)
27. McCrary, M.W.; Vaughn, N.E.; Hlavac, N.; Song, Y.H.; Wachs, R.A.; Schmidt, C.E. Novel Sodium Deoxycholate-Based Chemical Decellularization Method for Peripheral Nerve. *Tissue Eng Part C Methods* **2020**, *26*, 23–36. [\[CrossRef\]](#)
28. Lee, S.J.; Esworthy, T.; Stake, S.; Miao, S.; Zuo, Y.Y.; Harris, B.T.; Zhang, L.G. Advances in 3D Bioprinting for Neural Tissue Engineering. *Adv. Biosyst.* **2018**, *2*, 1700213. [\[CrossRef\]](#)
29. Pateman, C.J.; Harding, A.J.; Glen, A.; Taylor, C.S.; Christmas, C.R.; Robinson, P.P.; Rimmer, S.; Boissonade, F.M.; Claeysens, F.; Haycock, J.W. Nerve Guides Manufactured from Photocurable Polymers to Aid Peripheral Nerve Repair. *Biomaterials* **2015**, *49*, 77–89. [\[CrossRef\]](#)
30. Johnson, B.N.; Lancaster, K.Z.; Zhen, G.; He, J.; Gupta, M.K.; Kong, Y.L.; Engel, E.A.; Krick, K.D.; Ju, A.; Meng, F.; et al. 3D Printed Anatomical Nerve Regeneration Pathways. *Adv. Funct. Mater.* **2015**, *25*, 6205–6217. [\[CrossRef\]](#)
31. Kim, S.H.; Yeon, Y.K.; Lee, J.M.; Chao, J.R.; Lee, Y.J.; Seo, Y.B.; Sultan, M.T.; Lee, O.J.; Lee, J.S.; Yoon, S.-I.; et al. Precisely Printable and Biocompatible Silk Fibroin Bioink for Digital Light Processing 3D Printing. *Nat. Commun.* **2018**, *9*, 1–14. [\[CrossRef\]](#)
32. Weng, B.; Liu, X.; Shepherd, R.; Wallace, G.G. Inkjet Printed Polypyrrole/Collagen Scaffold: A Combination of Spatial Control and Electrical Stimulation of PC12 Cells. *Synth. Met.* **2012**, *162*, 1375–1380. [\[CrossRef\]](#)
33. Chen, Z.L.; Strickland, S. Laminin Gamma1 Is Critical for Schwann Cell Differentiation, Axon Myelination, and Regeneration in the Peripheral Nerve. *J. Cell Biol.* **2003**, *163*, 889–899. [\[CrossRef\]](#)

-
34. Lischer, M.; di Summa, P.G.; Oranges, C.M.; Schaefer, D.J.; Kalbermatten, D.F.; Guzman, R.; Madduri, S. Human Platelet Lysate Stimulated Adipose Stem Cells Exhibit Strong Neurotrophic Potency for Nerve Tissue Engineering Applications. *Regen. Med.* **2020**, *15*, 1399–1408. [[CrossRef](#)] [[PubMed](#)]
 35. Kakudo, N.; Morimoto, N.; Ma, Y.; Kusumoto, K. Differences between the Proliferative Effects of Human Platelet Lysate and Fetal Bovine Serum on Human Adipose-Derived Stem Cells. *Cells* **2019**, *8*, 1218. [[CrossRef](#)] [[PubMed](#)]

Outlook

As previously described, clinical success of peripheral nerve repair and replacement depends on various factors such as a biological active conduit and the availability of growth factors secreted by SCs. During this project, an acellular nerve graft was developed which supports cell engrafting and long-term survival and is expected to support axonal regeneration in clinical settings. The used decellularization steps were all previously tested and established in various decellularization protocols. Based on the previously described Hudson method we used several steps of anionic, zwitterionic, hypertonic and hypotonic solutions. The Hudson method became state of the art as first used in clinical settings. However, further improvements were developed over time. Using hypertonic and hypotonic solutions to disrupt cellular structures by osmotic pressure are described as less ECM disruptive but still efficient decellularization detergents⁴⁵. Further, the addition of enzymatic degradation steps was successful in targeted elimination of certain proteins and molecules which resulted in improved removal of cellular compartments and improved nerve regeneration. The addition of elastase improved axonal removal and reduced immunogenicity⁴⁶. Addition of chondroitinase ABC improved axonal elongation in subsequent transplantations⁴⁷. This study demonstrated that the combination of less invasive detergents, targeted enzymatic degradation over an extended period of time removed cellular compartments, reduced immunogenicity and was overall beneficial for cell engrafting and survival. Compared to the Hudson method, myelin removal was even more efficient and the preservation of the basal lamina comparable. One of the main components of the cellular membrane facing basal lamina is laminin⁴⁸. The preservation of the basal lamina is necessary to support SC and direct axonal sprouting⁴⁹. Further it could be shown that without laminin, SC cannot differentiate into a myelinating phenotype⁵⁰. Fragmentation of the basal lamina can be directly correlated to reduced reinnervation⁵¹. Therefore, it is of greatest importance to preserve the laminin structure during decellularization as shown in this study. Even though we lack direct prove of successful nerve regeneration using our acellular conduits we do expect efficient nerve reinnervation due to observed *in-vitro* results. However, final immunogenicity examination and axonal regeneration efficiency must be investigated *in-vivo*, preferably in farm animal suitable for large gap neurectomy and conduit transplantation.

However, the current gold standard for nerve replacement, the autograft still holds one great advantage. This is the presence of SCs which are crucial for efficient axonal elongation and reinnervation over larger distances by providing necessary growth factors. Therefore, there is a great interest of seeding SCs into acellular graft. It has been shown that murine SC transplantation

into acellular nerve graft could improve functional recovery after peripheral nerve defects in mice⁵². Autologous SC injection in human spinal cord injuries led to increased recovery in patients motor, sensory and autonomic measures⁵³. However, despite the evidence of therapeutic potential of SCs transplantation regarding promoting of axonal regeneration and myelination in the peripheral and the central nervous system, the harvest of SCs holds almost the same limitations as the use of autografts, i.e. the required sacrifice of an healthy nerve and the following functional impairment⁵⁴. Additionally, the isolation, culture and purification of primary human SCs is challenging due to their limited *in-vitro* proliferation capacity and the frequent contamination by fast expanding fibroblasts^{16,55,56}. However, SC-like cells which have comparable nerve regeneration potential can be differentiated from various other cell types such as pluripotent cells, namely induced pluripotent stem cells and embryonic stem cells and adult stem cells such as MSCs, neural crest stem cells and skin-derived precursory cells which can be isolated and expanded facing smaller challenges. Therefore, as part of this project a systemic review was written: „Schwann Cell-Like Cells: Origin and Usability for Repair and Regeneration of the Peripheral and Central Nervous System” which summarize different sources and methods of SC-like cells differentiation which potentially overcome the limitations of primary human SC and describes the state of research regarding clinical application¹. For clinical application of nerve allografts recellularized by SC-like cells, the cells need to distribute and engraft homogenously throughout the tissue. The most common recellularization technique for acellular nerve grafts, by direct microinjection leads to cell aggregation, poor engraftment and insufficient distribution throughout the scaffold as shown in acellular lungs, liver and heart valves⁵⁷. Seeding by perfusion within a bioreactor leads to better distribution among the scaffold and enhanced cell engraftment⁵⁸. However, which recellularization technique is the most favourable depends on the organ and the seeded cell types.

Recellularization of pig derived acellular nerve grafts with human derived SC-like cells has not yet been investigated, thus, this is a crucial future step of this project to proceed to clinical application.



Review

Schwann Cell-Like Cells: Origin and Usability for Repair and Regeneration of the Peripheral and Central Nervous System

Alois Hopf ^{1,2}, Dirk J. Schaefer ^{2,3} , Daniel F. Kalbermatten ^{1,3}, Raphael Guzman ^{2,4} and Srinivas Madduri ^{1,2,3,*}

¹ Department of Biomedical Engineering, University of Basel, Gewerbestrasse 14, 4123 Allschwil, Switzerland; aloisc.hopf@unibas.ch (A.H.); Daniel.Kalbermatten@usb.ch (D.F.K.)

² Department of Biomedicine, University Hospital Basel, Hebelstrasse 20, 4031 Basel, Switzerland; Dirk.Schaefer@usb.ch (D.J.S.); Raphael.Guzman@usb.ch (R.G.)

³ Department of Plastic, Reconstructive, Aesthetic and Hand Surgery, University Hospital Basel, University of Basel, Spitalstrasse 21, 4031 Basel, Switzerland

⁴ Department of Neurosurgery, University Hospital Basel, Spitalstrasse 21, 4031 Basel, Switzerland

* Correspondence: srinivas.madduri@usb.ch; Tel.: +41-0061-556-5049

Received: 8 June 2020; Accepted: 22 August 2020; Published: 29 August 2020



Abstract: Functional recovery after neurotmesis, a complete transection of the nerve fiber, is often poor and requires a surgical procedure. Especially for longer gaps (>3 mm), end-to-end suturing of the proximal to the distal part is not possible, thus requiring nerve graft implantation. Artificial nerve grafts, i.e., hollow fibers, hydrogels, chitosan, collagen conduits, and decellularized scaffolds hold promise provided that these structures are populated with Schwann cells (SC) that are widely accepted to promote peripheral and spinal cord regeneration. However, these cells must be collected from the healthy peripheral nerves, resulting in significant time delay for treatment and undesired morbidities for the donors. Therefore, there is a clear need to explore the viable source of cells with a regenerative potential similar to SC. For this, we analyzed the literature for the generation of Schwann cell-like cells (SCLC) from stem cells of different origins (i.e., mesenchymal stem cells, pluripotent stem cells, and genetically programmed somatic cells) and compared their biological performance to promote axonal regeneration. Thus, the present review accounts for current developments in the field of SCLC differentiation, their applications in peripheral and central nervous system injury, and provides insights for future strategies.

Keywords: Schwann cells; Schwann cell-like cells; human adipose stem cells; neurotrophic factors; peripheral nerve injuries; spinal injuries; brain injuries; axonal regeneration; myelin regeneration

1. Introduction

Every year about 1 million people suffer from peripheral nerve injuries (PNI) worldwide [1,2]. In the case of simple nerve transection, end-to-end suturing is sufficient. However, long-gap nerve injuries that are not amenable with end-to-end suturing result in a significant clinical challenge. For this, autologous nerve transplantation is the current clinical gold standard [1,2], where the regenerating axons are supported optimally by endogenous physical and biological guiding scaffold. However, autologous nerve grafts are associated with several drawbacks, such as limited donor sites, modality mismatch, and co-morbidities, i.e., neuroma formation [3–5]. Within this context, bio-engineered nerve grafts combining physical guidance structures with neurotrophic cells, guidance cues, and signaling molecules provide an innovative and viable option for treating PNI [6]. There is growing evidence for the therapeutic potential of Schwann cells (SC) transplantation for promoting axonal regeneration

and myelination in the peripheral and central nervous system (CNS) following injury [7,8]. In spite of the promising outcome, the harvest of autologous SC represents almost the same limitations that are associated with autologous nerve grafting, i.e., healthy nerve surgical harvest and related functional impairment [9]. Further isolation, culture, and purification has been shown to be challenging due to the limited expansion potential of SCs and frequent contamination with rapidly proliferating fibroblasts [10–13]. Therefore, a viable option would be to generate Schwann cell-like cells (SCLCs) from different sources with reduced limitations [10]. Thus, the need for stem cell-derived SCLC has evolved. For this, cells with self-renewal capacity, multi-lineage potential, and low immunogenicity are highly suitable. Additionally, cells that are easily accessible with abundant quantities become furthermore attractive. Thus, there is a great need for developing new strategies for the generation of therapeutic SCLC using stem cells of different origins (Figure 1 and Table 1).

1.1. Schwann Cell Development and Homeostasis

SCs are the glial cells of the peripheral nervous system (PNS), named after Theodor Schwann, one of the founders of the cell theory. Ramon y Cajal in 1928 concluded, among others like Ranvier and Waller, that axonal recovery in the PNS is a result of axo-glial bidirectional interaction [14]. Nowadays, SCs are recognized as one of the largest, ultra-structurally most complex cells in the body. However, they are still capable of rapid transformation in development and injury [15]. SCs originate from migrating neural crest cells. In vivo differentiation of neural crest into the SC lineage has not been fully elucidated. However, it is known that the transcription factor SRY-Box Transcription Factor 10 (SOX10) is an essential master regulator for generating the earliest cells in the SC lineage, as reviewed by Mirsky in 2008 [16]. During the development, SCs are associated with a bundle of axons and release a variety of neurotrophic factors, such as nerve growth factor (NGF), brain-derived neurotrophic factor (BDNF), glial cell line-derived neurotrophic factor (GDNF), and neurotrophin 3 (NT3), which are involved in axonal growth and pathfinding. By proliferation and extensive extension of SC structures, axons are segregated into smaller bundles in a process called radial sorting. Most of the small-diameter axons, including many sensory and autonomous axons, remain in such bundle associated with non-myelinating Remak SCs. In contrast to the CNS, single Remak SC wraps a single axon in PNS. Remak SCs remain proliferative throughout life and express several markers typically found in developing SCs, such as neural cell adhesion molecule (NCAM), p75 neurotrophin receptor (p75NTR), and glial fibrillary acid protein (GFAP) [17,18]. Radial sorting of large-diameter axons, including some sensory and many motor axons, proceeds until one SC surrounds one axon. Such SCs wrap myelin structures around the axons, resulting in the formation of mature myelin sheath [19]. Differentiation of myelinating SCs is controlled by the Krox20 transcription factor (Egr2), as evidenced by the inability of Krox20 deficient mice to form myelin sheaths in vitro and in vivo [15,20,21].

1.2. PNS Injury

SCs distal to the injury site lose their contact with axons following injury and undergo significant changes in their signaling environment due to missing contact with axonal-derived factors. Macrophages invade the injury site in large quantities and release a wide range of cytokines that will further influence the SC [10]. The hypoxic environment within the damaged nerve induces vascular endothelial growth factor A (VEGF-A) secretion by macrophages, resulting in the polarized vascularization, which, in turn, guides the SCs to bridge the nerve gap [22]. Following these changes within the injury microenvironment, the fully differentiated non-myelinating Remak SC as well as the myelinating SC converse to a repair SC phenotype [23]. Thus, the SC phenotype transition activates cellular mechanisms resembling developmental molecular sequences, such as up-regulation of neurotrophic factors (NTF), i.e., NGF, BDNF, ciliary neurotrophic factor (CNTF), NT3, extracellular matrix (ECM) proteins (laminin 1 and 2, and fibronectin), and NCAM, for regulating neuronal survival and axonal regeneration [24–27]. Further, SCs regulate self-renewal and survival by autocrine signaling, e.g., insulin-like growth factor 2 (IGF-2), platelet-derived growth factor (PDGF-BB), neurotrophin-2

(NT2), and leukemia inhibitory factor (LIF) [28]. By cellular elongation and branching, SCs form so-called bands of Büngner, “cellular tracks” in which axons can regenerate. This transition is further required for myelin autophagy and to secrete cytokines that attract the macrophages for later stages of myelin clearance [29]. These repaired SCs navigate the regenerating axons and remain functioning for a long time, often for months or even years in humans due to the slow axonal growth (i.e., <3 mm/day) [21]. Further, several studies have demonstrated that SC transplantation support functional axonal outgrowth in vitro and In vivo following injury [30–32].

1.3. CNS Injury

Myelin debris, astrocytes, and oligodendrocytes (OC) collectively become strong inhibitors of axonal regeneration in the CNS following injuries [33]. Myelin in the CNS is produced by OCs in contrast to PNS and contains inhibitory molecules, such as Nogo, OC-myelin glycoprotein, and myelin-associated glycoprotein (MAG). These molecules bind to Nogo receptors on the distal tip of regenerating axons to transmit inhibitory signals [34]. In contrast to SCs in the PNS, OCs in the CNS depend on an axonal-derived signal for survival. Therefore, OCs undergo apoptosis or enter a quiescent state after injury [35], resulting in reduced myelin clearance in the CNS. Remaining myelin can be found up to 22 months post-injury in a rat optic nerve injury model [36]. In addition to the uncleared myelin and associated inhibitory molecules, astrocytes start proliferating and extend their processes, resulting in the formation of astroglial scar that inhibits axonal regeneration physically and chemically [37,38]. One of those, monocyte chemoattractant protein-1 (MCP-1), promotes the recruitment of proinflammatory macrophages, releasing tumor necrosis factor α (TNF- α) and inducible nitric acid synthase (iNOS) [39]. TNF- α increases local expression of caspases, leading to apoptosis, and iNOS promotes the apoptosis of the damaged neuron. This process becomes inhibitory for the axonal regrowth over a prolonged period [40,41]. However, spontaneous regeneration of myelin sheaths often occurs following CNS demyelination, mainly by the differentiation of oligodendrocyte precursor cells (OPC) into myelinating OCs or SCs. Normally SCs are neither present in CNS nor migrate into the CNS due to mutual exclusivity of SCs and astrocytes [42,43]. Based on the earlier findings revealing the SCs presence and their myelin regeneration within the niche of spinal cord injury (SCI) of rodents as well as humans, it was concluded that SCs migrate into SCI niche from the periphery after the disruption of the astrocyte-SC exclusivity [42,44–47]. However, recent findings suggest that SCs from the PNS rarely enter the remyelinating spinal cord, but the vast majority of the SCs are derived from endogenous OPC [48,49]. The signals instructing the OPC differentiation into myelinating OC or myelinating SC are released by reactive astrocytes. Within this context, the inhibition of astrocyte activation has resulted in enhanced SC-myelination in contrast to OC-myelination [50]. Following demyelination, activated OPC and endothelial cells release ligands for bone morphogenetic protein (BMP) and Wnt signaling pathways, whereas reactive astrocytes release the BMP/Wnt antagonist *Soc1*. The BMP/Wnt signaling balance instructs OPC fate decisions shortly after activation. In the absence of *Soc1*, OPCs differentiation into SCs is favored within the astrocyte-free zone [51].

Chronic stage SCI in humans often results in schwannosis, which is an aberrant growth of SCs and nerve fibers in the CNS. Schwannosis impedes effective axonal outgrowth and promotes aberrant axonal growth, leading to pain, spasticity, and other abnormal responses in the patients suffering from chronic SCI [52]. In more than 80% of cases, patients with chronic SCI (i.e., >4 months) exhibit schwannosis in contrast to acute SCI [53]. Therefore, gaining a better understanding of endogenous SCs regulation may help developing new treatment strategies.

1.4. SC Transplantation

1.4.1. SC Transplantation in the PNS

Seddon first described autologous peripheral nerve grafting in 1947. He was the first to use autologous sensory nerve grafts for bridging the gaps in the peripheral nervous system [1], although

this procedure is associated with important drawbacks, such as sensory loss at the donor site, neuroma formation, and lack of sufficient graft material. Nonetheless, autologous nerve grafting has become the gold standard to treat long gap peripheral nerve injuries. There is a growing interest in the field for developing a viable alternative, as evidenced by 11 Food and Drug Administration (FDA)-approved nerve conduit devices and several in further development [2]. Although nerve conduits appear to enhance nerve regeneration in short gaps, it is increasingly difficult for supporting long-gap nerve injuries [3]. Therefore, functionalizing the nerve conduits with a variety of growth-promoting substrates has been widely considered for enhancing their biological function [4]. Within this context, the first successful SC transplantation in a rat model was demonstrated back in 1992 by Guenard et al. Transplantation of in vitro expanded SCs results in the axonal regeneration and myelin formation in a sciatic nerve injury model [5]. Further, the nerve conduit seeded with human SCs supports repair and regeneration of a 5 mm nerve gap injury in mice. Interestingly, transplanted human SCs survive for at least 6 weeks and form myelin around the regenerating axons [6]. Since then, several studies have demonstrated the benefits of SC transplantation for peripheral nerve regeneration in the variety of animal models. Applications of SCs and nerve conduits for treating nerve injuries was recently reviewed by Han et al., in 2019 [7]. Furthermore, successful autologous SC transplantation in humans was reported for the first time in 2016. Human SCs are isolated from the sural nerve as well as from the injured sciatic nerve stump and combined with a sural nerve graft to repair a 7.5 cm long sciatic nerve. For this, the cells are expanded in vitro for 7 days and incorporated into an autologous sural nerve graft for implantation. Patients treated with SCs-enriched nerve grafts restore significant sensory and motor functions, indicating the safety and feasibility of SCs clinical translation [4].

1.4.2. SC Transplantation in the CNS

An attractive option for CNS regeneration is to adopt and acquire the favorable properties of peripheral nerves, i.e., grafting of SC to revert scar formation and to promote axonal regeneration. Back in 1928, Ramon y Cajal, for the first time, demonstrated the potential of peripheral nerve transplantation to regenerate spinal axons. Further, he suggested that SCs could be used to overcome the non-permissive environment and to enable axonal regeneration [14]. In 1975, when techniques for glial cell isolation and purification were developed, Richard Bunge suggested the use of purified SC for the repair of the central nervous system. Richardson et al. in 1980 demonstrated the spinal axonal ingrowth into the transplanted peripheral nerve graft using an adult rat SCI model [54]. Since then, the beneficial effects of SC transplantation have been demonstrated by several studies for the repair and regeneration of axons in the CNS [55–57]. Transplanted SCs are capable of promoting remyelination and functional restoration [45,58]. As described previously, SCs express a multitude of factors, such as NGF, NT3, BDNF, fibroblast growth factor (FGF), GDNF, and CNTF, as well as ECM proteins—laminin and fibronectin, which are crucial for axonal growth and elongation [59,60]. In contrast to OCs in the CNS, SCs produce myelin sheaths, which is unlikely to be the target of an autoimmune reaction underlying autoimmune disease, such as multiple sclerosis (MS). In 2001, a phase 1 clinical trial was initiated at Yale University for treating five MS patients with SCs. However, the trial was terminated after the third patient due to the lack of evidence for the therapeutic benefits (myelination) of transplanted SCs [61]. Moreover, the inability of post-natal SC to migrate through normal white matter or astrocytes rich areas, such as glial scars, further limits the SCs therapy for MS patients [62]. Within this context, embryonic SC precursor cells exhibit enhanced migration to demyelinated lesion sites in a rat model and improve myelin regeneration [63]. In an alternative approach, genetic modification of adult SCs' adhesion properties results in effective migration, which, in turn, improves myelin regeneration and functional restoration in rats with SCI [64,65]. Thereby, modified SCs hold the potential for demyelinating diseases [42]. Even though there is growing evidence for the therapeutic potential of SCs for treating CNS, their clinical transition is still challenging. As described by Bunge in 2016, the need for combinatorial strategies has emerged for treating SCI due to the secondary tissue damage, cell death, inflammation, scar formation, inhibitory factors, and silenced

axons [66]. Within this context, various co-treatment strategies were developed in the Bunge lab in an attempt to increase the therapeutic efficacy of SC for CNS repair. Those include steroids, neurotrophins, enzymes, cyclic AMP, and olfactory ensheathing cells [67–71]. Furthermore, genetically modified SCs for their neurotrophic potency have resulted in increased neurotrophin release and enhanced functional axonal regeneration [72–74]. Thus, the combinatorial treatment approaches have positively increased the quality and quantity of axonal regeneration, remyelination, and functional recovery, i.e., loco-motor outcome of paralyzed rats [66]. These topics were reviewed in great detail by Fortun et al., in 2009, Tetzlaff et al., in 2011, and Griffin et al., in 2020 [75–77].

1.5. Biomaterial/Scaffolds

Effective regeneration of severed nerves largely depends on the injury size. The end-to-end suturing is feasible for small gap injuries. However, there exists a critical nerve gap length, allowing neither spontaneous regeneration nor end-to-end suturing. End-to-end suturing of large nerve gaps (>3 mm) leads to tension between the nerve segments and is often associated with poor outcomes [78]. Implantation of nerve auto or allograft can bridge such large gap injuries. However, these are coming with the aforementioned drawbacks, such as donor site morbidity, functional impairment, and immunological complications in the latter case. Therefore, there is an increased research focus on developing artificial nerve conduits. An ideal nerve conduit incorporates several attributes, such as biocompatibility, biodegradable, flexibility, stability, and bio-inspired functional design. Sarker et al. recently reviewed advancements in the field of artificial nerve conduits. In this review, varying structures from simple hollow tubes to complex conduits incorporating cells and bioactive molecules mimicking the autologous nerve were detailed and discussed. Shortly, it concludes that cell loaded nerve conduits possess superior biological performance over hollow structures, and SCs outperform among a wide variety of cells that are under investigation for nerve regeneration [79].

1.6. Immunosuppression Following PNI and SCI

Considerable evidence has been shown for the therapeutic potential of SC and stem cell transplantation in PNI and SCI. However, the downside of using non-autologous cells is immune rejection. Therefore, the efficiency of non-autologous cell transplantation relies on effective immune-suppressive drugs. Several studies have evaluated tacrolimus (FK506) and cyclosporine (cyclosporine A or CsA) as main adjuvants for stem cell transplantation. Tacrolimus is commercially available and is widely used for transplantation procedures. Its mode of action relies primarily on inhibition of T-lymphocyte proliferation. Similar to tacrolimus, cyclosporine inhibits T-cell activation. It has been shown that systematic cyclosporine, as well as tacrolimus administration, significantly reduces T-cell infiltration into allografts, resulting in the enhanced therapeutic efficacy of transplanted cells in PNI and SCI [80]. Furthermore, it has been shown that tacrolimus induces SC proliferation, which, in return, triggers axonal regeneration [81]. Sosa et al. reviewed the neuroprotective effects and functional recovery after PNI and SCI in response to cyclosporine and tacrolimus, in 2005 [82]. Numerous preclinical studies have investigated the use of tacrolimus and cyclosporine in an allogeneic stem cell transplantation for treating SCI, as reviewed by Antonios et al. in 2019 [41].

2. Origin and Therapeutic Effects of Schwann Cell-Like Cells (SCLC)

2.1. Mesenchymal Stem/Stromal Cells

Human mesenchymal stem/stromal cells (MSCs) are defined by the International Society for Cellular Therapy by three minimal criteria: (1) adherence to plastic; (2) >95% of cells must be CD105+, CD73+, or CD90+, as well as <2% CD45+, CD34+, CD14+, CD19+, major histocompatibility complex II (MHC II) positive; (3) multipotent differentiation potential [83]. MSCs with self-renewal capacity, high proliferation ability, multilineage potential, and neurotrophic potency hold promise for the clinical treatment of nerve injuries. For the first time, MSCs were discovered in the bone marrow (BM), which

is still the most studied MSC source. Later on, MSCs were isolated from the variety of tissues, including adipose tissue, umbilical cord tissue, Wharton's-jelly, hair follicles, and skin. Preferably, these cells should be easily accessible in abundant quantities for clinical applications. Nowadays, next to BM, the most preferred MSC source is adipose tissue due to their abundance per gram tissue and easy accessibility [84]. However, umbilical cord tissues, such as cord blood and Wharton's Jelly, enable non-invasive isolation procedures, thus making them an attractive source for MSCs (Figure 1). A wide range of MSCs is currently under clinical trials with a major focus on implantation techniques, safety, and efficacy. Even though preclinical studies encourage the use of MSCs for treating human SCI, the outcome of clinical trials remain controversial, as described by Soria-Zavala et al. in 2020 [85].

2.1.1. Biological/Chemical Induction

Dezawa et al. described the differentiation of rat MSCs into SCLC in vitro for the first time in 2001 [86]. This original protocol by Dezawa was developed for the differentiation of rat bone marrow-derived MSC (BM-MSC) into SCLCs. Shortly, sub-confluent MSCs are incubated in alpha-MEM containing 1 mM beta-mercaptoethanol (BME) for 24 h. BME is a reducing agent and is known to induce neurite-like processes in MSC culture, previously used to induce neuronal differentiation [87]. Then, the media is removed, and the cells are washed with phosphate-buffered-saline (PBS), followed by 72 h of incubation in alpha-MEM media supplemented with 10% FBS and 35 ng/mL all-trans-retinoic acid (RA). RA regulates the expression of various transcription factors during early neuronal differentiation and increases the responsiveness to neurotrophins [88]. After a PBS wash, MSCs are transferred to alpha-MEM supplemented with 10% FBS, 5 μ M forskolin (FSK), 10⁶ ng/mL recombinant human basic-fibroblast growth factor (bFGF), 5 ng/mL recombinant human platelet-derived growth factor-AA (PDGF-AA), and 200 ng/mL recombinant human heregulin-beta1 (HRG) for 7 days. PDGF-AA, bFGF, and HRG are neurotrophins involved in the differentiation and proliferation of glial cells (SC). Further, bFGF and PDGF-AA are potent mitogens for MSCs. In the meantime, HRG is found to induce neural crest cells selectively into SC [89,90]. FSK increases the level of intracellular cyclic adenosine monophosphate (cAMP) [91]. Further, the cAMP elevation is known to increase responsiveness to neurotrophic factors. Thus, the induction process is a result of the potential synergistic effect of bFGF, PDGF-AA, HRG, and FSK [86,92]. Based on the protocol by Dezawa, several derivatives are developed over time using MSCs of different origins. Improved differentiation of MSCs is achieved by adding the glial growth factor (GGF-2), which is a potent SC mitogen that stimulates peripheral nerve regeneration and restricts neural crest stem cell (NCSC) differentiation to the glial lineage [93–96]. Further, co-cultures of BM-MSC and adipose-derived MSC (Ad-MSC) in the presence of primary SCs result in the differentiation and expression of the SC markers—peripheral myelin protein 22 (PMP-22) and S100—for up to 12 days (Figure 1 and Table 1) [97].

2.1.2. Physical-Electrical Induction

Another approach, which was mainly studied for the differentiation of neural stem cells (NSC) into neurons, is electrical stimulation for the differentiation of MSCs into SCLCs [98–100]. Electrical stimulation only is successful in inducing MSCs into SCLCs using a flexible, highly conductive (sheet resistance < 1 k Ω /sq) inkjet-printed graphene interdigitated electrode circuit. Following electrical stimulation, the expression of the growth factors, i.e., NGF, GDNF, and BDNF, is up-regulated in comparison to chemical induction method. Further, electrically-induced MSCs show a high level of phenotypic markers specific for SC, i.e., p75, S100, and S100 β , compared to chemically-induced and naïve MSCs. The possible mechanism of differentiation by electrical stimulation is assumed to be associated with altering the cellular membrane potential through hyperpolarization and depolarization, modifying ion channel density, receptor distribution, and calcium channel activation [101]. Further, it has been shown that various signaling pathways, i.e., mitogen-activated protein kinase (MAPK), Phosphoinositide 3-kinases (PI3K), and Rho-associated protein kinase (ROCK) pathways, regulating MSC's proliferation and differentiation, are activated in response to electrical fields [102–104].

Another approach involving biomechanical forces or micro-nano patterned topographical surfaces has demonstrated the feasibility of controlling the fate of the stem cells. MSC cultured on imprinted SC topographies results in the direct differentiation into SCLC [105]. On the other hand, combining a micro-patterned substrate with chemical induction does not improve the differentiation process. Although the micro-pattern has a significant effect on cell alignment and elongation of the differentiated cells, the percentage of SCLC is not affected [106]. However, it is predicted that biophysical forces and mechanotransduction play a fundamental role in instructing the cell fate. It has been demonstrated that physical cues play an important role in embryonic stem cell (ESC) differentiation in vitro [103]. For example, shear stress is linked with ESC differentiation towards vascular endothelial cells, and the stretching of MSCs results in the up-regulation of smooth muscle cell markers [107,108]. Thus, the physical cues and structural features have gained increasing focus in the field, highlighting their important role in cell differentiation and transplantation (Figure 1 and Table 1) [105,109].

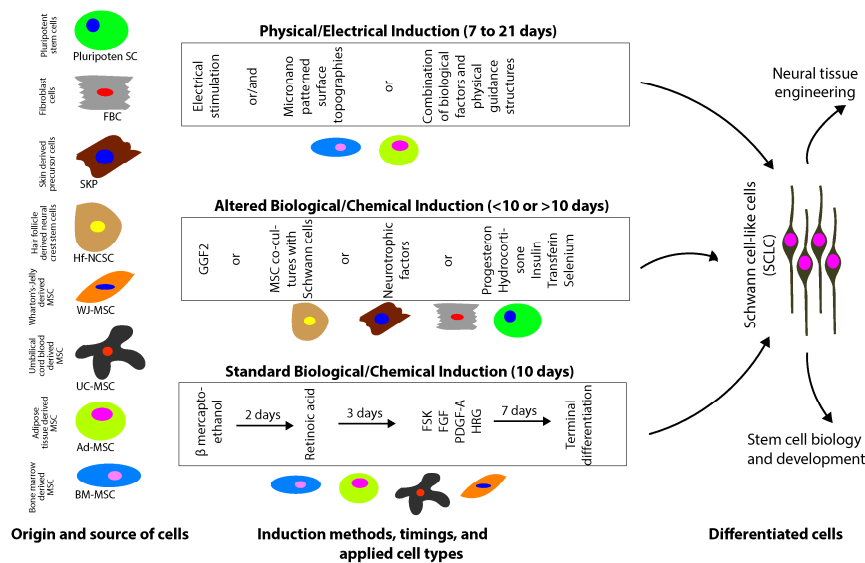


Figure 1. Mesenchymal stem cell (MSC) of different origin, current developments in the differentiation of MSC into Schwann cell-like cells (SCLC) and potential applications of SCLC.

2.1.3. Bone Marrow-Derived MSC

In Vitro Characterization

MSCs were isolated for the first time from BM, and these cells were extensively studied for various applications, as recently reviewed by Gomez-Salazar et al. in 2020 [110]. As shown for rat BM-MSCs, human BM-MSCs have the potential to differentiate into the glial lineage and express typical glial markers like S100B, GFAP, p75, and erbB3. Early morphological changes are observable within 4 to 5 days in the presence of differentiation media supplemented with GGF-2. BM-MSC morphology changes from flat, fibroblastic phenotype to a bipolar, elongated spindle-shaped, which is an SC's characteristic phenotype [111]. Human BM-MSCs-derived SCLCs promote neurite sprouting from rat dorsal root ganglion (DRG) neurons in vitro [111]. Further, BM-MSCs-derived SCLCs render the microenvironment more favorable for tissue repair by releasing various growth factors, such as VEGF-A and hepatocyte growth factor (HGF) (Figure 1 and Table 1) [112].

Application in the PNS

A crucial function of SCs in PNI regeneration is their ability to remyelinate the regenerating axons. Even if the axons would reach their target, proper myelination is crucial for normal neuronal function and conduction speed [109,113]. Therefore, Dezawa et al. transplanted BM-MSCs-derived SCLCs with a GFP marker within a 15 mm hollow conduit (Amicon, Beverly, MA, USA) using a nerve gap-injury model. Within 3 weeks, successful nerve regeneration, along with newly formed myelin structures, is visualized by GFP expressing cells [83]. Significant improvement in functional and behavioral recovery (gait analysis) is observed after 6 months [114,115]. In another study, transplantation of 10 mm hollow conduits (Amicon, Beverly, MA, USA) seeded with human BM-MSCs-derived SCLCs and tacrolimus co-treatment results in the recovery of sciatic nerve function, as measured by walking track analysis in rats within 3 weeks [116].

Application in the CNS

Rat BM-MSCs-derived SCLCs promote locomotor and sensory function when grafted into SCI through 3 mm atelocollagen honeycomb (Koken Inc., Tokyo, Japan) scaffold in comparison to cell-free scaffolds [117]. Follow up studies have further revealed the improvement in anatomical and functional features of regenerated spinal cord tissue in response to BM-MSCs and BM-MSCs-derived SCLCs. However, undifferentiated BM-MSCs better support axonal regeneration, while BM-MSCs-derived SCLCs promote significant remyelination. Therefore, the authors suggest that a combination of SCLCs and BM-MSCs may become effective in treating SCI [118]. The application of human-MSC-derived SCLCs in SCI is still lacking. However, it has been shown that human-MSC-derived SCLC supports axonal outgrowth in an ex-vivo SCI model by secreting HGF and VEGF [112].

Limitations

To overcome the shortfall in terms of phenotypical stability of SCLCs, neuroectodermal progenitors from human BM-MSCs are selectively expanded and induced into SCLCs via an intermediate neurosphere. For this, a sphere-forming protocol used for skin precursor cells (SKPs) is adapted by Dezawa et al. in 2001 to foster the expansion of neuroglial progenitors within the BM-MSCs population [86,119,120]. Resulting SCLCs promote axonal outgrowth and myelination in vitro. Implantation into a rat PNI model involving 16 mm long chitosan conduit reveals the formation of human myelin basic protein (MBP) and compact myelin sheath after 8-weeks. The rats are co-treated with cyclosporine A [121]. However, BM-MSCs possess important limitations for their clinical transition. Firstly, the isolation of BM-MSCs is an invasive and painful procedure. Secondly, the ratio of MSCs in the bone marrow is relatively low (<1/100,000), and lastly, the quantity of bone marrow that can be harvested from patients is strictly limited [122]. Thus, there is a need for an alternative viable source of cells.

2.1.4. Adipose Tissue-Derived MSC

In Vitro Characterization

Compared to BM-MSCs, Ad-MSCs are easily accessible from patients in abundant quantities (i.e., 500 times higher cell count). Further, it has been shown that Ad-MSCs possess rapid proliferation capacity and immune-privileged [123–125]. Kingham et al., using rat cells, reported the first successful differentiation of Ad-MSCs into SCLCs. For this, they used the previously established Dezawa's protocol with a slight modification of increasing induction time and concentration of FSK and GGF-2 [126]. Rat Ad-MSCs-derived SCLCs are well studied for their expression of a neuroglial marker, neurotrophic factors, neurotransmitter, and related receptors. Their potential to promote axonal regeneration and myelin formation has been demonstrated by several studies in vitro and in vivo [127–132]. Differentiation of human Ad-MSCs into SCLCs results in the change of morphology from flat, fibroblast-like structure to elongated, spindle-shape, resembling the primary human SC.

The secretion of GDNF, NGF, BDNF, VEGF-A, and angiopoietin-1 proteins is found to increase in the differentiated Ad-MSCs in vitro [133,134]. Ad-MSCs-derived SCLCs enhance neurite outgrowth from DRG neurons in vitro (Figure 1 and Table 1) [133].

Application in the PNS

Self-aligned rat Ad-MSCs-derived SCLCs in a collagen matrix support the axonal regeneration in a 15 mm rat PNI model. After 8 weeks, a 3.5-fold greater amount of axons is observed in conduits with SCLC than in cell-free conduits [135]. Further, rats treated with SCLC-seeded fibrin or silicon conduits following gap-injury exhibit improved nerve regeneration and functional outcome postoperatively at 2 weeks [128], 16 weeks [136], and 6 months [137]. Transplantation of human SCLCs into a rat tibial nerve crush injury supports the axonal regeneration and enriches the distal nerve with regenerating axons and MBP-positive myelin structures after 8 weeks of implantation [134]. Tubular fibrin conduit loaded with human Ad-MSCs-derived SCLCs results in enhanced angiogenesis and early nerve regeneration within 2 weeks in a rat 10 mm sciatic nerve injury model that is co-treated with cyclosporine A [133].

Application in the CNS

Collagen scaffolds loaded with Ad-MSC-derived SCLCs significantly enhance locomotor and sensory scores in rats with 3 mm hemisection SCI in comparison to cell-free implants. Further, a comparison of functional outcomes between BM-MSC-derived SCLCs and Ad-MSC-derived SCLCs reveals no significant difference, suggesting their comparable therapeutic performance [138]. In a 3 mm deep brain contusion, it has been shown that Ad-MSC-derived SCLCs improve behavioral performance after 30 days of implantation [139]. These results prove the ability of Ad-MSC-derived SCLCs to survive and exert their therapeutic function, i.e., neuronal survival, axonal regeneration, and remyelination within the microenvironment of CNS injury.

Limitations

Withdrawal of differentiation media from human SCLCs results in the rapid reversal of the SCLCs phenotype to stem cell-like characteristics [140]. These observations suggest that the differentiation process is reversible, and the long-term stability of SCLC is subjective to the constant availability of differentiation factors. GGF-2 is a key axonal-derived factor for SC maintenance *In vivo*, while SCs release BDNF and GDNF for neuronal maintenance [26,141]. Stimulation of Ad-MSCs with differentiation media containing a high concentration of GGF-2 mimics paracrine signaling and eventually results in BDNF and GDNF expression. However, the increased expression of GDNF and BDNF and the reduced NT-3 expression in response to GGF-2 stimulation may not indicate true differentiation. In an attempt to improve the quality of the differentiation process for human Ad-MSCs (stability and functional characteristics), the protocol by Dezawa et al. is modified and additional factors, i.e., progesterone (Prog), hydrocortisone, and insulin-transferrin-selenium, are added [142,143]. SCLCs, resulting from the modified protocol, exhibit enhanced performance *in vitro* and *In vivo*. Collagen sponge loaded with human SCLCs is implanted into a 10 mm sciatic nerve gap, and the outcome analysis reveals the enhanced stability (long-term survival), proliferation, myelination, and improved motor function within 4 months. Experimental rats are immunosuppressed by cyclosporine A [143]. However, the heterogeneity of stromal-vascular fraction (SVF)-derived Ad-MSCs represents the important limitation for their therapeutic efficiency. For effective clinical applications and reproducibility, it would be crucial to identify specific subpopulations within the SVF Ad-MSC pool. Furthermore, it is worth comparing the therapeutic performance of the cells resulting from the following two different strategies; 1) High purity Ad-MSC-derived SCLCs and 2) *In vivo* transdifferentiation of Ad-MSC into SCLCs in response to the localized release of growth factors.

2.1.5. Umbilical Cord-Derived MSC

MSCs can be isolated from various tissues that are generated during childbirth, i.e., umbilical cord blood, placenta, perivascular tissue, amniotic fluid, and Wharton's jelly (tissue surrounding the umbilical cord vessels). The isolation from these tissues is easier, non-invasive, and economical than bone marrow aspirate or adipose tissue [144]. Therefore, these tissues represent a potential alternative to Ad-MSCs and BM-MSCs involving invasive procedures. MSCs from the umbilical cord can be harvested without risk for either mother or child and cryopreserved [145]. Interestingly, Umbilical cord derived MSCs (UC-MSCs) are currently subject of dozens of clinical trials for various diseases, including spinal cord injuries. However, in-vitro UC-MSCs-derived SCLCs are not yet a subject of a clinical trial. But the usage of naive UC-MSCs shows safety, survival, and integration capabilities in human patients, as reviewed by Couto et al. in 2019 (Figure 1 and Table 1) [146].

Umbilical Cord Blood-Derived MSC

In Vitro Characterization

Human umbilical cord blood-derived MSCs (UCB-MSCs) differentiation into SCLCs consists of a two-step process. First, UCB-MSCs are induced into free-floating neurospheres that are positive for nestin while being negative for GFAP and S100. Further differentiation of neurospheres into SCLCs is achieved by treating with RA, FSK, bFGF, PDGF-AA, and HRG, as described by Dezewa et al. Resulting cells do express the SC markers—S100 and GFAP—and support neuronal differentiation and axonal outgrowth in vitro. However, UCB-MSCs-derived SCLCs begin to revert to a flat morphology after passage three, indicating the need for the continuous support of the differentiation factors [147]. On the other hand, direct differentiation of UCB-MSCs into SCLCs is achieved by the previously established protocol by Dezawa et al. For this, pretreatment with BME and bFGF is followed by RA treatment and differentiation process involving FSK, bFGF, PDGF-BB, NGF, and HRG. Notably, the composition of the differentiation media is adapted to the new cell origin by including PDGF-BB in the place of PDGF-AA [148]. In contrast to PDGF-AA, PDGF-BB plays an important role in actin reorganization [149]. Furthermore, NGF is also added to the media, which is shown to promote neural precursor cell differentiation into mature neurons and glial cells in vitro [148,150].

In Vivo Application

The biological performance of UCB-MSCs-derived SCLCs still remains to be elusive for treating PNI or SCI. However, undifferentiated UCB-MSC transplantation into a sciatic nerve crush model results in enhanced BDNF and TrkB expression and improved functional recovery [151]. Transplantation following a spinal cord contusion injury by weight drop reveals the survival and differentiation of human UCB-MSCs into neurons, OCs, and astrocytes, resulting in the enhanced functional recovery [152,153]. Therefore, we hypothesize that in vitro differentiated UCB-MSCs may have a beneficial effect on neuronal survival, axonal regrowth, remyelination, and functional restoration in PNS and CNS.

Limitations

The vast abundance, availability of donors, and reliability of sample collection make UCB-MSCs be highly promising cell source. However, the clinical applicability of UCB-MSC-derived SCLCs is limited due to the long two-step differentiation process and lack of studies demonstrating their therapeutic capacity In vivo. In addition, functional and phenotype stability of transplanted cells are considered to be crucial for maintaining the safety and efficacy. Moreover, UCB-MSCs are isolated from the umbilical cord; therefore, their application as an allograft for many sections of the patients is obvious, and thus, it is inevitable to follow immune suppression procedure. However, UCB-MSCs are less mature than other types of adult stem cells, indicating their low-immunogenicity [154].

Wharton's-Jelly-Derived MSC

In Vitro Characterization

Human Wharton's-Jelly-derived MSCs (WJ-MSCs) can be differentiated into SCLCs using the protocol established by Dezawa et al., with minor modifications. Within eight days, WJ-MSCs change to an SC-like morphology. From large and flat WJ-MSC morphology, they change to a bi-polar spindle-shaped morphology and exhibit continuous proliferation, resulting in high density than undifferentiated WJ-MSCs. Resulting WJ-MSC-derived SCLCs express typical SC markers, i.e., GFAP, p75, S100 β , and MBP. Further, these differentiated cells well support the axonal outgrowth in vitro from DRG neurons (Figure 1 and Table 1) [155].

Application in the PNS

Human WJ-MSC-derived SCLCs are seeded on to hollow fibers (Amicon, Beverly, MA, USA) and transplanted into an 8 mm PNI rat model that is co-treated with tacrolimus. Interestingly, SCLCs maintain their phenotype *In vivo* and contribute to myelin tissue formation around regenerative axons. Furthermore, the motor function of the animals treated with WJ-MSC-derived SCLCs is found to be significantly higher than undifferentiated WJ-MSCs and comparable to human SCs [156].

Application in the CNS

WJ-MSC-derived SCLCs still remain to be evaluated in animals for treating PNI/SCI. However, the beneficial effects of undifferentiated WJ-MSC transplantation in SCI are demonstrated by several studies [157,158]. Clinical studies using WJ-MSC transplantation show the positive impact on motor function, self-care ability, and muscular tension of patients with thoracolumbar SCI grade A [159]. The regenerative effects of WJ-MSCs are mainly associated with their paracrine signals [160]. Within this context, we hypothesize that WJ-MSC-derived SCLCs with improved neurotrophic potency may hold the improved capacity for treating SCI lesions.

Limitations

UCB-MSCs and WJ-MSCs are isolated from the umbilical cord, and therefore, a large section of the patients who failed to bank their umbilical cord depend on the allograft source. International standards and quality management are required for long-term cell banking of these potential MSCs [161]. However, further evaluation of the WJ-MSC-derived SCLCs for treating PNI and SCI is required in complete detail.

2.2. Hair Follicle/Skin-Derived Stem Cells

Cellular homeostasis and regeneration of the mammalian epidermis rely on the variety of precursor cells, which can be found in the epidermis and in the hair follicle epithelium [162]. Hair follicles possess abundant stem cells with easy accessibility. The hair bulge is a well-characterized niche for adult stem cells, i.e., epithelial stem cells, melanocyte stem cells, and neural crest stem cells (NCSCs) [163–167]. The mesenchymal compartment of the hair follicle harbors dermal sheath, dermal papilla, and dermal precursors. These unique populations of epidermal and dermal cells within the hair follicles possess high differentiation potential (Figure 1 and Table 1).

2.2.1. Neural Crest Stem Cells

In Vitro Characterization

Hair follicle-derived NCSCs (Hf-NCSCs) are of high interest for regenerative medicine, given their multi-lineage capacity and wider availability [168]. Similar to endogenous SCs, Hf-NCSCs originate from the embryonic neural crest. Thus, Hf-NCSCs are of great choice for generating SCLCs *in vitro*. Hf-NCSCs are readily accessible in the bulge of hair follicles and can be isolated with high purity for

further expansion [169]. Briefly, hair follicles are dissected, and the bulge sections are placed in adherent culture. Due to their migratory ability, Hf-NCSCs emigrate from the bulge explants. These migratory Hf-NCSCs can be expanded and cryopreserved [170]. Differentiation of rat and human Hf-NCSCs can be achieved *in vitro* using media supplemented with GGF-2, which is known to suppress neural differentiation while promoting glial differentiation [96]. Within 4 weeks, human Hf-NCSCs become S100- and GFAP-positive [168]. Alternatively, a faster differentiation can be achieved when human Hf-NCSCs are treated with BME and RA, followed by manipulation of the WNT, sonic hedgehog, and transforming growth factor β (TGF- β) signaling pathways and further exposure to bFGF, PDGF-BB, FSK, and GGF-2. Within 4 days after induction, Hf-NCSCs change to a more slender and elongated morphology, representing the characteristic feature of SCs. Further, Hf-NCSC-derived SCLCs show enhanced expression of SOX10, KROX20, p75, MBP, and S100 β and become mature within 2 weeks of differentiation. Hf-NCSC-derived SCLCs interact with axons and co-localize with myelin *in vitro* (Figure 1 and Table 1) [169].

Application in the PNS

Multiple studies have demonstrated enhanced axonal regeneration and functional restoration when NCSCs are transplanted into the niche of PNI [171–173]. Hf-NCSCs transplanted into a 2 mm PNI mouse model become GFAP-positive SCLCs and support the axonal regeneration and innervation [174]. Hf-NCSCs also regulate the neuroinflammatory responses, and Stratton et al. in 2017 showed myelin regeneration by Hf-NCSCs. However, studies demonstrating the effect of Hf-NCSC-derived SCLCs on PNI are still missing.

Application in the CNS

When transplanted into an SCI mouse model, murine Hf-NCSCs differentiate into GFAP/CNPase-positive SCLCs, leading to myelin regeneration and improved motor and sensory function [175–177]. However, *In vivo* applications of Hf-NCSC-derived SCLCs are still missing. Given the potential of Hf-NCSCs to differentiate into SCLCs *in vitro* as well as *In vivo*, we hypothesize that Hf-NCSC-derived SCLCs may possess high stability and enhanced neurotrophic potency, leading to better performance.

Limitations

An extended or prolonged differentiation process involving several weeks and complex procedure is certainly a major drawback. Further, the lack of *In vivo* studies showing the therapeutic ability of Hf-NCSC-derived SCLCs is the main limitation. However, the high regeneration potential of Hf-NCSCs, as evidenced by enhanced axonal regeneration, myelin, and functional recovery following PNI and SCI, may circumvent extended time required for *in vitro* differentiation.

2.2.2. Skin-Derived Precursory Cells

In Vitro Characterization

Similar to Hf-NCSCs, SKPs can be harvested from skin and hair follicles. Resulting SKPs can be differentiated *in vitro* into SCLCs [178–181]. Briefly, single-cell suspension of skin tissue will be achieved by enzymatic, i.e., collagenase digestion, followed by mechanical dissociation and filtration. These cells are then cultured with epidermal growth factor (EGF) and FGF-2. Within 3–7 days, the floating spheres of SKPs are formed. Further expansion can be achieved by the dissociation of these spheres into single cells and by further subculture. SKPs do express the neural marker nestin; however, they lack the expression of the NCSC markers—p75NTR and PSA-NCAM. Further, it has been shown that SKPs could reconstitute the dermis and induce hair follicle morphogenesis. Thus, it is clear that SKPs originate from embryonic mesenchymal precursors [181]. Differentiation of human and rodent SKPs is achieved by culturing dissociated SKP spheres on poly-D-lysine and laminin-coated plates in

the presence of FSK and HRG. Within 10 days, the cells become bipolar and express the SC markers, such as S100 β , MBP, PMP22, GFAP, and P75NTR. Further, DRG co-cultures reveal the myelination capability of SKP-derived SCLCs in vitro (Figure 1 and Table 1) [178,182].

Application in the PNS

SKP-derived SCLC transplantation into the distal segment of a crushed sciatic nerve reveals the association of transplanted cells with regenerating axons and the expression of MBP and PMP22 after 2 weeks. Interestingly, naive SKP transplant shows a similar expression of myelin proteins; however, expression levels appear to be lower than the SKP-derived SCLCs. Interestingly, a subpopulation of SKP-derived SCLCs expresses GFAP but not MBP while aligning with axons, suggesting that these cells may belong to non-myelinating SCLCs [178]. The 12 mm decellularized nerve graft seeded with SKP-derived SCLCs promotes significant loco-motor function when implanted into a 10 mm sciatic nerve gap injury. Seventeen weeks post-operatively, SKP-derived SCLCs accelerate functional regeneration that can be comparable to Sham control groups, as evidenced by the tapered beam task in contrast to other groups receiving isografts, nerve-derived SC, or media alone. Further, the amount of axons, action potential amplitudes, and muscle weights are found to be significantly higher for the animals treated with SKP-derived SCLCs [183].

Application in the CNS

SKPs, when transplanted into the brains of newborn shiverer mice, differentiate into myelinating cells, presumably a response to axonal-derived factors within the niche of developing brain. The CNS of shiverer mice is characterized by extensive demyelination. Compact myelin formation is observed following SKP transplantation, further confirming the myelination potential of in vivo differentiated SKPs [178,184]. In ex vivo studies, it has been shown that in vitro SKP-derived SCLCs express MBP and S100 β within the cerebellar white matter in cerebellar slice cultures [178]. Immediate injection of rodent SKP-derived SCLCs into the lesion site of an SCI crush model promotes repair and functional recovery within 6 weeks. SKP-derived SCLCs implantation results in increased usage of the injury-affected forelimb, enhanced axonal density in the rubrospinal tract rostral to the lesion, and significant EMG thresholds that are comparable to uninjured animals. Further, no significant differences between nerve-derived SCs and SKP-derived SCLCs are found in several measures, such as motor function, electrophysiological properties, graft survival, neuroprotection, myelination, and integration into the host parenchyma [185]. Transplantation of SKP-derived SCLCs into a rat chronic SCI model reflects a more clinically relevant approach than acute injury. Therefore, SKP-derived SCLCs are transplanted into chronic SCI of rats, i.e., 8 weeks after injury. Subsequent analysis reveals the survival of transplanted SCLCs for 5 months, their integration into host tissue, neural protection, axonal regeneration, and myelination. Further, the functional analysis reveals improved locomotion after 8 weeks of SCLCs transplantation [186].

Limitations

Human SKPs display varied gene expression profiles that are subjective to the anatomical region of cell isolation [187,188]. Such heterogeneity is a potential risk factor for their clinical transition. Moreover, there are no markers to distinguish purified human SKPs from the rest of the cells originating from hair follicles [189]. However, by sequential passaging of SKP-derived SCLCs, the purity of the cells could be raised over 95% [178]. Subsequently, it is crucial to study the utility of human SKP-derived SCLCs in order to assess their suitability for clinical applications.

2.3. Pluripotent Stem Cells

Pluripotent stem cells, i.e., ESCs, as well as induced pluripotent stem cells (iPSCs), are of great interest for the generation of SCLCs. iPSCs are highly similar to ESCs in terms of gene signature, epigenetic status, and differentiation potential [190,191]. Therefore, iPSCs are attractive autologous cells,

represent a viable alternative to ESCs, which are accessible from the inner cell mass of pre-implantation blastocysts only [192,193].

2.3.1. In Vitro Characterization

SCLCs generation from pluripotent progenitors generally relies on an intermediate stage called NCSCs. These NCSCs can be either derived from neural rosettes formed on an MS-5 stromal feeder cell layer or from non-adherent neurospheres that are induced by PA6 stromal cells [194,195]. ESC-derived NCSCs can be further differentiated into neural crest derivatives like sensory and sympathetic neurons, smooth muscle cells, and SCs [196,197]. ESC-derived NCSC differentiation towards SCs can be achieved by various combinations of factors, such as HRG, BDNF, GNF, NGF, FSK, bFGF, and cAMP. Further, myelin formation can be induced by ascorbic acid [198]. Human ESC-derived SCLCs wrap and myelinate rat DRG neurons in vitro [199–201]. ESC differentiation into SCLCs involving an intermediate step is a time-consuming process, requiring several weeks to months. Direct differentiation, involving no NCSC stage, can be achieved by inducing ESCs or iPSCs into SC precursors (SCP). First, neural rosettes from human pluripotent stem cells can be derived by modulating the Glycogen synthase kinase 3 (GSK-3) and TGF- β pathways using inhibitors in the absence of feeder cells [202,203]. Next, neuregulin1 (NRG1) induces neural rosettes differentiation towards self-renewing SOX10-positive SCP, which can be further differentiated into immature SCLCs using NRG1, RA, PDGF-BB, and FSK. Resulting cells express trophic factors, such as BDNF, GDNF, NGF, and NT-3, and promote axonal regeneration from rat DRG neurons and deposit the myelin around the axons.

2.3.2. In Vivo Application

ESC-derived SCLCs support the anatomical regeneration and enhanced motor function within 8 weeks after matrigel-assisted transplantation into PNI [204]. Further structural analysis reveals the co-localization of MBP with S100-positive ESC-derived SCLCs, indicating their myelination potential. These observations are further strengthened by accelerated sciatic functional recovery assessed by walking track analysis [204].

2.3.3. Limitations

The therapeutic use of ESCs in clinics is associated with ethical, safety, and regulatory considerations. Within this context, autologous-derived iPSC holds better chances for the clinical transition than ESCs. However, iPSC-based applications are limited due to the increased safety risks associated with the genetic reprograms involving genome-integrating viruses and proto-oncogenes, i.e., c-Myc used for the induction of pluripotency can lead to genomic instability and tumorigenesis [190,205]. Moreover, teratoma formation is reported to be another major risk linked to iPSCs' clinical applications. Low numbers of undifferentiated ESCs or iPSCs can result in teratoma formation after implantation [30,206]. Thus, there is a need to explore more effective yet safe strategies for the differentiation of ESC/iPSC into SCLCs.

2.4. Fibroblasts

Recent studies in the field of cellular reprogramming have demonstrated the feasibility of somatic cell direct conversion into target cell type without passing through a pluripotent intermediate state. Thus, the resulting cells with complete pre-differentiation would be suitable for transplantation therapies without being tumorigenic (Figure 1 and Table 1) [207–209].

Table 1. Differential origin of Schwann cell-like cells (SCLCs) and their biological performance.

Starting Cell	Induction Factors	Method	Phenotypic Markers	Growth Factor Expression	In Vitro Outcome	In Vivo Outcome	Time (Days)	Subacute/Chronic Injury	Injury	In Vivo Cotreatments	Application in PNS/CNS	Ref.
Ad-MSC	BME, RA, FSK, bFGF, PDGF, HRG	direct biochemical induction	morphology	BDNF, NGF, GDNF	increased neurites sprouting of NG108-15 neurons, increased neurites length and increased amount of neurites per neuron	increased myelination	18 days	subacute	rat tibial crush	-	PNS	[134]
Ad-MSC	BME, RA, FSK, bFGF, PDGF-AA, HRG	direct biochemical induction	-	BDNF, GDNF, VEGF-A, Angiopoietin-1	increased neurites length of rat DRG neurons	increased amount and length of axons, increased angiogenesis	18 days	subacute	10-mm rat sciatic nerve gap	14-mm tubular fibrin conduit, Cyclosporine A	PNS	[126]
Ad-MSC	BME, RA, FSK, bFGF, PDGF-AA, HRG	direct biochemical induction	morphology	BDNF, GDNF, NGF	withdrawal of differentiation media cause reversion of the induced SCLC phenotype	-	18 days	-	-	-	-	[131]
Ad-MSC	BME, RA, FSK, bFGF, PDGF, HRG, PROG, Hydrocortisone, Insulin	direct biochemical induction	morphology	BDNF, NGF	-	increased amount of axons, increased myelination, enhanced motor function recovery	13 days	subacute	10-mm rat sciatic nerve gap	collagen sponge, cyclosporine A	PNS	[143]
BM-MSC	BME, RA, FSK, bFGF, PDGF-AA, GGF-2	direct biochemical induction	morphology	-	increased neurite sprouting, increased neurite length, increase neurite density of rat DRG neuron	-	18 days	-	-	-	-	[111]
BM-MSC	BME, RA, FSK, bFGF, PDGF-AA, HRG	direct biochemical induction	morphology	HGF, VEGF	increased number and neurite length of Neuro2A cells	enhanced axonal outgrowth in ex vivo Spinal Cord slices	12 days	-	-	-	CNS (ex vivo)	[112]

Table 1. Cont.

Starting Cell	Induction Factors	Method	Phenotypic Markers	Growth Factor Expression	In Vitro Outcome	In Vivo Outcome	Time (Days)	Subacute/Chronic Injury	Injury	In Vivo Cor-treatments	Application in PNS/CNS	Ref.
BM-MSC	neurosphere induction: bFGF, EGF, B27; SC-like cell induction: FSK, PDGF-AA, bFGF, HRG	two step biochemical induction	morphology S100, p75	BDNF, VEGF, HGF, NGF	increased neurites sprouting, increased neurite length of Neuro2A cells and rat DRG neurons, myelination	functional myelination	21 days (neurospheres); 14 days (SC-like cells)	Subacute	5-mm rat sciatic nerve gap	16-mm chitosan conduit; Cyclosporine A	PNS	[121]
BM-MSC	BME, RA, FSK, bFGF, PDGF-AA, HRG	direct biochemical induction	morphology, GFAP, S100, p75, P0	-	-	increased amount of axons, enhanced motor function outcome	8-9 days	Subacute	10-mm rat sciatic nerve gap	10-mm trans-permeable tubes (Hollow fibers, Amicon, Beverly, MA); bacrolimus	PNS	[116]
BM-MSC; Ad-MSC	conditioned SC media	SC co-culture	PMP-22, S100	-	-	-	12 days	-	-	-	-	[97]
ESC	neurosphere induction: Stromal feeder cells, BME, SHH, FGF8, BDNF, TGFβ, cAMP; ascorbic acid; SC-like cell induction: HRG, CNTF, cAMP	two step biochemical induction: ESC to neural rosette to SC-like cells	GFAP, S100, MBP	-	-	-	16 days (rosette); 60 days (SC-like cells)	-	-	-	-	[201]
ESC	neurosphere induction: Stromal feeder cell, BME; SC-like cell induction: FSK, bFGF, HRG, ascorbic acid	two step biochemical induction: ESC to neurospheres to SC-like cells	morphology, GFAP, S100, p75, PMP-22, P0, MBP, Krox20	-	interaction with chicken & rat DRG neurons	-	14-16 days (neurospheres); 56 days (SC-like cells)	-	-	-	-	[200]

Table 1. Cont.

Starting Cell	Induction Factors	Method	Phenotypic Markers	Growth Factor Expression	In Vitro Outcome	In Vivo Outcome	Time (Days)	Subacute/Chronic Injury	Injury	In Vivo Cotreatments	Application in PNS/CNS	Ref.
ESC/iPSC	NCC induction: stromal feeder cell, B27, FGF2, Rock inhibitor, ascorbic acid; SC-like cell induction: HRG	two step biochemical induction; ESC/iPSC to NCC to SC-like cells	GFAP, S100, p75, erbB3, Sox9, PMP-22, MBP	-	myelination of rat DRG neurons	-	14 days (neurospheres); 40 days (SC-like cells)	-	-	-	-	[199]
ESC/iPSC	rosette induction: CHIR99021, SB431542; SCP induction: NRG1; SC-like cell induction: NRG1, RA, FSK, PDGF-BB	tree step biochemical induction; ESC/iPSC to rosette to SPCs to SC-like cells	morphology; GFAP, S100, PMP-22, PLP	BDNF; GDNF; NGF; CNTF; NT-3, NT-4	myelination of rat DRG neurons	enhanced myelination, enhanced motor function recovery	6 days (rosette); 18 days (SPC); 7 days (SC-like cells)	suacute	6–9 mm mouse sciatic nerve gap	matrigel	PNS	[204]
Fibroblasts	SOX10, Krox20 transduction; FSK, bFGF, PDGF, HRG	genetic modification	morphology; GFAP, p75, NG2	BDNF; GDNF; NGF	increased neurites sprouting of NG108-15 neurons, increased neurites length, increased amount of neurites per neuron, myelination of mice DRG neurons	enhanced myelination, enhanced motor function recovery	3 days	subacute	5 mm mouse sciatic nerve gap	5 mm gelatin hydrogel conduit	PNS	[207]
Fibroblasts	SOX10, Krox20 transduction; HRG, FSK	genetic modification	morphology; GFAP, erbB3, MAG, P0, MBP	-	interaction with murine DRG neurons, increased neurites length	-	14 days	-	-	-	-	[210]
Hf-NCC	mouse sciatic nerve	In vivo differentiation	GFAP	-	-	enhanced myelination, enhanced electrical signal transduction	-	Subacute	2-mm rat sciatic nerve gap	-	PNS	[174]

Table 1. Cont.

Starting Cell	Induction Factors	Method	Phenotypic Markers	Growth Factor Expression	In Vitro Outcome	In Vivo Outcome	Time (Days)	Subacute/Chronic Injury	Injury	In Vivo Cotreatments	Application in PNS/CNS	Ref.
HF-NCC	GGF-2	direct biochemical induction	GFAP, S100	-	-	-	28 days	-	-	-	-	[168]
	BME, RA, FSK, bFGF, PDGF-BB, GGF-2, CHIR99021 (GSK inhibitor, WNT activator), SB41542 (TGFβ1 receptor inhibitor)											
HF-NCC		direct biochemical induction	morphology: S100, p75, MBP, SOX10, Krox20	BDNF, FGF2, FGF5, IL6, VEGF	interaction with murine DRG neurons, myelination	-	4–17 days	-	-	-	-	[169]
SKP	FSK, HRG	direct biochemical induction	S100, p75, PMP-22, MBP	-	-	integration into CNS white matter in ex vivo spinal cord slices; compact myelin formation in vivo	10 days	chronic demyelination	shivver mice brain characterized by extensive demyelination	-	CNS	[178]
SKP	FSK, HRG	direct biochemical induction	morphology: S100, p75, p0	-	myelination of rat DRG neurons	alignment with newly formed myelin	10 days	chronic (implantation 6 days post demyelination)	local demyelination by lysolecithin injection in mice sciatic nerves	-	PNS	[182]
UCB-MSC	NCC induction: Epidermal Growth Factor, bFGF, B27; SC-like cell induction: RA, FSK, bFGF, PDGF-AA, HRG	two step biochemical induction: UCB-MSC to neurospheres to SC-like cells	morphology: GFAP, S100, Nestin	-	increased neurite sprouting of rat DRG neurons	-	>5 days (neurospheres); 4 days (SC-like cells)	-	-	-	-	[147]

Table 1. Cont.

Starting Cell	Induction Factors	Method	Phenotypic Markers	Growth Factor Expression	In Vitro Outcome	In Vivo Outcome	Time (Days)	Subacute/Chronic Injury	Injury	In Vivo Cotreatments	Application in PNS/CNS	Ref
UCB-MSC	BME, RA, FSK, bFGF, PDGF-BB, NCF, HRG	direct biochemical induction	morphology, GFAP, S100, p75	-	-	-	8 days	-	-	-	-	[148]
WJ-MSC	BME, RA, FSK, bFGF, PDGF, HRG	direct biochemical induction	morphology, GFAP, S100, p75, MBP	BDNF, NGF, NT-3	increased neurite sprouting, increased neurite length of rat DRG neurons	-	12 days	-	-	-	-	[155]
WJ-MSC	BME, RA, FSK, bFGF, PDGF, HRG	direct biochemical induction	morphology, GFAP, S100, p75, P0, O4	-	-	improved amount of axons, myelination, enhanced motor function recovery	6-7 days	Subacute	8-mm rat sciatic nerve gap	8-mm trans-permeable tubes (Hollow fibers, Amicon, Beverly, MA); tacrofintus	PNS	[156]

2.4.1. In Vitro Characterization

Human fibroblasts can be genetically reprogrammed using lentiviral vectors. Postnatal rat and human skin fibroblasts can be trans-differentiated into S100/O4-positive induced SCs (iSCs) by Sox10 and Krox20 reprogramming [203,206]. Prior to transduction, fibroblasts are placed in the media supplemented with FSK and HRG. The depletion of FSK and HRG in iSCs' media results in significant cell death, indicating their beneficial effects for the post-transduction survival of iSCs. Transcriptional profiling of resulting cells confirms that iSCs are positive for the SC markers, i.e., MBP, ERBB2, MAG, ERG2, SOX10, myelin protein zero (MPZ), GFAP, and MBP, while being negative for the oligodendrocyte-specific transcription factors and markers, i.e., Myelin oligodendrocyte glycoprotein (MOG), Oligodendrocyte transcription factor 1 & 2 (OLIG1, OLIG2), Neuron-gial antigen 2 (NG2), and NKX2-2. Strong activation and subsequent maintenance of distinct SC factors following transgene transduction clearly indicate the effective reprogramming. Resulting iSCs show potential for myelin formation, as demonstrated by DRG neuronal co-culture experiments. In response to bFGF-stimulation, iSCs exhibit three-fold potency for remyelination, which is closely matching with somatic SCs [210].

2.4.2. In Vivo Characterization

Human iSCs accelerate nerve regeneration and promote motor function within 12 weeks after gelatin hydrogel-assisted transplantation of iSCs into a 5 mm sciatic nerve gap injury in mice [207].

2.4.3. Limitations

The major drawback of genetically modified cells by lentiviral vectors is a random integration of the therapeutic genes that can potentially modify the activity of neighboring genes in close proximity and even inactivates genes completely by integrating into them [211]. Further limitations include ethical and regulatory constraints associated with genetically modified cells.

3. Conclusions

PNS and, particularly, CNS regeneration is highly challenging. SC transplantation enables overcoming the hurdles and reversal of the inhibitory microenvironment into a permissive niche. Due to the significant problems associated with SC harvest and culture, the need for stem cell therapy has emerged. Within this context, cells with the following traits, i.e., safety, homogeneity, non-immunogenicity (autologous), wider availability, functional stability, and therapeutic efficacy, are of great interest. ESCs, iPSCs, and genetically modified cells will remain controversial and away from the clinical transition due to ethical, technical, and regulatory constraints. However, the methods to generate SCLCs using ESCs/iPSCs are of great importance for studying gliogenesis and peripheral neuropathies. All other cell types, particularly Ad-MSCs, UCB-MSCs, WJ-MSCs, Hf-NCSCs, and SKPs, hold promise for the clinical transition if provided the possibility of direct and fast differentiation with long-term functional stability and safety. In the clinical settings, the time window between donor cell isolation and patient implantation is of great importance. Following neurotmesis, it becomes absolutely crucial to minimize the time gap for immediate therapy in order to protect the patients from chronic denervation, secondary damage, and comorbidities. Indeed, delayed treatment often results in progressive muscle degeneration and function [13,212]. To overcome these problems, a highly efficient one-step differentiation without intermediate cell stage and extensive cell sorting would be highly desirable. In vitro generation of SCLCs allows vigorous characterization of transplantable cells but requires long-differentiation time. Therefore, the transplantation of progenitor cells, followed by In vivo differentiation, may become attractive and effective in terms of time. Within this context, undifferentiated MSCs hold better chances for the clinical transition in comparison to the differentiated cells that are linked with technical and regulatory hurdles. On the other hand, the development of safe and effective differentiation methods may foster the clinical transition of the differentiated SCLCs with improved therapeutic efficacy.

So far, there are no clinical trials registered using the SCLCs. However, the safety of autologous, in vitro expanded SC transplantation was demonstrated by the Miami clinical trial project in 2017 [29]. Furthermore, there are several studies reporting the therapeutic benefits of MSCs for SCI and other neurological diseases. Intravenous infusion of autologous Ad-MSCs exhibits no serious adverse events. Most importantly, no carcinogenic incidents are reported [60]. In another phase 1 clinical trial, the local injection of autologous BM-MSCs in patients with chronic SCI results in various improvements of tactile sensitivity in all patients. Some patients further gain lower limb motor function [213]. However, in phase 3 clinical trials, the injection of autologous BM-MSCs into chronic SCI only shows improved neurological outcomes in 2 out of 16 patients [214]. Thus, these results remain controversial and do not replicate previous pre-clinical studies. Therefore, the extended pre-clinical studies with clinically relevant models are highly required prior to the clinical studies, and the same is true for SCLCs.

Thus, preclinical studies involving chronic nerve injury models are extremely important in order to mirror the actual clinical scenario. For instance, studying the ways of rejuvenating the niche of chronically denervated distal segments. As shown in Table 1, currently, the studies using human SCLC for treating chronic PNI and SCI are largely missing. Furthermore, the homogeneity of the differentiated SCLCs and the efficiency of their reprogramming procedures are crucial for the success of preclinical and clinical studies.

Author Contributions: S.M. designed the topic and supervised the project. A.H. and S.M. conducted the literature search. A.H. analyzed the literature and wrote the manuscript. A.H. and S.M. organized the structure. S.M. revised the manuscript. All the authors contributed to the manuscript revision. All authors have read and agreed to the published version of the manuscript.

Funding: We acknowledge the research grants from EUROSTAR to Madduri Srinivas and the surgery foundation at the University Hospital Basel to Madduri Srinivas, Daniel Kalbermatten, and Raphael Guzman.

Conflicts of Interest: The authors declare no conflict of interest.

References

1. Johnson, E.O.; Zoubos, A.B.; Soucacos, P.N. Regeneration and repair of peripheral nerves. *Injury* **2005**, *36*. [[CrossRef](#)] [[PubMed](#)]
2. Hke, A. Mechanisms of Disease: What factors limit the success of peripheral nerve regeneration in humans? *Nat. Clin. Pract. Neurol.* **2006**, *2*, 448–454. [[CrossRef](#)] [[PubMed](#)]
3. Pfister, B.J.; Gordon, T.; Loverde, J.R.; Kochar, A.S.; Mackinnon, S.E.; Cullen, D.K. Biomedical Engineering Strategies for Peripheral Nerve Repair: Surgical Applications, State of the Art, and Future Challenges. *Crit. Rev. Biomed. Eng.* **2011**, *39*, 81–124. [[CrossRef](#)] [[PubMed](#)]
4. Mackinnon, S.E.; Hudson, A.R. Clinical application of peripheral nerve transplantation. *Plast. Reconstr. Surg.* **1992**, *90*, 695–699. [[CrossRef](#)]
5. Sun, X.; Zhu, Y.; Yin, H.-Y.; Guo, Z.-Y.; Xu, F.; Xiao, B.; Jiang, W.-L.; Guo, W.-M.; Meng, H.-Y.; Lu, S.-B.; et al. Differentiation of adipose-derived stem cells into Schwann cell-like cells through intermittent induction: Potential advantage of cellular transient memory function. *Stem Cell Res. Ther.* **2018**, *9*, 133. [[CrossRef](#)]
6. Johnson, P.J.; Wood, M.D.; Moore, A.M.; MacKinnon, S.E. Tissue engineered constructs for peripheral nerve surgery. *Eur. Sur.* **2013**, *45*, 122–135. [[CrossRef](#)]
7. Gunard, V.; Xu, X.M.; Bunge, M.B. The use of schwann cell transplantation to foster central nervous system repair. *Semin. Neurosci.* **1993**, *5*, 401–411. [[CrossRef](#)]
8. Aszmann, O.; Korak, K.; Luegmair, M.; Frey, M. Bridging Critical Nerve Defects through an Acellular Homograft Seeded with Autologous Schwann Cells Obtained from a Regeneration Neuroma of the Proximal Stump. *J. Reconstr. Microsurg.* **2008**, *24*, 151–158. [[CrossRef](#)]
9. Hilton, D.A.; Jacob, J.; Househam, L.; Tengah, C. Complications following sural and peroneal nerve biopsies. *J. Neurol. Neurosurg. Psychiatry* **2007**, *78*, 1271–1272. [[CrossRef](#)]
10. Stratton, J.A.; Kumar, R.; Sinha, S.; Shah, P.; Stykel, M.; Shapira, Y.; Midha, R.; Biernaskie, J. Purification and Characterization of Schwann Cells from Adult Human Skin and Nerve. *eNeuro* **2017**, *4*. [[CrossRef](#)]
11. Rutkowski, J.L.; Kirk, C.J.; Lerner, M.A.; Tennekoon, G.I. Purification and expansion of human Schwann cells in vitro. *Nat. Med.* **1995**, *1*, 80–83. [[CrossRef](#)] [[PubMed](#)]

12. Andersen, N.D.; Srinivas, S.; Piñero, G.; Monje, P.V. A rapid and versatile method for the isolation, purification and cryogenic storage of Schwann cells from adult rodent nerves. *Sci. Rep.* **2016**, *6*, 31781. [[CrossRef](#)] [[PubMed](#)]
13. Sulaiman, O.A.; Gordon, T. Role of chronic Schwann cell denervation in poor functional recovery after nerve injuries and experimental strategies to combat it. *Neurosurgery* **2009**, *65*, A105–A114. [[CrossRef](#)] [[PubMed](#)]
14. Cajal, S.R.y. Degeneration and Regeneration of the Nervous System. *Nature* **1930**, *125*, 230–231. [[CrossRef](#)]
15. Kidd, G.J.; Ohno, N.; Trapp, B.D. Biology of Schwann cells. *Handb. Clin. Neurol.* **2013**, *115*, 55–79. [[CrossRef](#)]
16. Mirsky, R.; Woodhoo, A.; Parkinson, D.B.; Arthur-Farraj, P.; Bhaskaran, A.; Jessen, K.R. Novel signals controlling embryonic Schwann cell development, myelination and dedifferentiation. *J. Peripher. Nerv. Syst.* **2008**, *13*, 122–135. [[CrossRef](#)]
17. Murinson, B.B.; Archer, D.R.; Li, Y.; Griffin, J.W. Degeneration of myelinated efferent fibers prompts mitosis in Remak Schwann cells of uninjured C-fiber afferents. *J. Neurosci.* **2005**, *25*, 1179–1187. [[CrossRef](#)]
18. Jessen, K.R.; Mirsky, R.; Lloyd, A.C. Schwann Cells: Development and Role in Nerve Repair. *Cold Spring Harb. Perspect. Biol.* **2015**, *7*, a020487. [[CrossRef](#)]
19. Webster, H.D. The geometry of peripheral myelin sheaths during their formation and growth in rat sciatic nerves. *J. Cell Biol.* **1971**, *48*, 348–367. [[CrossRef](#)]
20. Topilko, P.; Schneider-Maunoury, S.; Levi, G.; Baron-Van Evercooren, A.; Chennoufi, A.B.; Seitanidou, T.; Babinet, C.; Charnay, P. Krox-20 controls myelination in the peripheral nervous system. *Nature* **1994**, *371*, 796–799. [[CrossRef](#)]
21. Jessen, K.R.; Mirsky, R. The Success and Failure of the Schwann Cell Response to Nerve Injury. *Front. Cell. Neurosci.* **2019**, *13*, 1–14. [[CrossRef](#)] [[PubMed](#)]
22. Cattin, A.L.; Burden, J.J.; Van Emmenis, L.; Mackenzie, F.E.; Hoving, J.J.; Garcia Calavia, N.; Guo, Y.; McLaughlin, M.; Rosenberg, L.H.; Quereda, V.; et al. Macrophage-Induced Blood Vessels Guide Schwann Cell-Mediated Regeneration of Peripheral Nerves. *Cell* **2015**, *162*, 1127–1139. [[CrossRef](#)] [[PubMed](#)]
23. Jessen, K.R.; Mirsky, R. The repair Schwann cell and its function in regenerating nerves. *J. Physiol.* **2016**, *594*, 3521–3531. [[CrossRef](#)]
24. Richner, M.; Ulrichsen, M.; Elmegaard, S.L.; Dieu, R.; Pallesen, L.T.; Vaegter, C.B. Peripheral Nerve Injury Modulates Neurotrophin Signaling in the Peripheral and Central Nervous System. *Mol. Neurobiol.* **2014**, *50*, 945–970. [[CrossRef](#)] [[PubMed](#)]
25. Frostick, S.P.; Yin, Q.; Kemp, G.J. Schwann cells, neurotrophic factors, and peripheral nerve regeneration. *Microsurgery* **1998**, *18*, 397–405. [[CrossRef](#)]
26. Terenghi, G. Peripheral nerve regeneration and neurotrophic factors. *J. Anat.* **1999**, *194*, 1–14. [[CrossRef](#)] [[PubMed](#)]
27. Fawcett, J.W.; Keynes, R.J. Peripheral nerve regeneration. *Annu. Rev. Neurosci.* **1990**, *13*, 43–60. [[CrossRef](#)]
28. Jessen, K.R.; Mirsky, R. Signals that determine Schwann cell identity. *J. Anat.* **2002**, *200*, 367–376. [[CrossRef](#)]
29. Anderson, K.D.; Guest, J.D.; Dietrich, W.D.; Bartlett Bunge, M.; Curiel, R.; Dididze, M.; Green, B.A.; Khan, A.; Pearse, D.D.; Saraf-Lavi, E.; et al. Safety of Autologous Human Schwann Cell Transplantation in Subacute Thoracic Spinal Cord Injury. *J. Neurotrauma* **2017**, *34*, 2950–2963. [[CrossRef](#)]
30. Ma, M.S.; Boddeke, E.; Copray, S. Pluripotent Stem Cells for Schwann Cell Engineering. *Stem Cell Rev. Rep.* **2015**, *11*, 205–218. [[CrossRef](#)]
31. Rodríguez, F.J.; Verdú, E.; Ceballos, D.; Navarro, X. Nerve guides seeded with autologous schwann cells improve nerve regeneration. *Exp. Neurol.* **2000**, *161*, 571–584. [[CrossRef](#)] [[PubMed](#)]
32. Fansa, H.; Keilhoff, G. Comparison of different biogenic matrices seeded with cultured Schwann cells for bridging peripheral nerve defects. *Neurol. Res.* **2004**, *26*, 167–173. [[CrossRef](#)] [[PubMed](#)]
33. Llorens, F.; Gil, V.; del Río, J.A. Emerging functions of myelin-associated proteins during development, neuronal plasticity, and neurodegeneration. *FASEB J.* **2011**, *25*, 463–475. [[CrossRef](#)] [[PubMed](#)]
34. Zörner, B.; Schwab, M.E. Anti-Nogo on the go: From animal models to a clinical trial. *Ann. N. Y. Acad. Sci.* **2010**, *1198*, E22–E34. [[CrossRef](#)] [[PubMed](#)]
35. Barres, B.A.; Jacobson, M.D.; Schmid, R.; Sendtner, M.; Raff, M.C. Does oligodendrocyte survival depend on axons? *Curr. Biol.* **1993**, *3*, 489–497. [[CrossRef](#)]
36. Ludwin, S.K. Oligodendrocyte survival in Wallerian degeneration. *Acta Neuropathol.* **1990**, *80*, 184–191. [[CrossRef](#)]

37. Buffo, A.; Rite, I.; Tripathi, P.; Lepier, A.; Colak, D.; Horn, A.P.; Mori, T.; Götz, M. Origin and progeny of reactive gliosis: A source of multipotent cells in the injured brain. *Proc. Natl. Acad. Sci. USA* **2008**, *105*, 3581–3586. [[CrossRef](#)]
38. Pekny, M.; Pekna, M. Astrocyte intermediate filaments in CNS pathologies and regeneration. *J. Pathol.* **2004**, *204*, 428–437. [[CrossRef](#)]
39. Pineau, I.; Sun, L.; Bastien, D.; Lacroix, S. Astrocytes initiate inflammation in the injured mouse spinal cord by promoting the entry of neutrophils and inflammatory monocytes in an IL-1 receptor/MyD88-dependent fashion. *Brain. Behav. Immun.* **2010**, *24*, 540–553. [[CrossRef](#)]
40. Satake, K.; Matsuyama, Y.; Kamiya, M.; Kawakami, H.; Iwata, H.; Adachi, K.; Kiuchi, K. Nitric oxide via macrophage iNOS induces apoptosis following traumatic spinal cord injury. *Brain Res. Mol. Brain Res.* **2000**, *85*, 114–122. [[CrossRef](#)]
41. Antonios, J.P.; Farah, G.J.; Cleary, D.R.; Martin, J.R.; Ciacci, J.D.; Pham, M.H. Immunosuppressive mechanisms for stem cell transplant survival in spinal cord injury. *Neurosurg. Focus* **2019**, *46*, E9. [[CrossRef](#)] [[PubMed](#)]
42. Lavdas, A.A.; Papastefanaki, F.; Thomaidou, D.; Matsas, R. Schwann cell transplantation for CNS repair. *Curr. Med. Chem.* **2008**, *15*, 151–160. [[CrossRef](#)] [[PubMed](#)]
43. Franklin, R.J.; Blakemore, W.F. Requirements for Schwann cell migration within CNS environments: A viewpoint. *Int. J. Dev. Neurosci.* **1993**, *11*, 641–649. [[CrossRef](#)]
44. Hirano, A.; Zimmerman, H.M.; Levine, S. Electron microscopic observations of peripheral myelin in a central nervous system lesion. *Acta Neuropathol.* **1969**, *12*, 348–365. [[CrossRef](#)]
45. Gilmore, S.A.; Sims, T.J. Patterns of Schwann cell myelination of axons within the spinal cord. *J. Chem. Neuroanat.* **1993**, *6*, 191–199. [[CrossRef](#)]
46. Black, J.A.; Waxman, S.G.; Smith, K.J. Remyelination of dorsal column axons by endogenous Schwann cells restores the normal pattern of Nav1.6 and Kv1.2 at nodes of Ranvier. *Brain* **2006**, *129*, 1319–1329. [[CrossRef](#)]
47. Blakemore, W.F.; Franklin, R.J. Transplantation options for therapeutic central nervous system remyelination. *Cell Transplant.* **2000**, *9*, 289–294. [[CrossRef](#)]
48. Zawadzka, M.; Rivers, L.E.; Fancy, S.P.; Zhao, C.; Tripathi, R.; Jamen, F.; Young, K.; Goncharevich, A.; Pohl, H.; Rizzi, M.; et al. CNS-resident glial progenitor/stem cells produce Schwann cells as well as oligodendrocytes during repair of CNS demyelination. *Cell Stem Cell* **2010**, *6*, 578–590. [[CrossRef](#)]
49. Assinck, P.; Duncan, G.J.; Plemel, J.R.; Lee, M.J.; Stratton, J.A.; Manesh, S.B.; Liu, J.; Ramer, L.M.; Kang, S.H.; Bergles, D.E.; et al. Myelinogenic Plasticity of Oligodendrocyte Precursor Cells following Spinal Cord Contusion Injury. *J. Neurosci.* **2017**, *37*, 8635–8654. [[CrossRef](#)]
50. Monteiro de Castro, G.; Deja, N.A.; Ma, D.; Zhao, C.; Franklin, R.J. Astrocyte Activation via Stat3 Signaling Determines the Balance of Oligodendrocyte versus Schwann Cell Remyelination. *Am. J. Pathol.* **2015**, *185*, 2431–2440. [[CrossRef](#)]
51. Ulanska-Poutanen, J.; Mieczkowski, J.; Zhao, C.; Konarzewska, K.; Kaza, B.; Pohl, H.B.; Bugajski, L.; Kaminska, B.; Franklin, R.J.; Zawadzka, M. Injury-induced perivascular niche supports alternative differentiation of adult rodent CNS progenitor cells. *eLife* **2018**, *7*. [[CrossRef](#)] [[PubMed](#)]
52. Norenberg, M.D.; Smith, J.; Marcillo, A. The pathology of human spinal cord injury: Defining the problems. *J. Neurotrauma* **2004**, *21*, 429–440. [[CrossRef](#)] [[PubMed](#)]
53. Bruce, J.H.; Norenberg, M.D.; Kraydieh, S.; Puckett, W.; Marcillo, A.; Dietrich, D. Schwannosis: Role of gliosis and proteoglycan in human spinal cord injury. *J. Neurotrauma* **2000**, *17*, 781–788. [[CrossRef](#)] [[PubMed](#)]
54. Richardson, P.M.; McGuinness, U.M.; Aguayo, A.J. Axons from CNS neurons regenerate into PNS grafts. *Nature* **1980**, *284*, 264–265. [[CrossRef](#)]
55. Harvey, A.R.; Plant, G.W.; Tan, M.M. Schwann cells and the regrowth of axons in the mammalian CNS: A review of transplantation studies in the rat visual system. *Clin. Exp. Pharmacol. Physiol.* **1995**, *22*, 569–579. [[CrossRef](#)]
56. Bunge, M.B. Transplantation of purified populations of Schwann cells into lesioned adult rat spinal cord. *J. Neurol.* **1994**, *242*, S36–S39. [[CrossRef](#)]
57. Dezawa, M.; Nagano, T. Contacts between regenerating axons and the Schwann cells of sciatic nerve segments grafted to the optic nerve of adult rats. *J. Neurocytol.* **1993**, *22*, 1103–1112. [[CrossRef](#)]
58. Blight, A.R.; Young, W. Central axons in injured cat spinal cord recover electrophysiological function following remyelination by Schwann cells. *J. Neurol. Sci.* **1989**, *91*, 15–34. [[CrossRef](#)]
59. Bunge, R.P. The role of the Schwann cell in trophic support and regeneration. *J. Neurol.* **1994**, *242*, S19–S21. [[CrossRef](#)]

60. Ra, J.C.; Shin, I.S.; Kim, S.H.; Kang, S.K.; Kang, B.C.; Lee, H.Y.; Kim, Y.J.; Jo, J.Y.; Yoon, E.J.; Choi, H.J.; et al. Safety of intravenous infusion of human adipose tissue-derived mesenchymal stem cells in animals and humans. *Stem Cells Dev.* **2011**, *20*, 1297–1308. [[CrossRef](#)]
61. Halfpenny, C.; Benn, T.; Scolding, N. Cell transplantation, myelin repair, and multiple sclerosis. *Lancet Neurol.* **2002**, *1*, 31–40. [[CrossRef](#)]
62. Kocsis, J.D.; Waxman, S.G. Schwann cells and their precursors for repair of central nervous system myelin. *Brain* **2007**, *130*, 1978–1980. [[CrossRef](#)]
63. Woodhoo, A.; Sahni, V.; Gilson, J.; Setzu, A.; Franklin, R.J.; Blakemore, W.F.; Mirsky, R.; Jessen, K.R. Schwann cell precursors: A favourable cell for myelin repair in the Central Nervous System. *Brain* **2007**, *130*, 2175–2185. [[CrossRef](#)] [[PubMed](#)]
64. Lavdas, A.A.; Franceschini, I.; Dubois-Dalcq, M.; Matsas, R. Schwann cells genetically engineered to express PSA show enhanced migratory potential without impairment of their myelinating ability in vitro. *Glia* **2006**, *53*, 868–878. [[CrossRef](#)] [[PubMed](#)]
65. Papastefanaki, F.; Chen, J.; Lavdas, A.A.; Thomaidou, D.; Schachner, M.; Matsas, R. Grafts of Schwann cells engineered to express PSA-NCAM promote functional recovery after spinal cord injury. *Brain* **2007**, *130*, 2159–2174. [[CrossRef](#)]
66. Bunge, M.B. Efficacy of Schwann cell transplantation for spinal cord repair is improved with combinatorial strategies. *J. Physiol.* **2016**, *594*, 3533–3538. [[CrossRef](#)] [[PubMed](#)]
67. Chen, A.; Xu, X.M.; Kleitman, N.; Bunge, M.B. Methylprednisolone administration improves axonal regeneration into Schwann cell grafts in transected adult rat thoracic spinal cord. *Exp. Neurol.* **1996**, *138*, 261–276. [[CrossRef](#)]
68. Xu, X.M.; Guénard, V.; Kleitman, N.; Aebischer, P.; Bunge, M.B. A combination of BDNF and NT-3 promotes supraspinal axonal regeneration into Schwann cell grafts in adult rat thoracic spinal cord. *Exp. Neurol.* **1995**, *134*, 261–272. [[CrossRef](#)]
69. Takami, T.; Oudega, M.; Bates, M.L.; Wood, P.M.; Kleitman, N.; Bunge, M.B. Schwann cell but not olfactory ensheathing glia transplants improve hindlimb locomotor performance in the moderately contused adult rat thoracic spinal cord. *J. Neurosci.* **2002**, *22*, 6670–6681. [[CrossRef](#)]
70. Fouad, K.; Schnell, L.; Bunge, M.B.; Schwab, M.E.; Liebscher, T.; Pearse, D.D. Combining Schwann cell bridges and olfactory ensheathing glia grafts with chondroitinase promotes locomotor recovery after complete transection of the spinal cord. *J. Neurosci.* **2005**, *25*, 1169–1178. [[CrossRef](#)]
71. Pearse, D.D.; Pereira, F.C.; Marcillo, A.E.; Bates, M.L.; Berrocal, Y.A.; Filbin, M.T.; Bunge, M.B. cAMP and Schwann cells promote axonal growth and functional recovery after spinal cord injury. *Nat. Med.* **2004**, *10*, 610–616. [[CrossRef](#)] [[PubMed](#)]
72. Menei, P.; Montero-Menei, C.; Whittmore, S.R.; Bunge, R.P.; Bunge, M.B. Schwann cells genetically modified to secrete human BDNF promote enhanced axonal regrowth across transected adult rat spinal cord. *Eur. J. Neurosci.* **1998**, *10*, 607–621. [[CrossRef](#)] [[PubMed](#)]
73. Golden, K.L.; Pearse, D.D.; Blits, B.; Garg, M.S.; Oudega, M.; Wood, P.M.; Bunge, M.B. Transduced Schwann cells promote axon growth and myelination after spinal cord injury. *Exp. Neurol.* **2007**, *207*, 203–217. [[CrossRef](#)] [[PubMed](#)]
74. Flora, G.; Joseph, G.; Patel, S.; Singh, A.; Bleicher, D.; Barakat, D.J.; Louro, J.; Fenton, S.; Garg, M.; Bunge, M.B.; et al. Combining neurotrophin-transduced schwann cells and rolipram to promote functional recovery from subacute spinal cord injury. *Cell Transplant.* **2013**, *22*, 2203–2217. [[CrossRef](#)]
75. Fortun, J.; Hill, C.E.; Bunge, M.B. Combinatorial strategies with Schwann cell transplantation to improve repair of the injured spinal cord. *Neurosci. Lett.* **2009**, *456*, 124–132. [[CrossRef](#)]
76. Tetzlaff, W.; Okon, E.B.; Karimi-Abdolrezaee, S.; Hill, C.E.; Sparling, J.S.; Plemel, J.R.; Plunet, W.T.; Tsai, E.C.; Baptiste, D.; Smithson, L.J.; et al. A systematic review of cellular transplantation therapies for spinal cord injury. *J. Neurotrauma* **2011**, *28*, 1611–1682. [[CrossRef](#)]
77. Griffin, J.M.; Bradke, F. Therapeutic repair for spinal cord injury: Combinatory approaches to address a multifaceted problem. *EMBO Mol. Med.* **2020**, *12*, e11505. [[CrossRef](#)]
78. Terzis, J.; Faibisoff, B.; Williams, B. The nerve gap: Suture under tension vs. graft. *Plast. Reconstr. Surg.* **1975**, *56*, 166–170. [[CrossRef](#)]

79. Sarker, M.D.; Naghieh, S.; McInnes, A.D.; Schreyer, D.J.; Chen, X. Regeneration of peripheral nerves by nerve guidance conduits: Influence of design, biopolymers, cells, growth factors, and physical stimuli. *Prog. Neurobiol.* **2018**, *171*, 125–150. [[CrossRef](#)]
80. Gillon, R.S.; Cui, Q.; Dunlop, S.A.; Harvey, A.R. Effects of immunosuppression on regrowth of adult rat retinal ganglion cell axons into peripheral nerve allografts. *J. Neurosci. Res.* **2003**, *74*, 524–532. [[CrossRef](#)]
81. Fansa, H.; Keilhoff, G.; Horn, T.; Altmann, S.; Wolf, G.; Schneider, W. Stimulation of Schwann cell growth and axon regeneration of peripheral nerves by the immunosuppressive drug FK 506. *Handchir. Mikrochir. Plast. Chir.* **1999**, *31*, 323–329; discussion 330–322. [[CrossRef](#)] [[PubMed](#)]
82. Sosa, I.; Reyes, O.; Kuffler, D.P. Immunosuppressants: Neuroprotection and promoting neurological recovery following peripheral nerve and spinal cord lesions. *Exp. Neurol.* **2005**, *195*, 7–15. [[CrossRef](#)] [[PubMed](#)]
83. Dominici, M.; Le Blanc, K.; Mueller, I.; Slaper-Cortenbach, I.; Marini, F.; Krause, D.; Deans, R.; Keating, A.; Prockop, D.; Horwitz, E. Minimal criteria for defining multipotent mesenchymal stromal cells. The International Society for Cellular Therapy position statement. *Cytotherapy* **2006**, *8*, 315–317. [[CrossRef](#)]
84. Ayala-Cuellar, A.P.; Kang, J.H.; Jeung, E.B.; Choi, K.C. Roles of mesenchymal stem cells in tissue regeneration and immunomodulation. *Biomol. Ther.* **2019**, *27*, 25–33. [[CrossRef](#)]
85. Soria-Zavala, K.; Garcia-Sánchez, J.; Rodríguez-Barrera, R. Mesenchymal Stem Cells for Clinical Use after Spinal Cord Injury. *IntechOpen* **2020**.
86. Dezawa, M.; Takahashi, I.; Esaki, M.; Takano, M.; Sawada, H. Sciatic nerve regeneration in rats induced by transplantation of in vitro differentiated bone-marrow stromal cells. *Eur. J. Neurosci.* **2001**, *14*, 1771–1776. [[CrossRef](#)]
87. Woodbury, D.; Schwarz, E.J.; Prockop, D.J.; Black, I.B. Adult rat and human bone marrow stromal cells differentiate into neurons. *J. Neurosci. Res.* **2000**, *61*, 364–370. [[CrossRef](#)]
88. Takahashi, J.; Palmer, T.D.; Gage, F.H. Retinoic acid and neurotrophins collaborate to regulate neurogenesis in adult-derived neural stem cell cultures. *J. Neurobiol.* **1999**, *38*, 65–81. [[CrossRef](#)]
89. Shah, N.M.; Groves, A.K.; Anderson, D.J. Alternative neural crest cell fates are instructively promoted by TGFbeta superfamily members. *Cell* **1996**, *85*, 331–343. [[CrossRef](#)]
90. Chaudhary, L.R.; Avioli, L.V. Activation of extracellular signal-regulated kinases 1 and 2 (ERK1 and ERK2) by FGF-2 and PDGF-BB in normal human osteoblastic and bone marrow stromal cells: Differences in mobility and in-gel renaturation of ERK1 in human, rat, and mouse osteoblastic cells. *Biochem. Biophys. Res. Commun.* **1997**, *238*, 134–139. [[CrossRef](#)]
91. Kim, H.A.; Ratner, N.; Roberts, T.M.; Stiles, C.D. Schwann cell proliferative responses to cAMP and Nf1 are mediated by cyclin D1. *J. Neurosci.* **2001**, *21*, 1110–1116. [[CrossRef](#)] [[PubMed](#)]
92. Meyer-Franke, A.; Wilkinson, G.A.; Kruttgen, A.; Hu, M.; Munro, E.; Hanson, M.G., Jr.; Reichardt, L.F.; Barres, B.A. Depolarization and cAMP elevation rapidly recruit TrkB to the plasma membrane of CNS neurons. *Neuron* **1998**, *21*, 681–693. [[CrossRef](#)]
93. Tohill, M.; Mantovani, C.; Wiberg, M.; Terenghi, G. Rat bone marrow mesenchymal stem cells express glial markers and stimulate nerve regeneration. *Neurosci. Lett.* **2004**, *362*, 200–203. [[CrossRef](#)] [[PubMed](#)]
94. Caddick, J.; Kingham, P.J.; Gardiner, N.J.; Wiberg, M.; Terenghi, G. Phenotypic and functional characteristics of mesenchymal stem cells differentiated along a Schwann cell lineage. *Glia* **2006**, *54*, 840–849. [[CrossRef](#)] [[PubMed](#)]
95. Mahanthappa, N.K.; Anton, E.S.; Matthew, W.D. Glial Growth Factor 2, a Soluble Neuregulin, Directly Increases Schwann Cell Motility and Indirectly Promotes Neurite Outgrowth. *J. Neurosci.* **1996**, *16*, 4673–4683. [[CrossRef](#)] [[PubMed](#)]
96. Shah, N.M.; Marchionni, M.A.; Isaacs, I.; Stroobant, P.; Anderson, D.J. Glial growth factor restricts mammalian neural crest stem cells to a glial fate. *Cell* **1994**, *77*, 349–360. [[CrossRef](#)]
97. Krampera, M.; Marconi, S.; Pasini, A.; Galìè, M. Induction of neural-like differentiation in human mesenchymal stem cells derived from bone marrow, fat, spleen and thymus. *Bone* **2007**. [[CrossRef](#)] [[PubMed](#)]
98. Ariza, C.A.; Fleury, A.T.; Tormos, C.J.; Petruk, V.; Chawla, S.; Oh, J.; Sakaguchi, D.S.; Mallapragada, S.K. The Influence of Electric Fields on Hippocampal Neural Progenitor Cells. *Stem Cell Rev. Rep.* **2010**, *6*, 585–600. [[CrossRef](#)]

99. Pires, F.; Ferreira, Q.; Rodrigues, C.A.V.; Morgado, J.; Ferreira, F.C. Neural stem cell differentiation by electrical stimulation using a cross-linked PEDOT substrate: Expanding the use of biocompatible conjugated conductive polymers for neural tissue engineering. *Biochim. Biophys. Acta Gen. Subj.* **2015**, *1850*, 1158–1168. [[CrossRef](#)]
100. Stewart, E.; Kobayashi, N.R.; Higgins, M.J.; Quigley, A.F.; Jamali, S.; Moulton, S.E.; Kapsa, R.M.I.; Wallace, G.G.; Crook, J.M. Electrical stimulation using conductive polymer polypyrrole promotes differentiation of human neural stem cells: A biocompatible platform for translational neural tissue engineering. *Tissue Eng. Part C Methods* **2015**, *21*, 385–393. [[CrossRef](#)]
101. Das, S.R.; Uz, M.; Ding, S.; Lentner, M.T.; Hondred, J.A.; Cargill, A.A.; Sakaguchi, D.S.; Mallapragada, S.; Claussen, J.C. Electrical Differentiation of Mesenchymal Stem Cells into Schwann-Cell-Like Phenotypes Using Inkjet-Printed Graphene Circuits. *Adv. Healthc. Mater.* **2017**, *6*, 1601087. [[CrossRef](#)] [[PubMed](#)]
102. Thrivikraman, G.; Madras, G.; Basu, B. Intermittent electrical stimuli for guidance of human mesenchymal stem cell lineage commitment towards neural-like cells on electroconductive substrates. *Biomaterials* **2014**, *35*, 6219–6235. [[CrossRef](#)] [[PubMed](#)]
103. Park, J.E.; Seo, Y.K.; Yoon, H.H.; Kim, C.W.; Park, J.K.; Jeon, S. Electromagnetic fields induce neural differentiation of human bone marrow derived mesenchymal stem cells via ROS mediated EGFR activation. *Neurochem. Int.* **2013**, *62*, 418–424. [[CrossRef](#)] [[PubMed](#)]
104. Hammerick, K.E.; Longaker, M.T.; Prinz, F.B. In vitro effects of direct current electric fields on adipose-derived stromal cells. *Biochem. Biophys. Res. Commun.* **2010**, *397*, 12–17. [[CrossRef](#)] [[PubMed](#)]
105. Moosazadeh Moghaddam, M.; Bonakdar, S.; Shokrgozar, M.A.; Zaminy, A.; Vali, H.; Faghihi, S. Engineered substrates with imprinted cell-like topographies induce direct differentiation of adipose-derived mesenchymal stem cells into Schwann cells. *Artif. Cells Nanomed. Biotechnol.* **2019**, *47*, 1022–1035. [[CrossRef](#)]
106. Sharma, A.D.; Zbarska, S.; Petersen, E.M.; Marti, M.E.; Mallapragada, S.K.; Sakaguchi, D.S. Oriented growth and transdifferentiation of mesenchymal stem cells towards a Schwann cell fate on micropatterned substrates. *J. Biosci. Bioeng.* **2016**, *121*, 325–335. [[CrossRef](#)]
107. Yamamoto, K.; Sokabe, T.; Watabe, T.; Miyazono, K.; Yamashita, J.K.; Obi, S.; Ohura, N.; Matsushita, A.; Kamiya, A.; Ando, J. Fluid shear stress induces differentiation of Flk-1-positive embryonic stem cells into vascular endothelial cells in vitro. *Am. J. Physiol. Heart Circ. Physiol.* **2005**, *288*, H1915–H1924. [[CrossRef](#)]
108. Kurpinski, K.; Chu, J.; Hashi, C.; Li, S. Anisotropic mechanosensing by mesenchymal stem cells. *Proc. Natl. Acad. Sci. USA* **2006**, *103*, 16095–16100. [[CrossRef](#)]
109. Clause, K.C.; Liu, L.J.; Tobita, K. Directed stem cell differentiation: The role of physical forces. *Cell Commun. Adhes.* **2010**, *17*, 48–54. [[CrossRef](#)]
110. Gomez-Salazar, M.; Gonzalez-Galofre, Z.N.; Casamitjana, J.; Crisan, M.; James, A.W.; Péault, B. Five Decades Later, Are Mesenchymal Stem Cells Still Relevant? *Front. Bioeng. Biotechnol.* **2020**, *8*, 148. [[CrossRef](#)]
111. Brohlin, M.; Mahay, D.; Novikov, L.N.; Terenghi, G.; Wiberg, M.; Shawcross, S.G.; Novikova, L.N. Characterisation of human mesenchymal stem cells following differentiation into Schwann cell-like cells. *Neurosci. Res.* **2009**, *64*, 41–49. [[CrossRef](#)] [[PubMed](#)]
112. Park, H.W.; Lim, M.J.; Jung, H.; Lee, S.P.; Paik, K.S.; Chang, M.S. Human mesenchymal stem cell-derived Schwann cell-like cells exhibit neurotrophic effects, via distinct growth factor production, in a model of spinal cord injury. *Glia* **2010**. [[CrossRef](#)] [[PubMed](#)]
113. Saab, A.S.; Nave, K.A. Myelin dynamics: Protecting and shaping neuronal functions. *Curr. Opin. Neurobiol.* **2017**, *47*, 104–112. [[CrossRef](#)] [[PubMed](#)]
114. Mimura, T.; Dezawa, M.; Kanno, H.; Sawada, H.; Yamamoto, I. Peripheral nerve regeneration by transplantation of bone marrow stromal cell-derived Schwann cells in adult rats. *J. Neurosurg.* **2004**, *101*, 806–812. [[CrossRef](#)]
115. Wang, X.; Luo, E.; Li, Y.; Hu, J. Schwann-like mesenchymal stem cells within vein graft facilitate facial nerve regeneration and remyelination. *Brain Res.* **2011**, *1383*, 71–80. [[CrossRef](#)]
116. Shimizu, S.; Kitada, M.; Ishikawa, H.; Itokazu, Y.; Wakao, S.; Dezawa, M. Peripheral nerve regeneration by the in vitro differentiated-human bone marrow stromal cells with Schwann cell property. *Biochem. Biophys. Res. Commun.* **2007**, *359*, 915–920. [[CrossRef](#)]
117. Zaminy, A.A. Mesenchymal stem cells as an alternative for Schwann cells in rat spinal cord injury. *Iran. Biomed. J.* **2013**, *17*, 113–122. [[CrossRef](#)]

118. Galhom, R.A.; Hussein Abd El Raouf, H.H.; Mohammed Ali, M.H. Role of bone marrow derived mesenchymal stromal cells and Schwann-like cells transplantation on spinal cord injury in adult male albino rats. *Biomed. Pharmacother.* **2018**, *108*, 1365–1375. [[CrossRef](#)]
119. Biernaskie, J.; Sparling, J.S.; Liu, J.; Shannon, C.P.; Plemel, J.R.; Xie, Y.; Miller, F.D.; Tetzlaff, W. Skin-derived precursors generate myelinating Schwann cells that promote remyelination and functional recovery after contusion spinal cord injury. *J. Neurosci.* **2007**, *27*, 9545–9559. [[CrossRef](#)]
120. Shea, G.K.; Tsui, A.Y.; Chan, Y.S.; Shum, D.K. Bone marrow-derived Schwann cells achieve fate commitment—A prerequisite for remyelination therapy. *Exp. Neurol.* **2010**, *224*, 448–458. [[CrossRef](#)]
121. Cai, S.; Tsui, Y.P.; Tam, K.W.; Shea, G.K.; Chang, R.S.; Ao, Q.; Shum, D.K.; Chan, Y.S. Directed Differentiation of Human Bone Marrow Stromal Cells to Fate-Committed Schwann Cells. *Stem Cell Rep.* **2017**, *9*, 1097–1108. [[CrossRef](#)] [[PubMed](#)]
122. Sabatino, M.A.; Santoro, R.; Gueven, S.; Jaquiere, C.; Wendt, D.J.; Martin, I.; Moretti, M.; Barbero, A. Cartilage graft engineering by co-culturing primary human articular chondrocytes with human bone marrow stromal cells. *J. Tissue Eng. Regen. Med.* **2015**. [[CrossRef](#)] [[PubMed](#)]
123. Kern, S.; Eichler, H.; Stoeve, J.; Kluter, H.; Bieback, K. Comparative analysis of mesenchymal stem cells from bone marrow, umbilical cord blood, or adipose tissue. *Stem Cells* **2006**, *24*, 1294–1301. [[CrossRef](#)] [[PubMed](#)]
124. Ema, H.; Morita, Y.; Yamazaki, S.; Matsubara, A.; Seita, J.; Tadokoro, Y.; Kondo, H.; Takano, H.; Nakauchi, H. Adult mouse hematopoietic stem cells: Purification and single-cell assays. *Nat. Protoc.* **2006**, *1*, 2979–2987. [[CrossRef](#)]
125. Zuk, P.A.; Zhu, M.; Mizuno, H.; Huang, J.; Futrell, J.W.; Katz, A.J.; Benhaim, P.; Lorenz, H.P.; Hedrick, M.H. Multilineage cells from human adipose tissue: Implications for cell-based therapies. *Tissue Eng.* **2001**, *7*, 211–228. [[CrossRef](#)]
126. Kingham, P.J.; Kalbermatten, D.F.; Mahay, D.; Armstrong, S.J.; Wiberg, M.; Terenghi, G. Adipose-derived stem cells differentiate into a Schwann cell phenotype and promote neurite outgrowth in vitro. *Exp. Neurol.* **2007**, *207*, 267–274. [[CrossRef](#)]
127. di Summa, P.G.; Kalbermatten, D.F.; Raffoul, W.; Terenghi, G.; Kingham, P.J. Extracellular matrix molecules enhance the neurotrophic effect of Schwann cell-like differentiated adipose-derived stem cells and increase cell survival under stress conditions. *Tissue Eng. Part A* **2013**, *19*, 368–379. [[CrossRef](#)]
128. di Summa, P.G.; Kingham, P.J.; Raffoul, W.; Wiberg, M.; Terenghi, G.; Kalbermatten, D.F. Adipose-derived stem cells enhance peripheral nerve regeneration. *J. Plast. Reconstr. Aesthet. Surg.* **2010**, *63*, 1544–1552. [[CrossRef](#)]
129. Kaewkhaw, R.; Scutt, A.M.; Haycock, J.W. Anatomical Site Influences the Differentiation of Adipose-Derived Stem Cells for Schwann-Cell Phenotype and Function. *Glia* **2011**, *749*, 734–749. [[CrossRef](#)]
130. Faroni, A.; Terenghi, G.; Magnaghi, V. Expression of functional γ -aminobutyric acid type A receptors in schwann-like adult stem cells. *J. Mol. Neurosci.* **2012**, *47*, 619–630. [[CrossRef](#)]
131. Faroni, A.; Rothwell, S.W.; Grolla, A.A.a. Differentiation of adipose-derived stem cells into Schwann cell phenotype induces expression of P2X receptors that control cell death. *Cell Death Dis.* **2013**, *4*, e743. [[CrossRef](#)] [[PubMed](#)]
132. Tomita, K.; Madura, T.; Mantovani, C.; Terenghi, G. Differentiated adipose-derived stem cells promote myelination and enhance functional recovery in a rat model of chronic denervation. *J. Neurosci. Res.* **2012**, *90*, 1392–1402. [[CrossRef](#)] [[PubMed](#)]
133. Kingham, P.J.; Kolar, M.K.; Novikova, L.N.; Novikov, L.N.; Wiberg, M. Stimulating the neurotrophic and angiogenic properties of human adipose-derived stem cells enhances nerve repair. *Stem Cells Dev.* **2014**, *23*, 741–754. [[CrossRef](#)] [[PubMed](#)]
134. Tomita, K.; Madura, T.; Sakai, Y.; Yano, K.; Terenghi, G.; Hosokawa, K. Glial differentiation of human adipose-derived stem cells: Implications for cell-based transplantation therapy. *Neuroscience* **2013**, *16*, 55–65. [[CrossRef](#)] [[PubMed](#)]
135. Georgiou, M.; Golding, J.P.; Loughlin, A.J.; Kingham, P.J.; Phillips, J.B. Engineered neural tissue with aligned, differentiated adipose-derived stem cells promotes peripheral nerve regeneration across a critical sized defect in rat sciatic nerve. *Biomaterials* **2015**, *37*, 242–251. [[CrossRef](#)] [[PubMed](#)]
136. di Summa, P.G.; Kalbermatten, D.F.; Pralong, E.; Raffoul, W.; Kingham, P.J.; Terenghi, G. Long-term in vivo regeneration of peripheral nerves through bioengineered nerve grafts. *Neuroscience* **2011**, *181*, 278–291. [[CrossRef](#)]

137. Orbay, H.; Uysal, A.C.; Hyakusoku, H.; Mizuno, H. Differentiated and undifferentiated adipose-derived stem cells improve function in rats with peripheral nerve gaps. *J. Plast. Reconstr. Aesthet. Surg.* **2012**, *65*, 657–664. [\[CrossRef\]](#)
138. Zaminy, A.; Shokrgozar, M.A.; Sadeghi, Y.; Norouzian, M.; Heidari, M.H.; Piryaee, A. Transplantation of schwann cells differentiated from adipose stem cells improves functional recovery in rat spinal cord injury. *Arch. Iran. Med.* **2013**, *16*, 533–541.
139. Yang, L.; Fang, J.; Liao, D.; Wang, W. Schwann cells differentiated from adipose-derived stem cells for the treatment of brain contusion. *Mol. Med. Report.* **2014**, *9*, 567–573. [\[CrossRef\]](#)
140. Faroni, A.; Smith, R.J.P.; Lu, L.; Reid, A.J. Human Schwann-like cells derived from adipose-derived mesenchymal stem cells rapidly de-differentiate in the absence of stimulating medium. *Eur. J. Neurosci.* **2016**, *43*, 417–430. [\[CrossRef\]](#)
141. Topilko, P.; Murphy, P.; Charnay, P. Embryonic development of Schwann cells: Multiple roles for neuregulins along the pathway. *Mol. Cell. Neurosci.* **1996**, *8*, 71–75. [\[CrossRef\]](#)
142. Liu, Y.; Chen, J.; Liu, W.; Lu, X.; Liu, Z.; Zhao, X.; Li, G.; Chen, Z. A Modified Approach to Inducing Bone Marrow Stromal Cells to Differentiate into Cells with Mature Schwann Cell Phenotypes. *Stem Cells Dev.* **2016**, *25*, 347–359. [\[CrossRef\]](#) [\[PubMed\]](#)
143. Kang, Y.; Liu, Y.; Liu, Z.; Ren, S.; Xiong, H.; Chen, J.; Duscher, D.; Machens, H.G.; Liu, W.; Guo, G.; et al. Differentiated human adipose-derived stromal cells exhibit the phenotypic and functional characteristics of mature Schwann cells through a modified approach. *Cytotherapy* **2019**, *21*, 987–1003. [\[CrossRef\]](#)
144. Weiss, M.L.; Troyer, D.L. Stem cells in the umbilical cord. *Stem Cell Rev.* **2006**, *2*, 155–162. [\[CrossRef\]](#) [\[PubMed\]](#)
145. Lee, M.W.; Choi, J.; Yang, M.S.; Moon, Y.J.; Park, J.S.; Kim, H.C.; Kim, Y.J. Mesenchymal stem cells from cryopreserved human umbilical cord blood. *Biochem. Biophys. Res. Commun.* **2004**. [\[CrossRef\]](#) [\[PubMed\]](#)
146. Couto, P.S.; Shatirishvili, G.; Bersenev, A.; Verter, F. First decade of clinical trials and published studies with mesenchymal stromal cells from umbilical cord tissue. *Regen. Med.* **2019**, *14*, 309–319. [\[CrossRef\]](#) [\[PubMed\]](#)
147. Zhang, H.T.; Cheng, H.Y.; Zhang, L.; Fan, J.; Chen, Y.Z.; Jiang, X.D.; Xu, R.X. Umbilical cord blood cell-derived neurospheres differentiate into Schwann-like cells. *Neuroreport* **2009**. [\[CrossRef\]](#)
148. Xiao, Y.Z.; Wang, S. Differentiation of Schwannlike cells from human umbilical cord blood mesenchymal stem cells in vitro. *Mol. Med. Report.* **2015**, *11*, 1146–1152. [\[CrossRef\]](#)
149. Lassing, I.; Mellström, K.; Nistr, M. Comparison of PDGF-AA- and PDGF-BB-induced phosphoinositide formation in human and mouse fibroblasts. *Exp. Cell Res.* **1994**, *211*, 286–295. [\[CrossRef\]](#)
150. Benoit, B.O.; Savarese, T.; Joly, M.; Engstrom, C.M.; Pang, L.; Reilly, J.; Recht, L.D.; Ross, A.H.; Quesenberry, P.J. Neurotrophin channeling of neural progenitor cell differentiation. *J. Neurobiol.* **2001**, *46*, 265–280. [\[CrossRef\]](#)
151. Sung, M.A.; Jung, H.J.; Lee, J.W.; Lee, J.Y.; Pang, K.M.; Yoo, S.B.; Alrashdan, M.S.; Kim, S.M.; Jahng, J.W.; Lee, J.H. Human umbilical cord blood-derived mesenchymal stem cells promote regeneration of crush-injured rat sciatic nerves. *Neural Regen. Res.* **2012**, *7*, 2018–2027. [\[CrossRef\]](#) [\[PubMed\]](#)
152. Dasari, V.R.; Spomar, D.G.; Gondi, C.S.; Sloffer, C.A.; Saving, K.L.; Gujrati, M.; Rao, J.S.; Dinh, D.H. Axonal remyelination by cord blood stem cells after spinal cord injury. *J. Neurotrauma* **2007**, *24*, 391–410. [\[CrossRef\]](#) [\[PubMed\]](#)
153. Cui, B.; Li, E.; Yang, B.; Wang, B. Human umbilical cord blood-derived mesenchymal stem cell transplantation for the treatment of spinal cord injury. *Exp. Ther. Med.* **2014**, *7*, 1233–1236. [\[CrossRef\]](#) [\[PubMed\]](#)
154. Berebichez-Fridman, R.; Montero-Olvera, P.R. Sources and Clinical Applications of Mesenchymal Stem Cells: State-of-the-art review. *Sultan Qaboos Univ. Med. J.* **2018**, *18*, e264–e277. [\[CrossRef\]](#)
155. Peng, J.; Wang, Y.; Zhang, L.; Zhao, B.; Zhao, Z.; Chen, J.F.; Guo, Q.Y.; Liu, S.Y.; Sui, X.; Xu, W.J.; et al. Human umbilical cord Wharton’s jelly-derived mesenchymal stem cells differentiate into a Schwann-cell phenotype and promote neurite outgrowth in vitro. *Brain Res. Bull.* **2011**. [\[CrossRef\]](#)
156. Matsuse, D.; Kitada, M.; Kohama, M.; Nishikawa, K.; Makinoshima, H.; Wakao, S.; Fujiyoshi, Y.; Heike, T.; Nakahata, T.; Akutsu, H.; et al. Human umbilical cord-derived mesenchymal stromal cells differentiate into functional Schwann cells that sustain peripheral nerve regeneration. *J. Neuropathol. Exp. Neurol.* **2010**, *69*, 973–985. [\[CrossRef\]](#)
157. Krupa, P.; Vackova, I.; Ruzicka, J.; Zaviskova, K.; Dubisova, J.; Koci, Z.; Turnovcova, K.; Urdzikova, L.M.; Kubinova, S.; Rehak, S.; et al. The Effect of Human Mesenchymal Stem Cells Derived from Wharton’s Jelly in Spinal Cord Injury Treatment Is Dose-Dependent and Can Be Facilitated by Repeated Application. *Int. J. Mol. Sci.* **2018**, *19*, 1503. [\[CrossRef\]](#)

158. Chudickova, M.; Vackova, I.; Machova Urdzikova, L.; Jancova, P.; Kekulova, K.; Rehorova, M.; Turnovcova, K.; Jendelova, P.; Kubinova, S. The Effect of Wharton Jelly-Derived Mesenchymal Stromal Cells and Their Conditioned Media in the Treatment of a Rat Spinal Cord Injury. *Int. J. Mol. Sci.* **2019**, *20*, 4516. [[CrossRef](#)]
159. Cheng, H.; Liu, X.; Hua, R.; Dai, G.; Wang, X.; Gao, J.; An, Y. Clinical observation of umbilical cord mesenchymal stem cell transplantation in treatment for sequelae of thoracolumbar spinal cord injury. *J. Transl. Med.* **2014**, *12*, 253. [[CrossRef](#)]
160. Qu, J.; Zhang, H. Roles of Mesenchymal Stem Cells in Spinal Cord Injury. *Stem Cells Int.* **2017**, *2017*, 5251313. [[CrossRef](#)]
161. Kalaszczynska, I.; Ferdyn, K. Wharton's jelly derived mesenchymal stem cells: Future of regenerative medicine? Recent findings and clinical significance. *Biomed. Res. Int.* **2015**, *2015*, 430847. [[CrossRef](#)] [[PubMed](#)]
162. Blanpain, C.; Fuchs, E. Epidermal homeostasis: A balancing act of stem cells in the skin. *Nat. Rev. Mol. Cell Biol.* **2009**, *10*, 207–217. [[CrossRef](#)]
163. Yang, R.; Xu, X. Isolation and Culture of Neural Crest Stem Cells from Human Hair Follicles. *J. Vis. Exp.* **2013**. [[CrossRef](#)] [[PubMed](#)]
164. Sieber-Blum, M.; Grim, M.; Hu, Y.F.; Szeder, V. Pluripotent neural crest stem cells in the adult hair follicle. *Dev. Dyn.* **2004**, *231*, 258–269. [[CrossRef](#)] [[PubMed](#)]
165. Biernaskie, J. Human hair follicles: "bulging" with neural crest-like stem cells. *J. Investig. Dermatol.* **2010**, *130*, 1202–1204. [[CrossRef](#)] [[PubMed](#)]
166. Yu, H.; Fang, D.; Kumar, S.M.; Li, L.; Nguyen, T.K.; Acs, G.; Herlyn, M.; Xu, X. Isolation of a novel population of multipotent adult stem cells from human hair follicles. *Am. J. Pathol.* **2006**, *168*, 1879–1888. [[CrossRef](#)]
167. Fernandes, K.J.L.; McKenzie, I.A.; Mill, P.; Smith, K.M.; Akhavan, M.; Barnab-Heider, F.; Biernaskie, J.; Junek, A.; Kobayashi, N.R.; Toma, J.G.; et al. A dermal niche for multipotent adult skin-derived precursor cells. *Nat. Cell Biol.* **2004**, *6*, 1082–1093. [[CrossRef](#)]
168. Ni, Y.; Zhang, K.; Liu, X.; Yang, T.; Wang, B.; Fu, L.; A, L.; Zhou, Y. miR-21 promotes the differentiation of hair follicle-derived neural crest stem cells into Schwann cells. *Neural. Regen. Res.* **2014**, *9*, 828–836. [[CrossRef](#)]
169. Sakaue, M.; Sieber-Blum, M. Human epidermal neural crest stem cells as a source of schwann cells. *Development (Cambridge)* **2015**, *142*, 3188–3197. [[CrossRef](#)]
170. Clewes, O.; Narytnyk, A.; Gillinder, K.R.; Loughney, A.D.; Murdoch, A.P.; Sieber-Blum, M. Human epidermal neural crest stem cells (hEPI-NCSC)—characterization and directed differentiation into osteocytes and melanocytes. *Stem Cell Rev. Rep.* **2011**, *7*, 799–814. [[CrossRef](#)]
171. Du, J.; Chen, H.; Zhou, K.; Jia, X. Quantitative Multimodal Evaluation of Passaging Human Neural Crest Stem Cells for Peripheral Nerve Regeneration. *Stem Cell Rev. Rep.* **2018**, *14*, 92–100. [[CrossRef](#)] [[PubMed](#)]
172. Jones, I.; Novikov, L.N.; Renardy, M.; Kingham, P.J. Regenerative effects of human embryonic stem cell-derived neural crest cells for treatment of peripheral nerve injury. *J. Tissue Eng. Regen. Med.* **2018**. [[CrossRef](#)] [[PubMed](#)]
173. Kimura, H.; Ouchi, T.; Shibata, S.; Amemiya, T.; Nagoshi, N.; Nakagawa, T.; Matsumoto, M.; Okano, H.; Nakamura, M.; Sato, K. Stem cells purified from human induced pluripotent stem cell-derived neural crest-like cells promote peripheral nerve regeneration. *Sci. Rep.* **2018**, *8*, 10071. [[CrossRef](#)]
174. Amoh, Y.; Kanoh, M.; Niiyama, S.; Hamada, Y.; Kawahara, K.; Sato, Y.; Hoffman, R.M.; Katsuoka, K. Human hair follicle pluripotent stem (hfPS) cells promote regeneration of peripheral-nerve injury: An advantageous alternative to ES and iPS cells. *J. Cell. Biochem.* **2009**, *107*, 1016–1020. [[CrossRef](#)] [[PubMed](#)]
175. Amoh, Y.; Li, L.; Katsuoka, K.; Hoffman, R.M. Multipotent nestin-expressing hair follicle stem cells. *J. Dermatol.* **2009**, *36*, 1–9. [[CrossRef](#)]
176. Amoh, Y.; Li, L.; Katsuoka, K.; Hoffman, R.M. Multipotent hair follicle stem cells promote repair of spinal cord injury and recovery of walking function. *Cell Cycle* **2008**, *7*, 1865–1869. [[CrossRef](#)] [[PubMed](#)]
177. Hu, Y.F.; Gourab, K.; Wells, C.; Clewes, O.; Schmit, B.D.; Sieber-Blum, M. Epidermal neural crest stem cell (EPI-NCSC)—mediated recovery of sensory function in a mouse model of spinal cord injury. *Stem Cell Rev. Rep.* **2010**, *6*, 186–198. [[CrossRef](#)]
178. McKenzie, I.A.; Biernaskie, J.; Toma, J.G.; Midha, R.; Miller, F.D. Skin-derived precursors generate myelinating Schwann cells for the injured and dysmyelinated nervous system. *J. Neurosci.* **2006**, *26*, 6651–6660. [[CrossRef](#)]

179. Toma, J.G.; Akhavan, M.; Fernandes, K.J.; Barnabé-Heider, F.; Sadikot, A.; Kaplan, D.R.; Miller, F.D. Isolation of multipotent adult stem cells from the dermis of mammalian skin. *Nat. Cell Biol.* **2001**, *3*, 778–784. [[CrossRef](#)]
180. Toma, J.G.; McKenzie, I.A.; Bagli, D.; Miller, F.D. Isolation and Characterization of Multipotent Skin-Derived Precursors from Human Skin. *Stem Cells* **2005**, *23*, 727–737. [[CrossRef](#)]
181. Biernaskie, J.; Paris, M.; Morozova, O.; Fagan, B.M.; Marra, M.; Pevny, L.; Miller, F.D. SKPs derive from hair follicle precursors and exhibit properties of adult dermal stem cells. *Cell Stem Cell* **2009**, *5*, 610–623. [[CrossRef](#)] [[PubMed](#)]
182. Krause, M.P.; Dworski, S.; Feinberg, K.; Jones, K.; Johnston, A.P.W.; Paul, S.; Paris, M.; Peles, E.; Bagli, D.; Forrest, C.R.; et al. Direct genesis of functional rodent and human schwann cells from skin mesenchymal precursors. *Stem Cell Rep.* **2014**, *3*, 85–100. [[CrossRef](#)] [[PubMed](#)]
183. Khuong, H.T.; Kumar, R.; Senjaya, F.; Grochmal, J.; Ivanovic, A.; Shakhbazau, A.; Forden, J.; Webb, A.; Biernaskie, J.; Midha, R. Skin derived precursor Schwann cells improve behavioral recovery for acute and delayed nerve repair. *Exp. Neurol.* **2014**, *254*, 168–179. [[CrossRef](#)] [[PubMed](#)]
184. Yandava, B.D.; Billingham, L.L.; Snyder, E.Y. "Global" cell replacement is feasible via neural stem cell transplantation: Evidence from the dysmyelinated shiverer mouse brain. *Proc. Natl. Acad. Sci. USA* **1999**, *96*, 7029–7034. [[CrossRef](#)]
185. Sparling, J.S.; Bretzner, F.; Biernaskie, J.; Assinck, P.; Jiang, Y.; Arisato, H.; Plunet, W.T.; Borisoff, J.; Liu, J.; Miller, F.D.; et al. Schwann cells generated from neonatal skin-derived precursors or neonatal peripheral nerve improve functional recovery after acute transplantation into the partially injured cervical spinal cord of the rat. *J. Neurosci.* **2015**, *35*, 6714–6730. [[CrossRef](#)]
186. Assinck, P.; Sparling, J.S.; Dworski, S.; Duncan, G.J.; Wu, D.L.; Liu, J.; Kwon, B.K.; Biernaskie, J.; Miller, F.D.; Tetzlaff, W. Transplantation of Skin Precursor-Derived Schwann Cells Yields Better Locomotor Outcomes and Reduces Bladder Pathology in Rats with Chronic Spinal Cord Injury. *Stem Cell Rep.* **2020**, *15*, 140–155. [[CrossRef](#)]
187. Ruetze, M.; Knauer, T.; Gallinat, S.; Wenck, H.; Achterberg, V.; Maerz, A.; Deppert, W.; Knott, A. A novel niche for skin derived precursors in non-follicular skin. *J. Dermatol. Sci.* **2013**, *69*, 132–139. [[CrossRef](#)]
188. Yoshikawa, K.; Naitoh, M.; Kubota, H.; Ishiko, T.; Aya, R.; Yamawaki, S.; Suzuki, S. Multipotent stem cells are effectively collected from adult human cheek skin. *Biochem. Biophys. Res. Commun.* **2013**, *431*, 104–110. [[CrossRef](#)]
189. Dai, R.; Hua, W.; Xie, H.; Chen, W.; Xiong, L.; Li, L. The Human Skin-Derived Precursors for Regenerative Medicine: Current State, Challenges, and Perspectives. *Stem Cells Int.* **2018**, *2018*, 8637812. [[CrossRef](#)]
190. Okita, K.; Ichisaka, T.; Yamanaka, S. Generation of germline-competent induced pluripotent stem cells. *Nature* **2007**, *448*, 313–317. [[CrossRef](#)]
191. Maherali, N.; Sridharan, R.; Xie, W.; Utikal, J.; Eminli, S.; Arnold, K.; Stadtfeld, M.; Yachechko, R.; Tchieu, J.; Jaenisch, R.; et al. Directly Reprogrammed Fibroblasts Show Global Epigenetic Remodeling and Widespread Tissue Contribution. *Cell Stem Cell* **2007**, *1*, 55–70. [[CrossRef](#)] [[PubMed](#)]
192. Evans, M.J.; Kaufman, M.H. Establishment in culture of pluripotential cells from mouse embryos. *Nature* **1981**, *292*, 154–156. [[CrossRef](#)] [[PubMed](#)]
193. Thomson, J.A. Embryonic stem cell lines derived from human blastocysts. *Science* **1998**, *282*, 1145–1147. [[CrossRef](#)] [[PubMed](#)]
194. Perrier, A.L.; Tabar, V.; Barberi, T.; Rubio, M.E.; Bruses, J.; Topf, N.; Harrison, N.L.; Studer, L. Derivation of midbrain dopamine neurons from human embryonic stem cells. *Proc. Natl. Acad. Sci. USA* **2004**, *101*, 12543–12548. [[CrossRef](#)]
195. Pomp, O.; Brokhman, I.; Ziegler, L.; Almog, M.; Korngreen, A.; Tavian, M.; Goldstein, R.S. PA6-induced human embryonic stem cell-derived neurospheres: A new source of human peripheral sensory neurons and neural crest cells. *Brain Res.* **2008**, *1230*, 50–60. [[CrossRef](#)]
196. Rathjen, J.; Haines, B.P.; Hudson, K.M.; Nesci, A.; Dunn, S.; Rathjen, P.D. Directed differentiation of pluripotent cells to neural lineages: Homogeneous formation and differentiation of a neuroectoderm population. *Development* **2002**, *129*, 2649–2661.
197. Pomp, O.; Brokhman, I.; Ben-Dor, I.; Reubinoff, B.; Goldstein, R.S. Generation of Peripheral Sensory and Sympathetic Neurons and Neural Crest Cells from Human Embryonic Stem Cells. *Stem Cells* **2005**, *23*, 923–930. [[CrossRef](#)]

198. Eldridge, C.F.; Bunge, M.B.; Bunge, R.P.; Wood, P.M. Differentiation of axon-related Schwann cells in vitro. I. Ascorbic acid regulates basal lamina assembly and myelin formation. *J. Cell Biol.* **1987**, *105*, 1023–1034. [[CrossRef](#)]
199. Liu, Q.; Spusta, S.C.; Mi, R.; Lassiter, R.N.T.; Stark, M.R.; Hke, A.; Rao, M.S.; Zeng, X. Human Neural Crest Stem Cells Derived from Human ESCs and Induced Pluripotent Stem Cells: Induction, Maintenance, and Differentiation into Functional Schwann Cells. *STEM CELLS Transl. Med.* **2012**, *1*, 266–278. [[CrossRef](#)]
200. Ziegler, L.; Grigoryan, S.; Yang, I.H.; Thakor, N.V.; Goldstein, R.S. Efficient Generation of Schwann Cells from Human Embryonic Stem Cell-Derived Neurospheres. *Stem Cell Reviews and Reports* **2011**, *7*, 394–403. [[CrossRef](#)]
201. Lee, G.; Kim, H.; Elkabetz, Y.A. Isolation and directed differentiation of neural crest stem cells derived from human embryonic stem cells. *Nat. Biotechnol.* **2007**, *25*, 1468–1475. [[CrossRef](#)] [[PubMed](#)]
202. Li, W.; Sun, W.; Zhang, Y.; Wei, W.; Ambasadhan, R.; Xia, P.; Talantova, M.; Lin, T.; Kim, J.; Wang, X.; et al. Rapid induction and long-term self-renewal of primitive neural precursors from human embryonic stem cells by small molecule inhibitors. *Proc. Natl. Acad. Sci. USA* **2011**, *108*, 8299–8304. [[CrossRef](#)] [[PubMed](#)]
203. Smith, J.R.; Vallier, L.; Lupo, G.; Alexander, M.; Harris, W.A.; Pedersen, R.A. Inhibition of Activin/Nodal signaling promotes specification of human embryonic stem cells into neuroectoderm. *Dev. Biol.* **2008**, *313*, 107–117. [[CrossRef](#)] [[PubMed](#)]
204. Kim, H.S.; Lee, J.; Lee, D.Y.; Kim, Y.D.; Kim, J.Y.; Lim, H.J.; Lim, S.; Cho, Y.S. Schwann Cell Precursors from Human Pluripotent Stem Cells as a Potential Therapeutic Target for Myelin Repair. *Stem Cell Reports* **2017**, *8*, 1714–1726. [[CrossRef](#)]
205. Melino, G. p53 is a suppressor of tumorigenesis and metastasis interacting with mutant p53. *Cell Death Differ.* **2011**, *18*, 1487–1499. [[CrossRef](#)]
206. Li, J.Y.; Christophersen, N.S.; Hall, V.; Soulet, D.; Brundin, P. Critical issues of clinical human embryonic stem cell therapy for brain repair. *Trends Neurosci.* **2008**, *31*, 146–153. [[CrossRef](#)]
207. Sowa, Y.; Kishida, T.; Tomita, K.; Yamamoto, K.; Numajiri, T.; Mazda, O. Direct conversion of human fibroblasts into schwann cells that facilitate regeneration of injured peripheral nerve in vivo. *Stem Cells Transl. Med.* **2017**, *6*, 1207–1216. [[CrossRef](#)]
208. Yamamoto, K.; Kishida, T.; Sato, Y.; Nishioka, K.; Ejima, A.; Fujiwara, H.; Kubo, T.; Yamamoto, T.; Kanamura, N.; Mazda, O. Direct conversion of human fibroblasts into functional osteoblasts by defined factors. *Proc. Natl. Acad. Sci. USA* **2015**, *112*, 6152–6157. [[CrossRef](#)]
209. Pang, Z.P.; Yang, N.; Vierbuchen, T.; Ostermeier, A.; Fuentes, D.R.; Yang, T.Q.; Citri, A.; Sebastiano, V.; Marro, S.; Sdhof, T.C.; et al. Induction of human neuronal cells by defined transcription factors. *Nature* **2011**, *476*, 220–223. [[CrossRef](#)]
210. Mazzara, P.G.; Massimino, L.; Pellegatta, M.; Ronchi, G.; Ricca, A.; Iannielli, A.; Giannelli, S.G.; Cursi, M.; Cancellieri, C.; Sessa, A.a. Two factor-based reprogramming of rodent and human fibroblasts into Schwann cells. *Nature Commun.* **2017**, *8*. [[CrossRef](#)]
211. Smyth Templeton, N.; Zwaka, T. Use of Genetically Modified Stem Cells in Experimental Gene Therapies. *Gene Cell Ther.* **2008**. [[CrossRef](#)]
212. Sulaiman, O.A.; Gordon, T. Effects of short- and long-term Schwann cell denervation on peripheral nerve regeneration, myelination, and size. *Glia* **2000**, *32*, 234–246. [[CrossRef](#)]
213. Mendonça, M.V.; Laroocca, T.F.; de Freitas Souza, B.S.; Villarreal, C.F.; Silva, L.F.; Matos, A.C.; Novaes, M.A.; Bahia, C.M.; de Oliveira Melo Martinez, A.C.; Kaneto, C.M.; et al. Safety and neurological assessments after autologous transplantation of bone marrow mesenchymal stem cells in subjects with chronic spinal cord injury. *Stem Cell. Res. Ther.* **2014**, *5*, 126. [[CrossRef](#)] [[PubMed](#)]
214. Oh, S.K.; Choi, K.H.; Yoo, J.Y.; Kim, D.Y.; Kim, S.J.; Jeon, S.R. A Phase III Clinical Trial Showing Limited Efficacy of Autologous Mesenchymal Stem Cell Therapy for Spinal Cord Injury. *Neurosurgery* **2016**, *78*, 436–447; discussion 447. [[CrossRef](#)] [[PubMed](#)]



© 2020 by the authors. Licensee MDPI, Basel, Switzerland. This article is an open access article distributed under the terms and conditions of the Creative Commons Attribution (CC BY) license (<http://creativecommons.org/licenses/by/4.0/>).

Second project:

***In-vitro* neuromodulation targeting microglia activity**

Alois Conradin Hopf

Supervisors: Dr. Bekim Osmani, Dr. Catherine Brégère

Patents:

Tissue regeneration patch and corresponding fabrication process⁶

Inventors: Bekim Osmani, Raphael Guzman, Tino Töpfer, Bert Müller, Carina Luchsinger

Salinas, **Alois Hopf**, Mahyar Joodaki

Submitted to the European Patent Office, Application No.: EP21172804.3

Submission date: 07. May 2021

Neural implant based on a cellulose thin film and corresponding fabrication process³

Inventors: Bekim Osmani, Raphael Guzman, Tino Töpfer, Bert Müller, Carina Luchsinger

Salinas, **Alois Hopf**, Mahyar Joodaki

Submitted to the European Patent Office, Application No.: EP21172809.2

Submission date: 07. May 2021

Spin-Off company:

Bottneuro AG

„Digital solutions for Alzheimer’s patients”

Founders: Bekim Osmani, Tino Töpfer, Bert Müller, Pascal Brenneisen, Rolf Wildermuth,

Alois Hopf, Raphael Guzman, Cornelia Gut-Villa, Guido Sigron, Magnus Kristiansen

Incorporation date: 20. January 2021

Abstract

Chronic neuroinflammation is prevalent in various neurodegenerative diseases and chronic health conditions such as Alzheimer's Disease (AD) and chronic pain. Neuromodulation therapies has been successful in treating neuroinflammation by suppressing microglia activity using defined stimulation parameters *in-vivo*. The benefits of neuromodulation are mainly attributed to direct effects on neuronal excitability or modulation of neuronal networks followed by indirect effects on glia cells only. However, recent developments indicate a direct effect of electric fields on microglia activity. During this project an *in-vitro* neuromodulation device was developed to electrically stimulate microglia directly in a controlled cell culture environment. Using this newly developed device microglia activity was modulated. Applying alternate current (AC) at 40 Hz suppressed microglia activity and reduced secretion of pro-inflammatory cytokines. This effect is specific to the stimulation protocol and cannot be replicated using direct current (DC) stimulation. Based on the demonstrated impact on microglia activity, we expect that the progression of neuroinflammation can be suppressed by 40 Hz AC stimulation which brings lasting benefits to patients suffering from conditions related to chronic neuroinflammation. Therefore, Bottneuro, a Spin-Off company from the University of Basel was founded. Bottneuro focuses on non-invasive brain stimulation targeting microglia to reduce their inflammatory activity and suppress the release of neurotoxic compounds in AD patients.

Introduction

Microglia

Microglia are the primary immune cells of the CNS. Depending on the anatomical region, they account for up to 15% of the cells in the mammalian CNS^{59,60}. The key roles of microglia are immune surveillance, pathogen clearance and neuronal and glial maintenance. Different to other glia cells in the CNS, namely astrocytes and oligodendrocytes which are derived from the neuroectoderm, microglia are tissue-resident macrophages which are derived from the mesoderm during embryonic development⁶¹. Tissue macrophage haematopoiesis occurs in two waves during rodent embryonic development. First, primitive haematopoiesis in the extraembryonic yolk sac as first source of hematopoietic progenitor cells before establishing of blood circulation. This primitive haematopoiesis provides erythromyeloid precursors (EMP) which seed the developing CNS^{62,63}. Second, definitive haematopoiesis where the fetal liver provides the bulk of tissue macrophage precursors and hematopoietic stem/progenitor cells which will then give rise to all mature blood and immune cells^{62,64}. Microglia arise solely from EMP from the first wave of primitive haematopoiesis and is dependent on the transcription factors PU.1, IRF8 and SALL1^{65,66}. Whereas peripheral monocytes, macrophages and hematopoietic stem cell development is Myb dependent⁶⁵. Adult microglia are long lived cells with a relatively low proliferation capacity under homeostatic conditions. However, during neurodegeneration induced by certain CNS insults, microglia can self-renew and undergo clonal expansion^{67,68}. Microglia as innate immune cells in the CNS play an important role in CNS homeostasis. Distinct phenotypic subpopulations with distinct biological functions in response to environmental cues have been defined in *in-vitro* settings. Microglia are classically activated into M1 state in response to Lipopolysaccharide (LPS) and Interferon (IFN)- γ exposure. This shift from a quiescent to an activated state leads to the release of a wide range of pro-inflammatory mediators such as interleukin (IL)-1 β , Tumour Necrosis Factors (TNF), IL-6 and reactive oxygen species (ROS) contributing to chronic neuroinflammation⁶⁹. Exposure to interleukin (IL)-4 leads to alternative activation of M2 microglia which release cytokines and mediators such as IL-4, IL-13, IL-10 related to resolving inflammation, phagocytosis of harmful substances and wound healing⁷⁰. Traditionally, the M1 pro-inflammatory and M2 anti-inflammatory phenotypes are considered extreme activation states of microglia in response to environmental cues. Although useful for certain applications, this simplistic M1/M2 microglia activation model is considered outdated nowadays⁷¹⁻⁷³. Recent transcriptomic analyses extend the current M1/M2 model to a spectrum model with at least nine distinct macrophage/microglia activation patterns displaying distinct biological functions⁷². Microglia

phagocytosis is described in a three-step model of the initial “find-me”, the subsequent “eat-me” and the final “digest-me” step⁷⁴. Damaged and dead cells release chemoattractant molecules which act as “find-me” signals under physiological conditions. These signals initiate chemotactic motility of microglia. Subsequently, an engulfment synapse is formed which internalizes the harmful particles and substances. Finally, the engulfed particles are degraded in phagolysosomes, which are formed by fusion of lysosomes and phagosomes⁷⁵. In addition to phagocytosis, proliferation and migration, microglia are important for synaptic plasticity, development of neural circuits, immune response and vascular development⁷⁶⁻⁸¹.

Microglia and Chronic Pain

Chronic pain is defined by the International Association for the study of pain as persistent pain for more than 3 months⁸². Chronic pain is a major health concern affecting up to 30% of the world’s population resulting in a significant economic burden⁸³. Acute pain, often due to acute inflammation has a biological relevance, namely to protect wounded tissue, remove harmful stimuli, initiate healing process and to restore tissue integrity. In contrast, chronic pain brings no biological benefit and results from a biological maladaptation. The persistency of pain, even after healing and resolving the initial source of pain indicates that chronic pain results from pathological changes of the nervous system functions⁸⁴. Chronic pain is characterized by spontaneous pain, evoked pain sensation as response to noxious (hyperalgesia) and non-noxious (allodynia) stimuli. Chronic pain is, at least partially maintained by central sensitization driven by neuroinflammation which leads to the described phenomena⁸⁵. Activity dependent release of glial activators like neurotransmitters, chemokines, proteases and WNT ligands by the central terminals of primary afferent neurons lead to neuroinflammation. The release of these activators results in microglia activation and proliferation which contributes to increased production and secretion of pro-inflammatory cytokines and chemokines in the dorsal root ganglia⁸⁶. In addition, microglia are involved in synaptic pruning especially of inhibitory synapses which results in an imbalance between excitation and inhibition⁸⁷. Thus, the induction of chronic pain after the initial pain source is healed can be explained by microgliosis and its impact on neuroplasticity and synaptogenesis. Further, the pro-inflammatory cytokines TNF, IL-1 β and IL-6 can modulate both excitatory and inhibitory signal transmission which leads to prolonged, even permanent central sensitization and chronic pain^{86,88}. The release of IL-1 β by activated microglia in the spinal dorsal horn influences central sensitization by enhancing glutamate release from the central terminalis of dorsal root ganglion neurons. TNF not only modulates neuronal excitability but also binds to its receptor on microglia and astrocytes themselves, resulting in a microglial activation loop^{89,90}. The main role of

IL-6 is activation of the JAK/STAT pathway on spinal cord microglia. The JAK/STAT pathway is essential in development and function of the innate and adaptive immune response and altered activation can be found in chronic neuroinflammation. Inhibition of the JAK/STAT pathway attenuates both mechanical allodynia and thermal hypersensitivity^{91,92}. Pharmacological suppression of microglia activation in the spinal cord was shown to significantly alleviate mechanical hypersensitivity^{93,94}.

Microglia modulation in chronic pain

Spinal Cord Stimulation (SCS) in chronic pain can reduce or even stop the need for opioid medication and is more cost-effective than pharmacological treatments^{95,96}. Spinal cord implants enter the epidural space and deliver mild electric currents, causing a hyperpolarization of the neurons and therefore masking the pain signal from reaching the brain. The mechanism is based on the gate control theory as described by Wall and Melzack in 1965. In brief, it states that stimulation of large diameter afferent nerve fibers can inhibit pain transmission of second-order neurons through gating at the substantia gelatinosa in the dorsal root ganglion of the spinal cord. By this, noxious signal transmission to the thalamus and cerebral cortex is suppressed⁹⁷. However, as previously described, microglia and astrocyte induced neuroinflammation is a key mechanism underlying chronic pain^{85,90,98,99}. Interestingly, the analgesic effect of SCS persists over the stimulation duration which indicates a different mode of action than masking nociceptive signal transmission solely^{100,101}. An explanation is given by the observed reduction of microglia (CD11b) and astrocytes (GFAP) activity marker in the spinal cord and the release of inhibitory neurotransmitter (GABA, serotonin, opioids) in the spinal dorsal horn^{100,102,103}. These inhibitory neurotransmitters can directly inhibit glia activity via GABAergic, serotonergic and opioidergic receptors expressed by microglia and astrocytes^{104,105}. Additionally, excitatory neurotransmitter such as glutamate can directly induce microglia activity and trigger the secretion of even more excitatory neurotransmitter by microglia which can result in perpetuation of the nociceptive response. In this case, inhibitory neurotransmitters reduce microglia activity indirectly by reducing neuronal release of excitatory neurotransmitters. The underlying mechanism explaining the lasting analgesic effect over the duration of the SCS therapy itself is expected to be a combination of the increased inhibitory neurotransmitter secretion leading to reduced microglia activity and the subsequent reduced central excitability¹⁰⁰.

Microglia and Alzheimer's Disease

Life expectancy has increased dramatically in industrialized countries, making us more vulnerable to many age-related diseases such as AD or Parkinson's disease. AD is characterized by cognitive decline due to two pathological hallmarks. First, the extracellular accumulation of amyloid- β ($A\beta$) forming dense plaques and second, intracellular neurofibrillary tangles composed of hyperphosphorylated tau protein bound to microtubuli¹⁰⁶. These pathological hallmarks result in proliferation and activation of microglia and reactive gliosis which leads to neurotoxicity and neuronal loss^{107,108}. Extracellular $A\beta$ is produced by cleavage of the membrane-bound amyloid precursor protein in neurons by intracellular α - or β -secretase, and cleavage within the transmembrane domain by γ -secretase. Following cleavage, soluble $A\beta$ accumulates in the extracellular space and eventually leads to insoluble aggregation and dense core plaques. This aggregation is β -secretase dependent. Soluble and insoluble $A\beta$ is potentially cleared by microglia via different mechanisms. Soluble $A\beta$ is cleared via macropinocytosis in microglia. Following uptake by microglia, soluble $A\beta$ is targeted for intracellular proteolytic degradation^{109,110}. Proteolytic degradation can be enhanced by the lipidation status of ApoE high-density lipoproteins¹¹¹. It was shown that therapeutic enhancement of ApoE production leads to beneficial outcomes in AD¹¹⁰. Clearance of insoluble $A\beta$ depends on a microglia surface receptors complex and the delivery of insoluble $A\beta$ to lysosomes¹¹². It could be shown that the presence of anti-inflammatory cytokines and mediators such as IL-4 leads to moderate microglia activation which have a neuroprotective effect by phagocytosis of insoluble $A\beta$, especially in early stages of AD^{113,114}. In early stages of AD, scavenger's receptor (SR) activation on microglia promotes $A\beta$ clearance and hinder disease progression¹¹⁵. However, microglia phagocytosis of $A\beta$ clearance does not occur rapidly enough and therefore leads to extracellular accumulation of $A\beta$ over time¹¹⁶. The persistent activation of CD36 receptor, FC receptors, toll-like receptors (TLR) and complement receptors advanced glycation end products (RAGE) increase insoluble $A\beta$ production and decreases $A\beta$ clearance^{112,117,118}. Microglia envelopment of $A\beta$ plaques and therefore continuing activation stimuli induce the secretion of pro-inflammatory cytokines TNF, IL-6, IL-1 β which blocks $A\beta$ phagocytosis in microglia and leads to chronic neuroinflammation^{108,119} (Figure 1). Additionally, the microglia dependent release of the pro-inflammatory cytokines IL-6, TNF and complement protein C1q induces the conversion of quiescent astrocytes into reactive, neurotoxic astrocytes¹²⁰. Further, C1q facilitate synapse and neurons removal by microglia during developmental and homeostasis¹²¹. Therefore, $A\beta$ -induced upregulation of C1q exacerbate AD pathology by inducing synapse elimination and neurodegeneration¹²². Even though, microglia become less efficient in $A\beta$ phagocytosis over time, they maintain contact with the plaques and form a barrier around them¹²³.

This barrier limits newly formed soluble A β to binding to existing insoluble A β and reduces damage induced by direct contact of healthy neurites to the plaques¹²⁴.

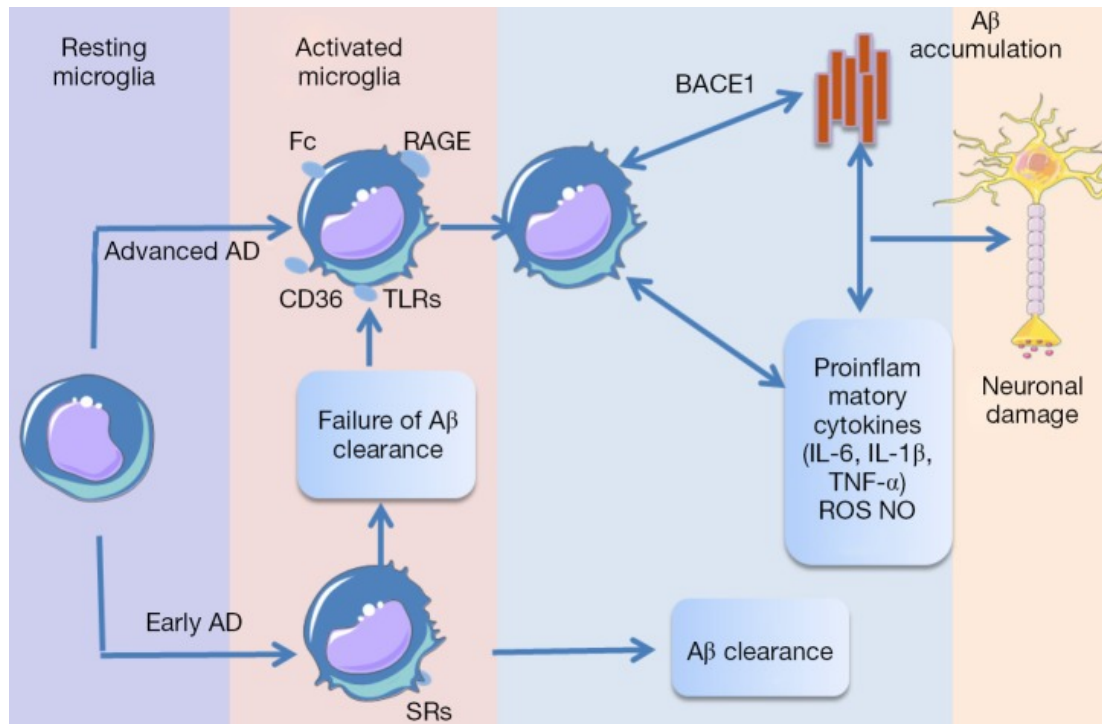


Figure 1: possible mechanism of microglial activation and contribution to AD progression

Microglia activation due to A β deposition and following release of pro-inflammatory cytokines. Early-stage microglia activation leads to A β clearance via microglia's SR. Persistent microglia activation by insoluble A β via FC, CD36, RAGE and Toll-like receptors leads to failure of A β clearance and A β accumulation. Induced neuroinflammation, especially IL-6 increases A β generation via induction of β -secretase (BACE1) synthesis. Therefore, resulting in a feed forward loop of microglia activation, neuroinflammation and A β deposition, ultimately causing neuronal damage. Figure adapted from Wang et al., 2015¹¹⁹.

Microglia modulation in AD

It was shown that induced neuronal activity at 40 Hz, but no other frequencies, leads to a reduction of soluble and insoluble A β in 5xFAD amyloidosis mice. The observed reduction of A β was accompanied by morphological adaption of microglia surrounding A β plaques. Microglia morphology changed upon 40 Hz stimulation into a more phagocytic ameboid phenotype. Co-localization of microglia and A β indicates A β phagocytosis. Further it was shown that by induced neuronal oscillations at 40 Hz the number and the size of remaining A β plaques were reduced. In conclusion, gamma rhythm stimulation at 40 Hz can induce a microglia response which attenuates AD-associated-pathology¹²⁵. Follow up studies have shown that by 40 Hz stimulation not only a

reduction of A β can be achieved but also a reduction of hyperphosphorylated tau and a reduction in the inflammatory response of microglia. Additionally, a neuroprotective effect of induced gamma oscillations was shown as seen by reduced neurodegeneration in a CK-p25 neurodegenerative mouse model. These pathological improvements were shown to have a beneficial impact on cognitive functions, namely on recognition & spatial memory in mice models of AD^{126,127}.

A recently published study showed enhanced cognitive functions in patients with mild to moderate AD following gamma stimulation. Overall, induced 40 Hz neuronal oscillations were well tolerated by all subjects. Patients receiving gamma sensory stimulation showed significantly reduced night-time active periods, in contrast to deterioration in sleep quality in sham group patients. Patients in the sham group also showed the expected, significant decline in ADCS-ADL scores, whereas patients in the gamma sensory stimulation group fully maintained their functional abilities over the 6-month period¹²⁸. Neuronal activity at defined frequencies cannot only be induced by sensory stimulation but by transcranial electrical stimulation as well. The firing pattern of individual neurons can be affected, specifically timing of spiking activity at defined frequency in targeted brain regions can be induced¹²⁹. Based on that the effect of non-invasive transcranial alternating current stimulation at gamma-frequency on memory function and cholinergic transmission in mild cognitive impairment due to AD was examined. Following a single 60 min session of 40 Hz transcranial AC stimulation (tACS), a significant improvement of memory performance was observed in gamma-stimulated but not in sham stimulated subjects. Further, Cholinergic transmission, as measured by short latency afferent inhibition has shown a significant increase due to gamma-stimulation¹³⁰. Repeated application of 40 Hz tACS led to a lasting improvement of cognitive functions in patients suffering from early-stage AD. The improvement in cognitive functions lasted over the course of tACS itself, indicating a modulation of the underlying disease pathology¹³¹.

Aim of the project

Neuroinflammation is prevalent in various long-lasting diseases such as AD, Parkinson's Disease, amyotrophic lateral sclerosis, stroke, chronic pain, but also in psychiatric disorders like schizophrenia, major depressive disorder and obsessive-compulsive disorder¹³²⁻¹³⁴. Being able to understand, interfere with and alter the progression of neuroinflammation in a controlled manner would have great clinical potential. As described in previous sections, neuromodulation therapy can have a lasting effect by modulating not only neuronal cells but also glia cells and neuroinflammation. However, the mechanism of glia cell modulation by electricity is poorly understood. Especially if observed effects are due to indirect glia cell stimulation via paracrine signalling of neuronal cells which are known to be electrically active or if the electric field influences glia cells behaviour directly. Based on the reviewed literature we hypothesize that microglia activity states can be modulated by defined electrical stimulation protocols directly. We expect to be able to control neuroinflammation progression and to modulate the phagocytic capacities of microglia.

The project was divided into three aims:

First aim of the project: The development of a system for *in-vitro* neuromodulation. To test our hypothesis that microglia activity can be directly modulated by defined electrical stimulation parameters. Cells are stimulated under standard cell culture conditions without including further variables into the experimental design. Therefore, a lid including electrodes for standard 6 well plates was designed which can be connected to an external function generator. Cells can be cultured as common and the lid can be added for electrical stimulation experiments in a 5% CO₂ incubator at 37°C. The lid is 3D printed and can be sterilized for repeated usage.

Second aim: Using this developed system, we have identified electrical stimulation protocols to alter the cytokine secretion pattern of stand-alone microglia. Therefore, microglia activation was first induced by external factors to induce microglia M1 polarization as a model for harmful microglia activity *in-vivo*. Following induced activation, the secretion of pro-inflammatory cytokines such as TNF and IL-6 were suppressed by defined electrical stimulation parameters. Further development of the *in-vitro* stimulation device and the analysis pipeline will allow us to refine electrical stimulation protocols for more targeted and controlled manipulation of the microglial phenotype.

Third aim: The results of this study will be transferred to clinical application by a Spin-off company (Bottneuro AG) from the University of Basel, founded January 2021. By collaborating with our industrial partner, Bottneuro AG, this project will be continued to bring sustainable benefits to patients.

Bottneuro AG

Bottneuro AG was founded on January 6th 2021 as a Spin-off company from the University of Basel. Build on academic research such as the presented project in this thesis, Bottneuro AG is targeting the neuromodulation market. By development of a personalized cap for transcranial induction and measurement of brain oscillations the goal of the company is to bring sustainable benefits to people suffering from neuroinflammation. Based on results of this thesis, it is expected that using tACS microglia activity can be modulated at targeted brain regions. Thus, the progression of microglia induced neuroinflammation and following neuronal death in amyloid plaque burdened brains can be treated. The company's founder includes Dr. Bekim Osmani, Dr. Tino Töpfer as main shareholders and board members and Dr. Bekim Osmani as Chief Executive Officer (CEO), Prof. Raphael Guzman as clinical advisor and me, Alois C. Hopf as Chief Scientific Officer (CSO). The company successfully terminated their seed round in Q4/2021 to develop the required electronics, hard-, software and to progress to clinical trials expected to start in 2023. Within 1 year since incorporation, the company grew from an idea to 10 FTE (excl. the founders). Bottneuro AG will continue their close collaboration with their academic partners, especially with the research group of Prof. Raphael Guzman to examine the mode of action of electrical stimulation on glia cells *in-vitro* and to fully understand the impact of neuromodulation on neuroinflammation.

Methods & Material

BV-2 cells culture

Immortalized murine microglia cells (BV-2 cell line) (Elabscience, Cat. No. EP-CL-0493) were used for neuromodulation experiments. BV-2 cells seeding density was $16'666 \text{ cells/cm}^2$ ($1 \times 10^6 \text{ cells/100 mm}$ petri dish). BV-2 cells were cultured in DMEM, high glucose, no glutamine medium (ThermoFischer Scientific, Cat. No. 11960-044) supplemented with 10% foetal bovine serum (FBS) (Gibco, Cat. No. A3160801), 1% penicillin/streptomycin (Gibco, Cat. No. 15140122) and a final concentration of 2 mM L-Glutamine (Gibco). Cell cultures were kept in a 5% CO₂ incubator at 37°C. Culture medium was replaced every other day. Once the cells reached 80% confluency the culture was divided. Media was aspirated and dish washed using PBS without Ca²⁺ and Mg²⁺ (PBS-/-) once. Followed by trypsinization with 0.25% Trypsin-EDTA (Gibco), and centrifugation for 5 min at 250 rcf. Cells were counted using trypan blue and plated at a density of 20'000 cell/cm² for electrical modulation experiments.

Animals

Animals used for microglia isolation were C57BL/6 mice, bred and provided by the local animal facility, Department of Biomedicine, University Hospital Basel, University of Basel. Mice were euthanized by decapitation under the animal license 2652-31062. All sample collection and experiments were conducted in accordance to the Swiss Federal Veterinary Office guidelines and were approved by the Cantonal Veterinary Office (Canton of Basel-Stadt, Switzerland).

Primary murine microglia isolation and culture

Primary brain derived murine microglia were used to confirm findings with BV-2 cells. First, mixed glia cells were isolated from C57BL/6 mice P3 according to a published protocol for rat mixed glia isolation and adapted to mice neonates¹³⁵. In brief, mice pups were decapitated using sterile scissors. All solutions and dissection equipment were kept on ice. All dissection equipment such as scissors, forceps and scalpels were sterilized by autoclaving. Between animals, dissecting equipment was rinsed in 70% Ethanol and washed in PBS^(-/). Heads were collected in a 50 mL tube containing 70% Ethanol for 10 sec and transferred in a 50 mL tube containing culture media. As culture media for primary murine microglia DMEM/F12 (Gibco, Cat. No. 31330-038) supplemented with 10% FBS and 200 U/ml penicillin, 200 µg/ml streptomycin was used. The brains were carefully removed from the skull. Meninges were removed under a Stereo dissecting microscope (Carl Zeiss Microscopy GmbH, Germany). For meninges removal brain were cut in

half and the brain halves were placed in 5 mL culture media. All the following steps were performed in the cell culture laboratories under sterile conditions in the cell culture hood. The brains were centrifuged for 5 min @ 300rcf. The supernatant was aspirated. 1 mL of fresh culture media was added and the brain halves were homogenized by pipetting up and down for 15 times using a p1000 micropipette. The resulting cell suspension was strained through a 100 µm cell strainer in a 50 mL tube to remove debris and large clumps. The strainer was rinsed by additional 9 mL of culture media to collect the remaining cells. Cells were counted using Trypan blue and seeded at a density of 62'500 cells/cm². The cells suspension was transferred to a T75 flask and incubated for 20days in a 5% CO₂ incubator @ 37°C. Culture media was changed every 4 days. Microglia were isolated from mixed glia culture via mild trypsinization¹³⁶. In brief, culture media from mixed glia culture was aspirated and cells were washed with 10 mL serum free culture media. Following that, the mixed glia culture was exposed to 0.25 % Trypsin-EDTA in serum free culture media. Within 30-40 min the upper layer of cells detached whereas a thin layer of cells remained attached to the bottom of the wells. The upper cell layer was aspirated and adherent cells were rinsed with culture media to remove remaining trypsin-EDTA. Cells (microglia) were collected using a cell scraper, counted using trypan blue and seeded at a density of 29'000 cells/cm² for *in-vitro* neuromodulation experiments.

Experimental setup

To mimic the pro-inflammatory microglia phenotype *in-vitro*, cells were exposed to ultrapure LPS from Escherichia coli (List labs, Lot No. 4219A1). LPS titration was performed 10ng/mL-1000ng/mL for 24 h to find optimal LPS concentration for strong induction of pro-inflammatory cytokine release without reaching a plateau-effect. For *in-vitro* neuromodulation experiments cells were simultaneously exposed to 100ng/mL LPS and electrical current. Control groups included no LPS with electrical current, no electrical current with 100ng/mL LPS and neither electrical current nor LPS stimulation. Two electrical stimulation protocols were tested. First protocol used DC Stimulation, 1 V for one hour followed by one hour no electrical stimulation for a total of 24 h. Second protocol used 40 Hz AC stimulation, 2 V (bi-directional) for 24 h continuously. After cell stimulation by electrical current and LPS, cell culture media was aspirated and fresh media added, 6h later culture media was collected and further analysed. At the time of media collection, the cells were counted using Trypan blue.

3D printed electrical stimulation device

The device for electrical stimulation of cell was built in-house by the medical technology facility from the university hospital Basel, and is referred to as Electrical stimulation (ES) device. The design is based on a validated and published electrical chamber and was adjusted for our needs¹³⁷. The ES device consists out of a 3D printed Lid which fits 6 well dishes (VWR, Cat. No. 734-0019), commonly used in the laboratory and platinum electrodes. The printing material was Acrylonitrile Butadiene Styrene (ABS). ABS is an abrasion and strain-resistant thermoplastic with high chemical resistance. Due to its physical properties, ABS is used in a wide range of medical technologies from respiratory devices to miniature implants¹³⁸. The lid has 6 pairs of platinum electrode 1 mm in diameter incorporated for stimulating each well separately. Platinum is biologically inert and commonly used for medical implant. The electrodes are placed in a parallel circuit including a switch to turn off 3 out of 6 electrodes (Figure 2). For stimulation experiments the ES device is connected to a function generator (Arbitrary Function Generator AFG3021C, Tektronix). The ES device is heat and humidity-resistant, and can be used in a CO₂ incubator at 37°C. For repeated use, the ES device was cleaned and sterilized between experiments. In brief, the ES device was rinsed with autoclaved ddH₂O, followed by 24 h in autoclaved ddH₂O for protein dissolvment. Next, the ES device was submerged in 70% ethanol for 24 h followed by 24 h in autoclaved ddH₂O. Finally, the ES device was placed under UV light for 24 h. All washing and sterilization steps were performed under sterile conditions in the cell culture hood.

Cytokine analysis

The concentration of pro-inflammatory cytokines in the cell culture medium after the LPS titration experiment was determined using the V-PLEX Proinflammatory Panel 1 Kit (Mesoscale, Cat. No. K15048D-2) according to manufacturer's protocol. The following cytokines were quantified: IFN- γ , IL-1 β , IL-2, IL-4, IL-5, IL-6, IL-10, IL-12p70, KC/GRO and TNF. The cytokine concentrations were normalized to the number of cells.

Following electrical stimulation experiments, concentrations of the pro-inflammatory cytokines TNF, IL-6 and IL-1 α were determined using a colorimetric enzyme-linked immunosorbent assay (ELISA) developed in the laboratory. In brief, 96-well microplates were coated with 50 μ L/well of capture antibody in PBS^(-/-) (4 μ g/mL anti-TNF (Cat. No. 506102, BioLegend), 1 μ g/mL anti-IL-6 (Cat. No. 504506, BioLegend), 3 μ g/mL anti-IL-1 α (Cat. No. 503206, BioLegend). After initial shaking at 600rpm for 5 min, it was incubated overnight at room temperature. The next day, plates were washed 3 times with 150 μ L/well wash buffer (50 mM Tris,

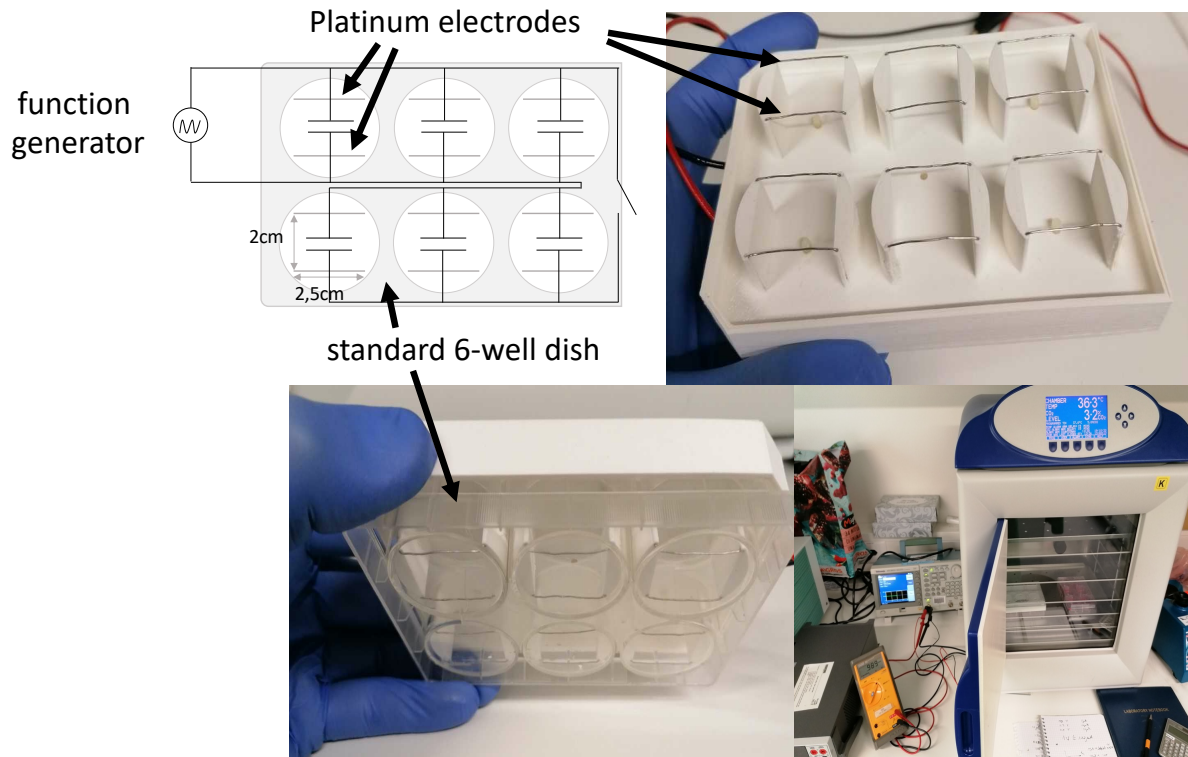


Figure 3: Electrical Stimulation (ES) device design

Electrical circuit diagram. Six platinum electrode pairs in a parallel circuit with a switch to connect/disconnect 3 electrode pairs. Electrodes connected to a function generator to control stimulation parameters. Acrylonitrile Butadiene Styrene (ABS) used for 3D printing the device. Manual incorporation of the platinum electrodes. The ES device fits standard 6 well plates (VWR, Cat. No. 734-0019). If the lid is on the plate, the electrodes touch the bottom of each well. For experiments the ES device is placed in a humidified CO₂ incubator @ 37°C and connected to a function generator outside the incubator.

60 mM NaCl, 0.1% Tween-20). After that, capture antibodies were blocked for 1 h at room temperature with 150µL/well blocking buffer (50 mM Tris, 60 mM NaCl, 0.1% Tween-20, 5% BSA). Samples were diluted in assay buffer at a 1:2 (IL-6 & IL-1α) or 1:100 (TNF) dilution. The recombinant proteins were prepared in assay buffer (range between 125 to 1.95pg/mL for recombinant TNF (Cat. No. 575209, BioLegend), 1000 to 7.81 pg/mL for recombinant IL-6 (Cat. No. 575709, BioLegend), 100 to 0.78 pg/mL for recombinant IL-1α (Cat. No. 580309, BioLegend). A total of 50µL of diluted samples and standards was added per well. Assay buffer consisted of 50 mM Tris, 60 mM NaCl, 0.1% Tween-20, 0.5% BSA. Standards and samples were incubated for 2h at room temperature on a rotational shaker at 600rpm. After 3 washes, 50µL/well biotinylated antibodies were added and incubated for 2h at room temperature at 600rpm.

Concentrations of detection antibodies were 0.25µg/mL biotin anti-TNF (Cat. No. 516003, BioLegend), 0.5µg/mL biotin anti-IL-6 (Cat. No. 504602, BioLegend) and 0.05µg/mL biotin anti-IL-1α (Cat. No. 512504, BioLegend). After 3 washes, 50 µl/well of 10ng/mL Streptavidin-Horse Radish Peroxidase in assay buffer (Cat. No. 21126, Pierce) was added and incubated for 1 h at room temperature in the dark. After 5 washes, 50µL/well 3,3',5,5'-Tetramethylbenzidin (TMB 1-Step Ultra) (Cat. No. 34028, Pierce) was added for 30 min at 450rpm protected from light exposure. The color reaction was stopped with 50µL/well 2N Hydrochloric acid (HCL). Absorbance was read on an ELISA microplate reader (SynergyH1 Hybrid Reader, BioTek) at 450nm and 570nm for background subtraction. Data were analyzed using the Gen5 Software (Gen5, version 3.05, BioTek).

Results

LPS dose-dependent release of cytokines

To mimic a pro-inflammatory phenotype *in-vitro*, immortalized murine microglia, BV-2 cells were exposed to various concentrations of LPS (0, 10ng/mL, 100ng/mL or 1000ng/mL) for 24 hours. The release of pro-inflammatory cytokines in response to LPS was dose-dependent, thereby confirming the suitability of LPS activated BV-2 cells as a model of neuroinflammation. The production of most pro-inflammatory cytokines was significantly increased in response to 100ng/ml LPS, and reached a plateau in response to 1000ng/ml LPS. The secretion of the anti-inflammatory cytokine IL-4 was significantly reduced upon exposure to 10ng/mL LPS, and remained low with higher concentrations of LPS (100ng/mL, 1000ng/mL). Low (10ng/mL) and intermediate (100ng/mL) concentrations of LPS had no significant impact on cell number and viability. Nevertheless, a high concentration of LPS (1000ng/mL) significantly reduced the number and viability of BV-2 cells (Figure 4). Thus, BV-2 cells were challenged with 100ng/ml LPS in subsequent experiments.

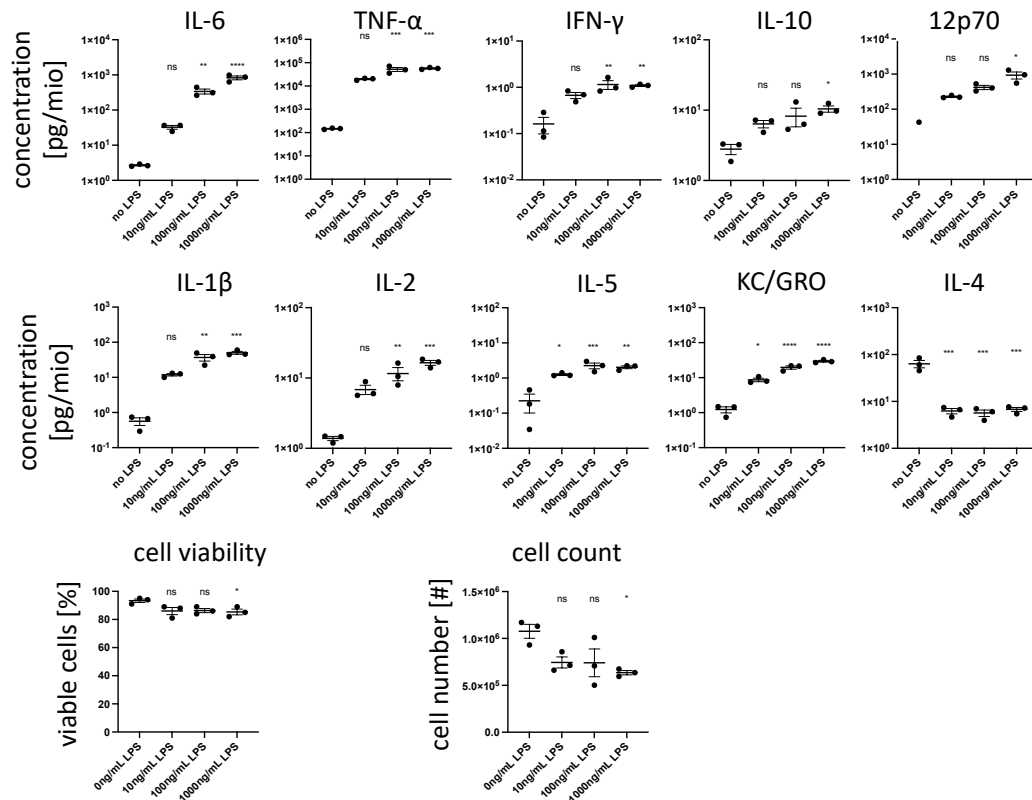


Figure 4: Lipopolysaccharide (LPS) titration and analysis of cytokine secretion, cell viability and cell number.

BV-2 cells were challenged with 0ng/mL, 10ng/mL, 100ng/mL, 1000ng/mL of LPS for 24 h. Cytokine concentration in the cell culture medium was determined by ELISA, normalized to the number of live cells and expressed in pg/million cells. Cell viability and cell count was assessed by trypan blue staining using an automated cell counter. For statistical analysis ordinary one-way ANOVA was performed. For multiple comparison Dunnett's multiple comparisons test was performed. Adjusted p-value: ns: $p > 0.05$; *=: $p < 0.05$; ** $p < 0.01$; ***=: $p < 0.001$; ****=: $p < 0.0001$.

Direct current stimulation reduces cell proliferation

The impact of DC stimulation on quiescent BV-2 cells and activated BV-2 cells by 100ng/mL LPS was analysed. Cells were seeded in 6-well dishes and exposed to 100ng/mL LPS for 24 h. For proliferation analysis cell were stimulated for 52h with 100ng/mL LPS and 1 V DC for 1 h every second hour for a total of 24 h or 52h respectively. To minimize variability due to different proliferation rates and resulting cell numbers, exposure time to 1 V DC and LPS was reduced to 24 h for cytokine analysis. Cell numbers were determined and normalized to initial cell number at beginning of the stimulation (0h). 1 V DC stimulation for 1 h every second hour alone negatively impacted BV-2 cell proliferation individually over 52h. The exposure of BV-2 cells to 100ng/mL LPS also negatively impacted cell proliferation. Combining 1 V DCS with 100ng/mL LPS treatment further reduced proliferation rate. After 24 h, 1 V DC stimulation led to a significant reduction in cell proliferation whereas LPS had no significant impact on proliferation rate (no DC/no LPS: 3.82 ± 0.18 , no DC/LPS: 3.35 ± 0.21 , DC/ no LPS: 3.0 ± 0.07 , DC/LPS: 2.91 ± 0.39). After 52h, LPS and/or DC stimulation induced a significant reduction in cell proliferation rates (no DC/no LPS: 11.23 ± 0.52 , no DC/LPS: 8.75 ± 1.08 , DC/ no LPS: 6.36 ± 1.07 , DC/LPS: 4.20 ± 0.88) (Figure 5, B). 100ng/mL LPS expectedly induced an elevation in IL-6 secretion by BV-2 cells. 1 V DC stimulation, either alone or in combination with 100ng/mL LPS had no impact on IL-6 secretion (Figure 5, C).

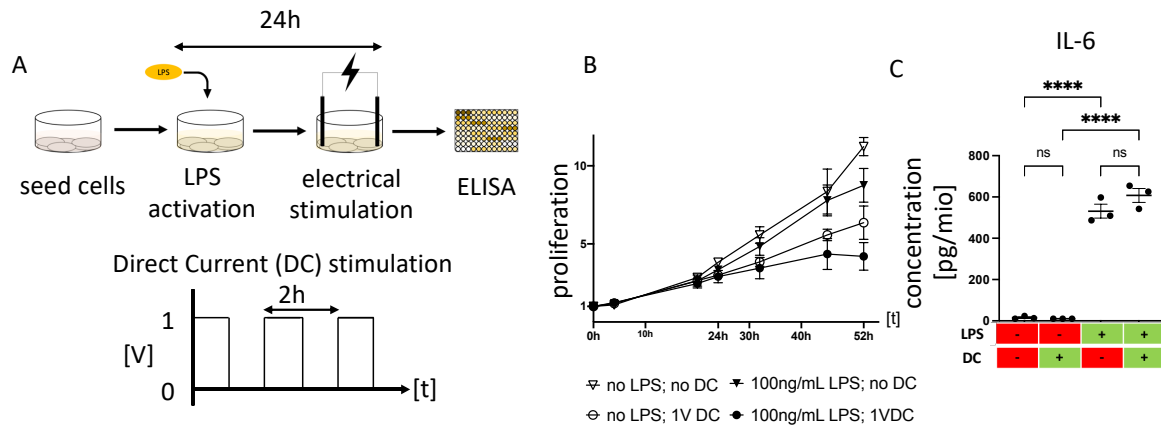


Figure 5: 1 V DC stimulation of BV-2 cells does not impact LPS-stimulated secretion of IL-6

A) *In-vitro* neuromodulation of BV-2 cells. BV-2 microglial cells are seeded in a 6-well dish. After cell attachment, the cells are exposed to 100 ng/mL LPS and 1 V DC for 1 h on 1 h off. **B)** Cells were stimulated for a total of 52 h. Start of stimulation at 0h. Cell numbers were counted under brightfield microscope. Proliferation rate defined as cell number at time x divided by cell number at time 0 h **C)** Concentration of IL-6 (pg per million cells) in the culture medium at 24 h after DC alone or in combination with LPS. Data points from three independent experiments performed in triplicates are shown. For statistical analysis ordinary one-way ANOVA was performed. For multiple comparisons, Dunnett's test was performed. Adjusted p-value: ns: $p > 0.05$; *=: $p < 0.05$; ** $p < 0.01$; ***=: $p < 0.001$; ****=: $p < 0.0001$

40 Hz Alternate current stimulation suppresses BV-2 cell activity

The impact of AC stimulation on quiescent BV-2 cells and LPS-activated BV-2 cells was tested. Cells were seeded in 6-well dishes and exposed to 100 ng/mL LPS for 24 h. During the time of LPS stimulation, the cells were continuously stimulated by AC, oscillating from -2 V to 2 V with a 40 Hz frequency (rectangular waveform) (Figure 6, A). In addition to IL-6, TNF and IL-1 α were also quantified in the culture medium. LPS activation of BV-2 cells stimulated the secretion of these three pro-inflammatory cytokines. The application of 40 Hz AC alone in BV-2 cells did not induce the release of any of these cytokines. Nevertheless, LPS induced secretion of cytokines was significantly suppressed following 40 Hz AC stimulation. IL-6 concentration in supernatant of LPS activated BV-2 was reduced to 13.0 % \pm 3.3% following 40 Hz AC stimulation. (332 pg/mio cells \pm 95 pg/mio cells under LPS only condition and 43 pg/mio cells \pm 11 pg/mio cells under LPS and 40 Hz AC condition). TNF concentration in supernatant of LPS activated BV-2 cells was reduced to 63.9% \pm 11.1% following 40 Hz AC stimulation. (252 pg/mio cells \pm

71 pg/mio cells under LPS only condition and 161 pg/mio cells \pm 28 pg/mio cells under LPS and 40 Hz AC condition). 40 Hz AC stimulation did not show a significant impact on cytokine secretion of non-LPS treated BV-2 cells. No effect of 40 Hz AC stimulation on IL-1 α secretion was observed (Figure 6, B).

LPS and AC stimulation of BV-2 cells does not impact cellular attachment to the well. Morphological appearance indicate overall survival of BV-2 cells following LPS and AC stimulation. Following LPS stimulation BV-2 cells become more amoeboid, regardless of additional AC stimulation (Figure 6, C).

40 Hz Alternate current stimulation suppresses primary murine microglia activity

To eliminate artifacts given by the immortalized cell line, stimulation experiments were reproduced using primary murine microglia. Comparable effects of LPS and 40 Hz AC stimulation can be seen in primary murine microglia. IL-6 concentration in supernatant of LPS activated primary murine microglia was reduced to 10.4% \pm 1.3% following 40 Hz AC stimulation. (845 pg/mio cells \pm 61 pg/mio cells under LPS only condition and 88 pg/mio cells \pm 11 pg/mio cells under LPS and 40 Hz AC condition). TNF concentration in supernatant of LPS activated primary murine microglia was reduced to 42.1% \pm 5.7% following 40 Hz AC stimulation. (38 pg/mio cells \pm 1 pg/mio cells under LPS only condition and 16 pg/mio cells \pm 2 pg/mio cells under LPS and 40 Hz AC condition). 40 Hz AC stimulation did not show a significant impact on cytokine secretion of non LPS treated primary murine microglia. No effect of 40 Hz AC stimulation on IL-1 α secretion was observed (Figure 6, B).

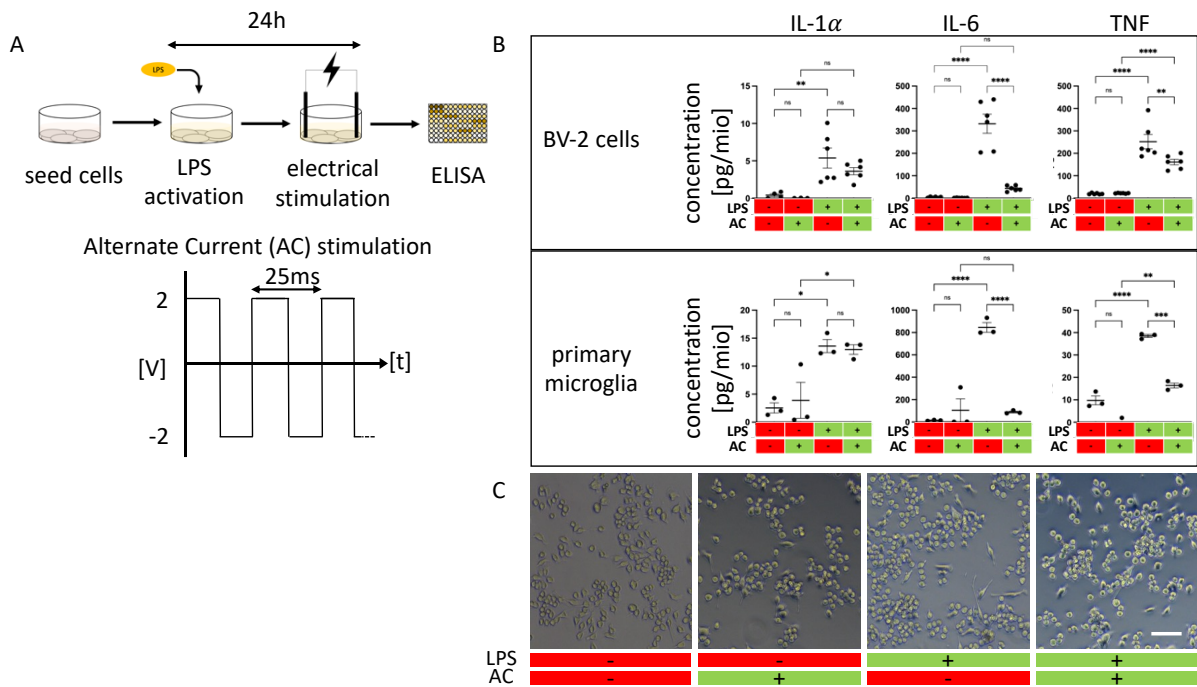


Figure 6: 40 Hz AC inhibits LPS-induced secretion of IL-6 and TNF by microglia

A) *In-vitro* neuromodulation of microglia cells. Microglial cells are seeded in a 6-well dish. After cell attachment, the cells are exposed to 100ng/mL LPS and A) for 24 h. Following stimulation, the secretion of pro-inflammatory cytokines is analyzed by an enzyme-linked immunosorbent assay (ELISA). The applied AC had a rectangular waveform with 40 Hz frequency and an Amplitude of 4 V (+2 V/-2 V). **B)** Cytokine concentration (pg per million cells) in secretome of BV-2 cells (top) or of primary microglia (bottom). For statistical analysis ordinary one-way ANOVA was performed. For multiple comparisons, Dunnett's test was performed. Adjusted p-value: ns: p>0.05; *= p<0.05; ** p<0.01; ***=: p<0.001; ****=: p<0.0001. **C)** Brightfield images of BV-2 following different stimulation protocols. Scale: 100µm.

Applied current depends on frequency and applied voltage

A frequency of 40 Hz and a set Voltage of 2 V results in a current of 3.27 mA applied to the cells. The root mean square (rms) value of the current [I_{rms}] in an AC electrical system depends on the Impedance (resistance and reactance) [Z] and the applied rms voltage [V_{rms}] according to Ohm's law ($[I_{rms}] = [Z] * [V_{rms}]$). V = 2 V set on the function generator corresponds to $V_{rms} = 1.41$ V ($V_{rms} = 2 \text{ V} / \sqrt{2}$). The impedance and the rms of the applied voltage were measured at increasing frequencies at a predefined Voltage of 2 V ($V_{rms} = 1.41$ V). At 40 Hz the total measured impedance

was 121Ω across 3 wells. Therefore, the impedance per well was 363Ω (in parallel circuit with same resistance per resistor: $[Z]_{\text{resistor}} = [Z]_{\text{total}} \times \# \text{ of resistors}$). The measured rms Voltage at 40 Hz was 1.18 V instead of 1.41 V as calculated. According to Ohm's law, measured that applied $V_{\text{rms}} = 1.18$ and $Z = 363 \Omega$, this results in an applied current of $I_{\text{rms}} = 3.27 \text{ mA}$ per well. With an increase in frequency the impedance gets reduced which results in higher current per well with fixed applied voltage (Figure 7).

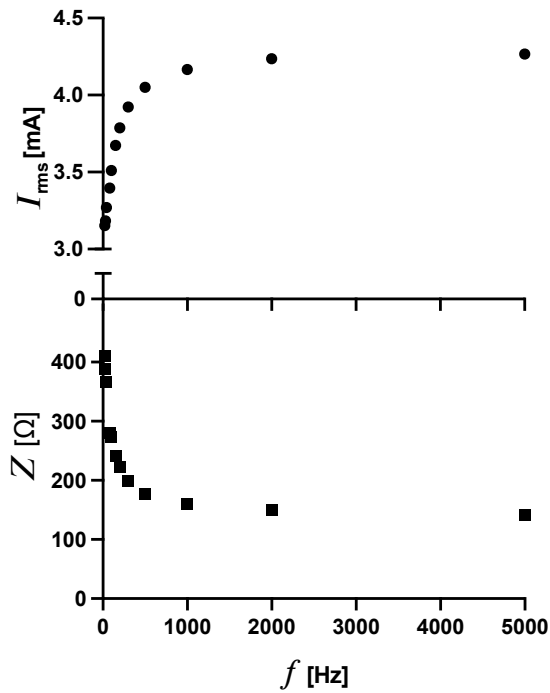


Figure 7: Applied Current and Impedance depends on frequency at set Voltage of 2 V

Impedance (Z) measurements at Voltage set to a peak value of 2 V. Current (I_{rms}) calculated according to Ohm's law for AC circuit ($[I_{\text{rms}}] = [Z] * [V]_{\text{rms}}$)

Discussion

Development of a new electrical stimulation device

The presented ES device developed in this project allows easy handling, sterilization, minimal evaporation and simple parallelization, ensuring high reproducibility of electrical stimulation experiments. Nowadays, the most common method to deliver electric current is to use an electrotactic chamber. For this, salt bridges are submerged in culture medium to avoid direct contact of the cells and the metallic electrodes. This separation prevents the release of electrochemical byproducts and a following pH change in the cell culture media. However, these setups come with significant limitations. First, the time for each experiment is limited. Temperature, calcium levels and pH level are stable for 30-60 min media only¹³⁹. Extended stimulation durations lead to diffusion of salt and temperature from the bridge reservoirs to the media and vice versa resulting in uncontrollable culture conditions. Platinum is a noble metal and provides therefore high oxidative resistance. By using platinum electrodes in our design, the potential cytotoxic release of electrochemical byproducts can be avoided. This allows us to electrically stimulate the cells over extended time periods without pH adjustments. Using culture media containing phenol red, no pH change due to electrical stimulation was observed.

Second, the experimental setup using electrotactic chambers in petri-dishes makes parallelization difficult and is challenging to maintain sterile. Using our ES device, we can stimulate six individual wells simultaneously and adding additional ES devices doesn't complicate the experimental setup. For our experiments we used two ES devices simultaneously which allows us to stimulate 12 wells at once. This allowed us to run each of the 4 conditions in triplicates which reduces technical variability. Sterility during the experiments was easily provided and no bacterial or fungal contamination was detected. Repeated use of the ES device requires sterilization between experiments. However, ABS plastic is not autoclavable. Therefore, another sterilization method was required. Submerging the ES device in ddH₂O for protein dissolution, followed by 70% Ethanol and exposure to UV light irradiation under laminar flow resulted in bacterial and fungal decontamination. Even though biological contamination was not detected, LPS negative samples have shown signs of activation by secreting pro-inflammatory factors in primary experiments. We conclude that this results from chemical contamination, namely from LPS contamination from previous experiments. LPS is known to have strong resistance e.g. requiring dry-heat sterilization at 250°C for 30 min or a UV fluence up to 500 mJ/cm² from a medium-pressure UV lamp in the wavelength range from 200 to 400 nm^{140,141}. Due to this strong resistance we have to assume that

endotoxins were not completely removed between experiments and at least partially remained on the electrodes. To make this effect neglectable, new ES device were produced and ES devices were kept separated from each other and designated to the use with LPS or the use without LPS. By designating the ES device to the use with or without LPS the unwanted induction of pro-inflammatory cytokine secretion in non LPS treated conditions was circumvented.

Last, the use of platinum electrodes resembles the clinical settings more closely. In clinical settings electric current is applied via metallic electrodes such as in patch electrodes for EEG, ECG or non-invasive brain stimulation or in implantable metallic electrodes as used in cardiac pacemakers, spinal cord implants or deep brain stimulation rather than via salt bridges.

LPS-stimulated production of pro-inflammatory cytokines as an *in vitro* model of neuroinflammation

A LPS concentration of 100ng/mL for 24 h was chosen to reliably induce cytokine secretion while maximizing the effect of additional factors on cytokine secretion. We determined that 100ng/mL LPS induced a robust secretion of pro-inflammatory cytokines without inducing significant cell death of BV-2 cells. LPS activated BV-2 cells are commonly used as a model for neuroinflammation¹⁴². However, used LPS concentrations and exposure time varies greatly between publications from 10ng/mL for 30 min up to 30µg/mL for 24 h, a factor of 144'000¹⁴³⁻¹⁴⁷. Therefore, finding the right concentration for an intermediate induction of pro-inflammatory cytokine release required the titration experiments. Our results are consistent with previous studies which have shown a strong dose dependency of the cytokine release over a broad range of LPS concentrations and exposure times^{143,144}.

Biphasic stimulation of glia cells has a neuroprotective effect

Our result indicate that neuromodulation therapies have a neuroprotective effect. Application of biphasic stimulation led to suppressed microglia activation by LPS. Monophasic stimulation did not have an effect. To reveal the direct impact of electrical stimulation on microglia cells and to exclude secondary effects of neuronal stimulation and subsequent paracrine signalling, we stimulated stand-alone microglia. LPS induced microglia activation can be suppressed by 40 Hz AC stimulation. Reduced concentrations of the pro-inflammatory cytokines TNF and IL-6 after 40 Hz AC stimulation in LPS activated microglia suggest the anti-inflammatory effect of 40 Hz AC stimulation. Commonly, the beneficial impact of neuromodulation is attributed to direct effects on neuronal excitability or modulation of neuronal networks followed by indirect effects on glia cells only. However, recent developments indicate direct impact of electrical stimulation

on glia cells¹⁴⁸⁻¹⁵¹. Previous *in-vivo* work indicates suppression of microglia activity due to electrical stimulation. 2 Hz and 10 Hz electric stimulation of the ischemic rat cortex resulted in lower infarct volume and reduced activation and proliferation of microglia¹⁵². Additionally, 100 Hz electroacupuncture stimulation inhibited TNF and IL-1 β mRNA upregulation in the ventral midbrains of medial-forebrain-bundle-axotomy activated microglia¹⁵³. Further, a lasting attenuation of neuropathic pain due to suppression of microglia activation was observed following 6h of 4 Hz and 60 Hz spinal cord stimulation in a sciatic nerve injury rat model¹⁵⁴. All these results indicate the suppression of microglia activation in the CNS by electrical stimulation. However, they cannot exclude the possibility that microglia activation is modulated by other environmental modifications induced by electrical stimulation. One previous study observed a direct effect of electrical stimulation on primary microglia activated by exposure to conditioned media of light damaged cone-derived cell line. A decrease in the number of amoeboid microglia and a downregulation of TNF and IL-1 β secretion was observed following 20 Hz biphasic electrical stimulation for 1 h with 1.6 mA¹⁵⁵. Comparing our findings to those previous published results we can confirm the direct anti-inflammatory effect of AC stimulation on microglia. Interestingly this anti-inflammatory effect is limited to AC stimulation. This is consistent with previous findings, where no influence of DC stimulation on secretion of neuroinflammatory markers was seen¹⁵⁶.

Studies in mice models of AD found that optogenetic and multisensory induced neuronal oscillations at 40 Hz but no other frequency lead to a reduction of A β and p-tau deposition^{125,126}. Pre-symptomatic stimulation further had a neuroprotective effect and prevented subsequent neurodegeneration and decline of cognitive functions^{127,157}. Microglia phenotype was altered into a more amoeboid morphology and a co-localization with A β was observed, indicating induced phagocytosis^{125,126}. The neuroprotective effect is consistent with previous findings and can be explained by suppression of neurotoxic cytokine release such as TNF. TNF does not only has a neurotoxic effect but also reduces the level of insulin degrading enzyme, a key protease for A β degradation and induces BACE1 synthesis and following A β production in cortical neurons^{158,159}. This may explain reduced A β burden due to the modulation of microglia activity into a less inflammatory and neurotoxic phenotype. Even though microglia underwent morphological transformation into a more amoeboid, phagocytic phenotype, transcriptomic analysis revealed reduced inflammatory markers. This strengthens the point that the classical definitions of M1/M2 microglia does not account for the microglia phenotype heterogeneity.

Oscillating transmembrane potential may mimic healthy brain state

Changes of the ionic homeostasis (Na^+ , Ca^{2+} , K^+ , H^+ , Cl^-) are closely associated with microglial activation, cytokine secretion, reactive oxygen species release and cell migration and proliferation¹⁶⁰. Pro-inflammatory microglia activation by LPS starts with cell surface receptor and ligand-gated ion channel activation, resulting in membrane depolarization. Microglial purinergic P2X4 receptor expression is enhanced by exposure to LPS *in-vitro*, but also following PNI in spinal microglia and in AD patients^{161–163}. P2X4 receptors are nonselective cationic-channels that open upon binding to ATP, released by damaged neuronal tissue and results in Ca^{2+} and Na^+ influx and K^+ efflux and subsequent depolarization¹⁶⁴. Microglia activation leads to persistent elevated intracellular Ca^{2+} concentration¹⁶⁵. An increase in intracellular Ca^{2+} is usually linked to morphological changes, migration, proliferation and induced cytokine secretion of microglia^{165,166}. As recently demonstrated, microglia express a variety of ion channels, including voltage gated potassium, calcium, sodium and proton channels¹⁶⁰. Interestingly, an upregulation of various voltage ion channels is observed in pro-inflammatory microglia activation^{160,167–169}. Upregulation of voltage gated ion channels makes activated microglia more susceptible to electrical potential differences between the intracellular and the extracellular environment as induced by electrical stimulation. This could explain the findings in this study in which cytokine secretion of LPS activated microglia were effectively modulated whereas no effect on cytokine secretion of non-LPS treated microglia was observed.

Activation of voltage gated ion channels depends on the difference between the intracellular potential with respect to the extracellular space. This is commonly induced by current flow through ligand-gated ion channels that open in response to the corresponding ligands which results in changing intracellular ion concentrations. In electrical stimulation experiments, electrons are brought into the system which results in a reduced net charge of the extracellular environment and altered transmembrane potential. Transiently de- or hyper- polarizing the cell results in voltage-gated ion channels activation¹⁷⁰. The change of the extracellular potential during AC stimulation depends on the applied frequency. Whereas during DC stimulation, the extracellular potential remains constant. Changing the extracellular potential from +2 V to -2 V repeatedly during 40 Hz AC stimulation the transmembrane potential fluctuates, resulting in continuous cellular de- and hyperpolarization. However, during DC stimulation, the extracellular potential remains constant and the transmembrane potential is regulated by ion in- and efflux across the membrane only. However, applying high voltages above physiological levels potentially results in continuous cellular hyperpolarization. Interestingly, under pathological conditions sustained

hyperpolarization is linked to chronically activated microglia^{169,171}. As described, DC stimulation potentially result in constant cellular hyperpolarization and therefore in continuous secretion of the pro-inflammatory cytokines as detected in this study. Transient hyperpolarization at the opposite, is linked to cellular process extension and an anti-inflammatory microglial phenotype^{166,171}. The externally induced transient de- and hyperpolarization potentially explains the suppressed pro-inflammatory cytokine release in LPS-activated microglia. Additionally, the demonstration of suppressed microglia activity by AC stimulation but not by DC stimulation suggest that an oscillating electric field may provide microglia with signals of a healthy brain. Indeed, it has been suggested that healthy neuronal activity suppress microglia activation and a lack of active suppression results in inducing microglial activity^{172,173}. This theory of oscillating de- and hyperpolarization induced by AC stimulation and continuous hyperpolarization due to DC stimulation could be tested by calcium imaging. Repeated de- and hyperpolarization would result in oscillating calcium concentration in the cells detectable via calcium imaging. Continuous hyperpolarization on the other hand would result in constant, non-fluctuating calcium signals. This theory of oscillating de- and hyperpolarization based on the frequency of the AC current could be further tested by applying pulsed DC stimulation at the same frequency. As the theory depends on the changing extracellular net charge rather than the direction of the current flow, the same results of pulsed DC and AC stimulation are expected. Revealing the involved signaling pathways would require transcriptomic analysis as performed in a study researching the effect of electroconvulsive therapy on microglia activity. Microglia response to immune challenges such as LPS was suppressed by electrical stimulation whereas no effect on resting microglia was detected. Transcriptomic analysis revealed activation of the retinoic acid receptor α response pathway which modulated microglial response to immune stimulations¹⁷³. However, our presented study did not target the mechanism of microglia activation and suppression and conclusions have to be taken carefully. Transcriptomic analysis would allow us to identify involved signaling pathways. Even though functionally similar, BV-2 cells as mainly used in this study, have shown to have a distinct gene expression profile upon LPS stimulation compared to primary murine microglia¹⁷⁴. Therefore, signaling pathway analysis should be conducted using primary microglia instead of microglial cell lines.

Microglia are the major immune cells of the CNS with the distinct role of immune surveillance, therefore, making them especially sensitive to changes in their microenvironment. Regardless of the isolation protocol, microglia are likely to be activated during isolation to a certain extent¹⁷⁵. This hinders definitive conclusions about suppression of microglia activity *in-vitro* as non-

LPS treated cells cannot be considered quiescent as in the healthy brain, nevertheless they were used as control group.

Relevance of *in-vitro* results for future neuromodulation strategies

The maximum applied current in our study was 3.27 mA for 24 h. For clinical application, the maximal applied current and time is limited. In general, stimulation is limited to a duration of 30 min and a current intensity of 2 mA, the advisable safety threshold for human studies^{176,177}. However, a phase I clinical safety study has shown safe and tolerable application of 4 mA DC stimulation in a single 30 min session in stroke patients¹⁷⁸. This leads to the conclusion that the maximum applied current in this study would be tolerated in human subjects. Another study has shown that transcranial applied AC stimulation is safe and tolerable if the maximum injected current was below 4 mA in total and below 2 mA per electrode¹³¹. We exceed stimulation duration for a single session drastically in this study and are on the upper limit with the applied current. However, we can conclude that microglia are directly responsive to electrical stimulation and that their activation phenotype can be modulated using defined sets of electrical stimulation parameters. Our study helps to understand the direct impact of neuromodulation therapies on microglia activation and subsequent neuroinflammation. However, for precise targeting and modulation of microglia activity, further studies using repeated stimulation session and potentially lower currents are required.

Conclusion/Outlook

While planning neuromodulation interventions, the effects on various cell types should be considered. First, the altered excitability of neurons by activation of voltage gated channels resulting in a rise of membrane potential and depolarization and overall neuronal synchronization. Second, as we have shown this study, microglia activation can be directly modulated by certain stimulation protocols. Therefore, the influence on microglia activity and potential other glia cells should be considered while planning neuromodulation therapies. Based on the discussed data and previous published clinical studies showing lasting effects of neuromodulation therapies, we conclude that the modulation of microglia activity and the suppression of the inflammatory response is responsible for the benefits brought to patients exceeding the course of the stimulation itself.

The presented research in this project will be continued with different academic and industrial partners and will be published in peer-reviewed journals. To consider direct microglia modulation for clinical application in a safe and patient tolerable way, an extended set of stimulation parameters have to be analyzed for targeted microglia modulation in the boundaries of clinical safety. Collaborating with the Department of Biomedical Engineering from the University of Basel for the development of a high throughput electrical stimulation device will help to fulfill this goal. Being able to test more stimulation parameters in parallel and to streamline the analysis will further reduce costs and save time. *In-vitro* development of stimulation protocols, within the boundaries of clinical safety, allows to identify beneficial neuromodulation protocols which can be directly tested and validated in clinical studies. This will be achieved by close collaboration with Bottneuro as implementation partner of transcranial applied electrical stimulation which conducts clinical trials and brings direct benefits to the patients.

Reference list

1. Hopf A, Schaefer DJ, Kalbermatten DF, Guzman R, Madduri S. Schwann Cell-Like Cells: Origin and Usability for Repair and Regeneration of the Peripheral and Central Nervous System. *Cells*. 2020;9(9):1990. doi:10.3390/cells9091990
2. Liu Z, Liu Y, Yushan M, Yusufu A. Enhanced Nerve Regeneration by Bionic Conductive Nerve Scaffold Under Electrical Stimulation. *Front Neurosci*. 2022;16. doi:10.3389/FNINS.2022.810676
3. Osmani B, Guzman R, Töpper T, et al. Neural implant based on a cellulose thin film and corresponding fabrication process. 2021.
4. Nguendon Kenhagho H, Canbaz F, Hopf A, Guzman R, Cattin P, Zam A. Toward optoacoustic sciatic nerve detection using an all-fiber interferometric-based sensor for endoscopic smart laser surgery. *Lasers Surg Med*. 2022;54(2):289-304. doi:10.1002/LSM.23473
5. Hopf A, Al-Bayati L, Schaefer DJ, Kalbermatten DF, Guzman R, Madduri S. Optimized Decellularization Protocol for Large Peripheral Nerve Segments: Towards Personalized Nerve Bioengineering. *Bioeng (Basel, Switzerland)*. 2022;9(9). doi:10.3390/BIOENGINEERING9090412
6. Osmani B, Guzman R, Töpper T, et al. Tissue regeneration patch and corresponding fabrication process. 2021.
7. Olsson Y. Microenvironment of the peripheral nervous system under normal and pathological conditions. *Crit Rev Neurobiol*. 1990;5(3):265-311. <https://europepmc.org/article/med/2168810>. Accessed May 12, 2022.
8. Akinrodoye MA, Lui F. Neuroanatomy, Somatic Nervous System. *StatPearls*. November 2021. <https://www.ncbi.nlm.nih.gov/books/NBK556027/>. Accessed May 12, 2022.
9. Ubogu EE. The Molecular and Biophysical Characterization of the Human Blood-Nerve Barrier: Current Concepts. *J Vasc Res*. 2013;50(4):289-303. doi:10.1159/000353293
10. Nave KA, Werner HB. Myelination of the nervous system: mechanisms and functions. *Annu Rev Cell Dev Biol*. 2014;30:503-533. doi:10.1146/ANNUREV-CELLBIO-100913-013101
11. Salzer JL, Zalc B. Myelination. *Curr Biol*. 2016;26(20):R971-R975. doi:10.1016/J.CUB.2016.07.074
12. Ioghen O, Manole E, Gherghiceanu M, Popescu BO, Ceafalan LC. Non-Myelinating Schwann Cells in Health and Disease. *Demyelination Disord*. April 2020. doi:10.5772/INTECHOPEN.91930

13. Cornbrooks CJ, Carey DJ, McDonald JA, Timpl R, Bunge RP. In vivo and in vitro observations on laminin production by Schwann cells. *Proc Natl Acad Sci U S A*. 1983;80(12):3850-3854. doi:10.1073/PNAS.80.12.3850
14. Balakrishnan A, Belfiore L, Chu TH, et al. Insights Into the Role and Potential of Schwann Cells for Peripheral Nerve Repair From Studies of Development and Injury. *Front Mol Neurosci*. 2021;13:270. doi:10.3389/FNMOL.2020.608442/BIBTEX
15. Daly WT, Yao L, Abu-rub MT, et al. The effect of intraluminal contact mediated guidance signals on axonal mismatch during peripheral nerve repair. *Biomaterials*. 2012;33(28):6660-6671. doi:10.1016/J.BIOMATERIALS.2012.06.002
16. Stratton JA, Kumar R, Sinha S, et al. Purification and characterization of schwann cells from adult human skin and nerve. *eNeuro*. 2017;4(3). doi:10.1523/ENEURO.0307-16.2017
17. Jessen KR, Mirsky R. The repair Schwann cell and its function in regenerating nerves. *J Physiol*. 2016;594(13):3521-3531. doi:10.1113/JP270874
18. Jessen KR, Mirsky R. The success and failure of the schwann cell response to nerve injury. *Front Cell Neurosci*. 2019;13:1-14. doi:10.3389/fncel.2019.00033
19. Navarro X, Vivó M, Valero-Cabré A. Neural plasticity after peripheral nerve injury and regeneration. *Prog Neurobiol*. 2007;82(4):163-201. doi:10.1016/J.PNEUROBIO.2007.06.005
20. Griffin JW, Hogan MC V., Chhabra AB, Deal DN. Peripheral nerve repair and reconstruction. *J Bone Joint Surg Am*. 2013;95(23):2144-2151. doi:10.2106/JBJS.L.00704
21. Sunderland S. Factors influencing the course of regeneration and the quality of the recovery after nerve suture. *Brain*. 1952;75(1):19-54. doi:10.1093/BRAIN/75.1.19
22. Pfister BJ, Gordon T, Loverde JR, Kochar AS, Mackinnon SE, Cullen DK. Biomedical Engineering Strategies for Peripheral Nerve Repair: Surgical Applications, State of the Art, and Future Challenges. *Crit Rev Biomed Eng*. 2011;39(2):81-124. doi:10.1615/CritRevBiomedEng.v39.i2.20
23. SK L, SW W. Peripheral nerve injury and repair. *J Am Acad Orthop Surg*. 2000;8(4):243-252. doi:10.5435/00124635-200007000-00005
24. Moore AM, MacEwan M, Santosa KB, et al. Acellular nerve allografts in peripheral nerve regeneration: A comparative study. *Muscle and Nerve*. 2011;44(2):221-234. doi:10.1002/mus.22033
25. Ray WZ, Mackinnon SE. Management of nerve gaps: autografts, allografts, nerve transfers, and end-to-side neurotaphy. *Exp Neurol*. 2010;223(1):77-85. doi:10.1016/j.expneurol.2009.03.031
26. Houdek MT, Shin AY. Management and complications of traumatic peripheral nerve

- injuries. *Hand Clin.* 2015;31(2):151-163. doi:10.1016/J.HCL.2015.01.007
27. Moore AM, Kasukurthi R, Magill CK, Farhadi HF, Borschel GH, Mackinnon SE. Limitations of Conduits in Peripheral Nerve Repairs. *HAND.* 2009;4(2):180-186. doi:10.1007/s11552-008-9158-3
 28. Griffin JW, Hogan M V., Chhabra AB, Deal DN. Peripheral Nerve Repair and Reconstruction. *J Bone Jt Surg.* 2013;95(23):2144-2151. doi:10.2106/JBJS.L.00704
 29. Grinsell D, Keating CP. Peripheral nerve reconstruction after injury: a review of clinical and experimental therapies. *Biomed Res Int.* 2014;2014:698256. doi:10.1155/2014/698256
 30. Muir D. The potentiation of peripheral nerve sheaths in regeneration and repair. *Exp Neurol.* 2010;223(1):102-111. doi:10.1016/J.EXPNEUROL.2009.05.038
 31. Mackinnon SE, Doolabh VB, Novak CB, Trulock EP. Clinical outcome following nerve allograft transplantation. *Plast Reconstr Surg.* 2001;107(6):1419-1429. doi:10.1097/00006534-200105000-00016
 32. Hiles RW. Freeze dried irradiated nerve homograft: a preliminary report. *Hand.* 1972;4(1):79-84. <http://www.ncbi.nlm.nih.gov/pubmed/5061383>. Accessed January 8, 2019.
 33. Sondell M, Lundborg G, Kanje M. Regeneration of the rat sciatic nerve into allografts made acellular through chemical extraction. *Brain Res.* 1998;795(1-2):44-54. <http://www.ncbi.nlm.nih.gov/pubmed/9622591>. Accessed January 8, 2019.
 34. TW G, TL S, SF B. Decellularization of tissues and organs. *Biomaterials.* 2006;27(19):3675-3683. doi:10.1016/J.BIOMATERIALS.2006.02.014
 35. Crapo PM, Gilbert TW, Badylak SF. An overview of tissue and whole organ decellularization processes. *Biomaterials.* 2011;32(12):3233-3243. doi:10.1016/j.biomaterials.2011.01.057
 36. Gilpin A, Yang Y. Decellularization Strategies for Regenerative Medicine: From Processing Techniques to Applications. *Biomed Res Int.* 2017;2017:9831534. doi:10.1155/2017/9831534
 37. Hudson TWI, Zawko S, Deister C, et al. Optimized acellular nerve graft is immunologically tolerated and supports regeneration. *Tissue Eng.* 2004;10(11-12):1641-1651. doi:10.1089/ten.2004.10.1641
 38. Graham JB, Muir D. Chondroitinase C selectively degrades chondroitin sulfate glycosaminoglycans that inhibit axonal growth within the endoneurium of peripheral nerve. *PLoS One.* 2016;11(12). doi:10.1371/journal.pone.0167682
 39. McKerracher L, Rosen KM. MAG, myelin and overcoming growth inhibition in the CNS. *Front Mol Neurosci.* 2015;8:51. doi:10.3389/fnmol.2015.00051

40. Gonzalez-Perez F, Udina E, Navarro X. Extracellular Matrix Components in Peripheral Nerve Regeneration. *Int Rev Neurobiol.* 2013;108:257-275. doi:10.1016/B978-0-12-410499-0.00010-1
41. Kehoe S, Zhang XF, Boyd D. FDA approved guidance conduits and wraps for peripheral nerve injury: A review of materials and efficacy. *Injury.* 2012;43(5):553-572. doi:10.1016/J.INJURY.2010.12.030
42. Brooks DN, Weber R V., Chao JD, et al. Processed nerve allografts for peripheral nerve reconstruction: a multicenter study of utilization and outcomes in sensory, mixed, and motor nerve reconstructions. *Microsurgery.* 2012;32(1):1-14. doi:10.1002/MICR.20975
43. Means KR, Rinker BD, Higgins JP, Payne SH, Merrell GA, Wilgis EFS. A Multicenter, Prospective, Randomized, Pilot Study of Outcomes for Digital Nerve Repair in the Hand Using Hollow Conduit Compared With Processed Allograft Nerve: <http://dx.doi.org/10.1177/1558944715627233>. 2016;11(2):144-151. doi:10.1177/1558944715627233
44. McCrary MW, Vaughn NE, Hlavac N, Song YH, Wachs RA, Schmidt CE. Novel Sodium Deoxycholate-Based Chemical Decellularization Method for Peripheral Nerve. <https://home.liebertpub.com/tec>. 2020;26(1):23-36. doi:10.1089/TEN.TEC.2019.0135
45. Kim JK, Koh Y Do, Kim JO, Seo DH. Development of a decellularization method to produce nerve allografts using less invasive detergents and hyper/hypotonic solutions. *J Plast Reconstr Aesthetic Surg.* 2016;69(12):1690-1696. doi:10.1016/j.bjps.2016.08.016
46. Hundepool CA, Nijhuis THJ, Kotsougiani D, Friedrich PF, Bishop AT, Shin AY. Optimizing decellularization techniques to create a new nerve allograft: an in vitro study using rodent nerve segments. *Neurosurg Focus.* 2017;42(3):E4. doi:10.3171/2017.1.FOCUS16462
47. Krekoski CA, Neubauer D, Zuo J, Muir D. Axonal Regeneration into Acellular Nerve Grafts Is Enhanced by Degradation of Chondroitin Sulfate Proteoglycan. *J Neurosci.* 2001;21(16):6206-6213. doi:10.1523/JNEUROSCI.21-16-06206.2001
48. Court FA, Wrabetz L, Feltri ML. Basal lamina: Schwann cells wrap to the rhythm of space-time. *Curr Opin Neurobiol.* 2006;16(5):501-507. doi:10.1016/J.CONB.2006.08.005
49. Ide C, Osawa T, Tohyama K. Nerve regeneration through allogeneic nerve grafts, with special reference to the role of the Schwann cell basal lamina. *Prog Neurobiol.* 1990;34(1):1-38. doi:10.1016/0301-0082(90)90024-B
50. Chen ZL, Strickland S. Laminin gamma1 is critical for Schwann cell differentiation, axon myelination, and regeneration in the peripheral nerve. *J Cell Biol.* 2003;163(4):889-899. doi:10.1083/JCB.200307068
51. Giannini C, Dyck PJ. The fate of Schwann cell basement membranes in permanently transected nerves. *J Neuropathol Exp Neurol.* 1990;49(6):550-563. doi:10.1097/00005072-

52. Udina E, Rodríguez FJ, Verdú E, Espejo M, Gold BG, Navarro X. FK506 enhances regeneration of axons across long peripheral nerve gaps repaired with collagen guides seeded with allogeneic Schwann cells. *Glia*. 2004;47(2):120-129. doi:10.1002/glia.20025
53. Zhou X-H, Ning G-Z, Feng S-Q, et al. Transplantation of Autologous Activated Schwann Cells in the Treatment of Spinal Cord Injury: Six Cases, more than Five Years of Follow-up. *Cell Transplant*. 2012;21(1_suppl):39-47. doi:10.3727/096368912X633752
54. Hilton DA, Jacob J, Househam L, Tengah C. Complications following sural and peroneal nerve biopsies. *J Neurol Neurosurg Psychiatry*. 2007. doi:10.1136/jnnp.2007.116368
55. Rutkowski JL, Kirk CJ, Lerner MA, Tennekoon GI. Purification and expansion of human Schwann cells in vitro. *Nat Med*. 1995;1(1):80-83. doi:10.1038/nm0195-80
56. Andersen ND, Srinivas S, Piñero G, Monje P V. A rapid and versatile method for the isolation, purification and cryogenic storage of Schwann cells from adult rodent nerves. *Sci Rep*. 2016;6(1):1-17. doi:10.1038/srep31781
57. Gao S, Zheng Y, Cai Q, et al. Combination of acellular nerve graft and Schwann cells-like cells for rat sciatic nerve regeneration. *Neural Plast*. 2014;2014. doi:10.1155/2014/139085
58. Scarritt ME, Pashos NC, Bunnell BA. A review of cellularization strategies for tissue engineering of whole organs. *Front Bioeng Biotechnol*. 2015;3:43. doi:10.3389/fbioe.2015.00043
59. Ochocka N, Kaminska B. Microglia Diversity in Healthy and Diseased Brain: Insights from Single-Cell Omics. *Int J Mol Sci*. 2021;22(6):1-26. doi:10.3390/IJMS22063027
60. Lawson LJ, Perry VH, Gordon S. Turnover of resident microglia in the normal adult mouse brain. *Neuroscience*. 1992;48(2):405-415. doi:10.1016/0306-4522(92)90500-2
61. Sierra A, de Castro F, del Río-Hortega J, Rafael Iglesias-Rozas J, Garrosa M, Kettenmann H. The “Big-Bang” for modern glial biology: Translation and comments on Pío del Río-Hortega 1919 series of papers on microglia. *Glia*. 2016;64(11):1801-1840. doi:10.1002/GLIA.23046
62. Ginhoux F, Greter M, Leboeuf M, et al. Fate mapping analysis reveals that adult microglia derive from primitive macrophages. *Science*. 2010;330(6005):841-845. doi:10.1126/SCIENCE.1194637
63. Palis J, Robertson S, Kennedy M, Wall C, Keller G. Development of erythroid and myeloid progenitors in the yolk sac and embryo proper of the mouse. *Development*. 1999;126(22):5073-5084. doi:10.1242/DEV.126.22.5073
64. Zhu Y, Wang T, Gu J, et al. Characterization and generation of human definitive

- multipotent hematopoietic stem/progenitor cells. *Cell Discov* 2020 61. 2020;6(1):1-18. doi:10.1038/s41421-020-00213-6
65. Schulz C, Perdiguero EG, Chorro L, et al. A lineage of myeloid cells independent of Myb and hematopoietic stem cells. *Science*. 2012;336(6077):86-90. doi:10.1126/SCIENCE.1219179
 66. Kierdorf K, Erny D, Goldmann T, et al. Microglia emerge from erythromyeloid precursors via Pu.1- and Irf8-dependent pathways. *Nat Neurosci*. 2013;16(3):273-280. doi:10.1038/NN.3318
 67. Fügler P, Hefendehl JK, Veeraraghavalu K, et al. Microglia turnover with aging and in an Alzheimer's model via long-term in vivo single-cell imaging. *Nat Neurosci*. 2017;20(10):1371-1376. doi:10.1038/NN.4631
 68. Cronk JC, Filiano AJ, Louveau A, et al. Peripherally derived macrophages can engraft the brain independent of irradiation and maintain an identity distinct from microglia. *J Exp Med*. 2018;215(6):1627-1647. doi:10.1084/JEM.20180247
 69. Martinez FO, Gordon S. The M1 and M2 paradigm of macrophage activation: Time for reassessment. *F1000Prime Rep*. 2014;6. doi:10.12703/P6-13
 70. Martinez FO, Helming L, Gordon S. Alternative Activation of Macrophages: An Immunologic Functional Perspective. <http://dx.doi.org/10.1146/annurev.immunol.021908.132532>. 2009;27:451-483. doi:10.1146/ANNUREV.IMMUNOL.021908.132532
 71. Martinez FO, Sica A, Mantovani A, Locati M. Macrophage activation and polarization. *Front Biosci*. 2008;13(2):453-461. doi:10.2741/2692
 72. Xue J, Schmidt S V., Sander J, et al. Transcriptome-based network analysis reveals a spectrum model of human macrophage activation. *Immunity*. 2014;40(2):274-288. doi:10.1016/J.IMMUNI.2014.01.006
 73. Ransohoff RM. A polarizing question: do M1 and M2 microglia exist? *Nat Neurosci*. 2016;19(8):987-991. doi:10.1038/NN.4338
 74. Sierra A, Abiega O, Shahraz A, Neumann H. Janus-faced microglia: beneficial and detrimental consequences of microglial phagocytosis. *Front Cell Neurosci*. 2013;7(JANUARY 2013). doi:10.3389/FNCEL.2013.00006
 75. Ravichandran KS. Find-me and eat-me signals in apoptotic cell clearance: progress and conundrums. *J Exp Med*. 2010;207(9):1807-1817. doi:10.1084/JEM.20101157
 76. Paolicelli RC, Bolasco G, Pagani F, et al. Synaptic pruning by microglia is necessary for normal brain development. *Science*. 2011;333(6048):1456-1458. doi:10.1126/SCIENCE.1202529

77. Kettenmann H, Kirchhoff F, Verkhratsky A. Microglia: new roles for the synaptic stripper. *Neuron*. 2013;77(1):10-18. doi:10.1016/J.NEURON.2012.12.023
78. Kettenmann H, Uwe Karsten H, Mami N, Alexei V. Physiology of microglia. *Physiol Rev*. 2011. doi:10.1152/physrev.00011.2010
79. Frost JL, Schafer DP. Microglia: Architects of the Developing Nervous System. *Trends Cell Biol*. 2016;26(8):587-597. doi:10.1016/J.TCB.2016.02.006
80. Shaked I, Porat Z, Gersner R, Kipnis J, Schwartz M. Early activation of microglia as antigen-presenting cells correlates with T cell-mediated protection and repair of the injured central nervous system. *J Neuroimmunol*. 2004;146(1-2):84-93. doi:10.1016/J.JNEUROIM.2003.10.049
81. Dudvarski Stankovic N, Teodorczyk M, Ploen R, Zipp F, Schmidt MHH. Microglia-blood vessel interactions: a double-edged sword in brain pathologies. *Acta Neuropathol*. 2016;131(3):347-363. doi:10.1007/S00401-015-1524-Y
82. Treede RD, Rief W, Barke A, et al. Chronic pain as a symptom or a disease: The IASP Classification of Chronic Pain for the International Classification of Diseases (ICD-11). *Pain*. 2019;160(1):19-27. doi:10.1097/J.PAIN.0000000000001384
83. Gereau RW, Sluka KA, Maixner W, et al. A pain research agenda for the 21st century. *J Pain*. 2014;15(12):1203-1214. doi:10.1016/j.jpain.2014.09.004
84. Basbaum A, Bautista D, Scherrer G, Cell DJ-, 2009 undefined. Cellular and molecular mechanisms of pain. *Elsevier*. <https://www.sciencedirect.com/science/article/pii/S0092867409012434>. Accessed May 9, 2022.
85. Ji RR, Nackley A, Huh Y, Terrando N, Maixner W. Neuroinflammation and central sensitization in chronic and widespread pain. *Anesthesiology*. 2018. doi:10.1097/ALN.0000000000002130
86. Ji RR, Xu ZZ, Gao YJ. Emerging targets in neuroinflammation-driven chronic pain. *Nat Rev Drug Discov* 2014 137. 2014;13(7):533-548. doi:10.1038/nrd4334
87. Ward H, West SJ. Microglia: sculptors of neuropathic pain? *R Soc Open Sci*. 2020;7(6):200260. doi:10.1098/RSOS.200260
88. Kawasaki Y, Zhang L, Cheng JK, Ji RR. Cytokine mechanisms of central sensitization: distinct and overlapping role of interleukin-1beta, interleukin-6, and tumor necrosis factor-alpha in regulating synaptic and neuronal activity in the superficial spinal cord. *J Neurosci*. 2008;28(20):5189-5194. doi:10.1523/JNEUROSCI.3338-07.2008
89. Vergne-Salle P, Bertin P. Chronic pain and neuroinflammation. *Jt Bone Spine*. 2021;88(6):105222. doi:10.1016/J.JBSPIN.2021.105222

90. Inoue K, Tsuda M. Microglia in neuropathic pain: Cellular and molecular mechanisms and therapeutic potential. *Nat Rev Neurosci.* 2018. doi:10.1038/nrn.2018.2
91. Dominguez E, Rivat C, Pommier B, Mauborgne A, Pohl M. JAK/STAT3 pathway is activated in spinal cord microglia after peripheral nerve injury and contributes to neuropathic pain development in rat. *J Neurochem.* 2008;107(1):50-60. doi:10.1111/J.1471-4159.2008.05566.X
92. Yan Z, Gibson SA, Buckley JA, Qin H, Benveniste EN. Role of the JAK/STAT signaling pathway in regulation of innate immunity in neuroinflammatory diseases. *Clin Immunol.* 2018;189:4-13. doi:10.1016/J.CLIM.2016.09.014
93. Jones M, Wen J, Selvaraj P, Tanaka M, Moran S, Zhang Y. Therapeutic Effect of the Substrate-Selective COX-2 Inhibitor IMMA in the Animal Model of Chronic Constriction Injury. *Front Pharmacol.* 2018;9. doi:10.3389/FPHAR.2018.01481
94. Gui Y, Duan S, Xiao L, Tang J, Li A. Bexarotene Attenuated Chronic Constriction Injury-Induced Spinal Neuroinflammation and Neuropathic Pain by Targeting Mitogen-Activated Protein Kinase Phosphatase-1. *J pain.* 2020;21(11-12):1149-1159. doi:10.1016/J.JPAIN.2019.01.007
95. Odonkor CA, Orman S, Orhurhu V, Stone ME, Ahmed S. Spinal Cord Stimulation vs Conventional Therapies for the Treatment of Chronic Low Back and Leg Pain: A Systematic Review of Health Care Resource Utilization and Outcomes in the Last Decade. *Pain Med (United States).* 2019;20(12):2479-2494. doi:10.1093/pm/pnz185
96. Kapural L, Yu C, Doust MW, et al. Novel 10-kHz High-frequency Therapy (HF10 Therapy) Is Superior to Traditional Low-frequency Spinal Cord Stimulation for the Treatment of Chronic Back and Leg Pain. *Anesthesiology.* 2015;123(4):851-860. doi:10.1097/ALN.0000000000000774
97. Melzack R, Wall PD. Pain mechanisms: A new theory. *Science (80-).* 1965. doi:10.1126/science.150.3699.971
98. Grace PM, Hutchinson MR, Maier SF, Watkins LR. Pathological pain and the neuroimmune interface. *Nat Rev Immunol.* 2014. doi:10.1038/nri3621
99. Costigan M, Scholz J, Woolf CJ. Neuropathic pain: A maladaptive response of the nervous system to damage. *Annu Rev Neurosci.* 2009. doi:10.1146/annurev.neuro.051508.135531
100. Sato KL, Johannek LM, Sanada LS, Sluka KA. Spinal cord stimulation reduces mechanical hyperalgesia and glial cell activation in animals with neuropathic pain. *Anesth Analg.* 2014;118(2):464-472. doi:10.1213/ANE.0000000000000047
101. Wolter T, Kieselbach K. Spinal cord stimulation for Raynaud's syndrome: long-term alleviation of bilateral pain with a single cervical lead. *Neuromodulation.* 2011;14(3):229-234. doi:10.1111/J.1525-1403.2011.00332.X

102. Sato KL, King EW, Johaneck LM, Sluka KA. Spinal cord stimulation reduces hypersensitivity through activation of opioid receptors in a frequency-dependent manner. *Eur J Pain*. 2013;17(4):551-561. doi:10.1002/J.1532-2149.2012.00220.X
103. Song Z, Meyerson BA, Linderoth B. Spinal 5-HT receptors that contribute to the pain-relieving effects of spinal cord stimulation in a rat model of neuropathy. *Pain*. 2011;152(7):1666-1673. doi:10.1016/J.PAIN.2011.03.012
104. Song P, Zhao ZQ. The involvement of glial cells in the development of morphine tolerance. *Neurosci Res*. 2001;39(3):281-286. doi:10.1016/S0168-0102(00)00226-1
105. Raghavendra V, Tanga F, Deleo JA. Inhibition of microglial activation attenuates the development but not existing hypersensitivity in a rat model of neuropathy. *J Pharmacol Exp Ther*. 2003;306(2):624-630. doi:10.1124/JPET.103.052407
106. Selkoe DJ, Hardy J. The amyloid hypothesis of Alzheimer's disease at 25 years. *EMBO Mol Med*. 2016;8(6):595-608. doi:10.15252/emmm.201606210
107. Selkoe DJ. Alzheimer's disease. *Cold Spring Harb Perspect Biol*. 2011;3(7):1-16. doi:10.1101/CSHPERSPECT.A004457
108. Block ML, Zecca L, Hong JS. Microglia-mediated neurotoxicity: uncovering the molecular mechanisms. *Nat Rev Neurosci*. 2007;8(1):57-69. doi:10.1038/NRN2038
109. Mandrekar S, Jiang Q, Lee CYD, Koenigsnecht-Talboo J, Holtzman DM, Landreth GE. Microglia mediate the clearance of soluble Abeta through fluid phase macropinocytosis. *J Neurosci*. 2009;29(13):4252-4262. doi:10.1523/JNEUROSCI.5572-08.2009
110. Skerrett R, Malm T, Landreth G. Nuclear receptors in neurodegenerative diseases. *Neurobiol Dis*. 2014;72 Pt A(Part A):104-116. doi:10.1016/J.NBD.2014.05.019
111. Jiang Q, Lee CYD, Mandrekar S, et al. ApoE promotes the proteolytic degradation of Abeta. *Neuron*. 2008;58(5):681-693. doi:10.1016/J.NEURON.2008.04.010
112. Bamberger ME, Harris ME, McDonald DR, Husemann J, Landreth GE. A cell surface receptor complex for fibrillar beta-amyloid mediates microglial activation. *J Neurosci*. 2003;23(7):2665-2674. doi:10.1523/JNEUROSCI.23-07-02665.2003
113. Koenigsnecht-Talboo J, Landreth GE. Microglial phagocytosis induced by fibrillar beta-amyloid and IgGs are differentially regulated by proinflammatory cytokines. *J Neurosci*. 2005;25(36):8240-8249. doi:10.1523/JNEUROSCI.1808-05.2005
114. Koenigsnecht J, Landreth G. Microglial phagocytosis of fibrillar beta-amyloid through a beta1 integrin-dependent mechanism. *J Neurosci*. 2004;24(44):9838-9846. doi:10.1523/JNEUROSCI.2557-04.2004
115. Yang CN, Shiao YJ, Shie FS, et al. Mechanism mediating oligomeric A β clearance by naïve

- primary microglia. *Neurobiol Dis.* 2011;42(3):221-230. doi:10.1016/J.NBD.2011.01.005
116. Akiyama H, Barger S, Barnum S, et al. Inflammation and Alzheimer's disease. *Neurobiol Aging.* 2000;21(3):383-421. doi:10.1016/S0197-4580(00)00124-X
 117. Arancio O, Zhang HP, Chen X, et al. RAGE potentiates Abeta-induced perturbation of neuronal function in transgenic mice. *EMBO J.* 2004;23(20):4096-4105. doi:10.1038/SJ.EMBOJ.7600415
 118. Carty M, Bowie AG. Evaluating the role of Toll-like receptors in diseases of the central nervous system. *Biochem Pharmacol.* 2011;81(7):825-837. doi:10.1016/J.BCP.2011.01.003
 119. Wang WY, Tan MS, Yu JT, Tan L. Role of pro-inflammatory cytokines released from microglia in Alzheimer's disease. *Ann Transl Med.* 2015;3(10):136. doi:10.3978/J.ISSN.2305-5839.2015.03.49
 120. Liddelow SA, Guttenplan KA, Clarke LE, et al. Neurotoxic reactive astrocytes are induced by activated microglia. *Nature.* 2017;541(7638):481-487. doi:10.1038/NATURE21029
 121. Li Q, Barres BA. Microglia and macrophages in brain homeostasis and disease. *Nat Rev Immunol.* 2018;18(4):225-242. doi:10.1038/NRI.2017.125
 122. Hong S, Beja-Glasser VF, Nfonoyim BM, et al. Complement and microglia mediate early synapse loss in Alzheimer mouse models. *Science.* 2016;352(6286):712-716. doi:10.1126/SCIENCE.AAD8373
 123. Bolmont T, Haiss F, Eicke D, et al. Dynamics of the microglial/amyloid interaction indicate a role in plaque maintenance. *J Neurosci.* 2008;28(16):4283-4292. doi:10.1523/JNEUROSCI.4814-07.2008
 124. Condello C, Yuan P, Grutzendler J. Microglia-Mediated Neuroprotection, TREM2, and Alzheimer's Disease: Evidence From Optical Imaging. *Biol Psychiatry.* 2018;83(4):377-387. doi:10.1016/J.BIOPSYCH.2017.10.007
 125. Iaccarino HF, Singer AC, Martorell AJ, et al. Gamma frequency entrainment attenuates amyloid load and modifies microglia. *Nature.* 2016;540(7632):230-235. doi:10.1038/nature20587
 126. Martorell A, Paulson A, Suk H-J, et al. Multi-sensory Gamma Stimulation Ameliorates Alzheimer's-Associated Pathology and Improves Cognition. *Cell.* 2019.
 127. Adaikkan C, Middleton SJ, Marco A, et al. Gamma Entrainment Binds Higher-Order Brain Regions and Offers Neuroprotection. *Neuron.* 2019. doi:10.1016/j.neuron.2019.04.011
 128. Cimenser A, Hempel E, Travers T, et al. Sensory-Evoked 40-Hz Gamma Oscillation Improves Sleep and Daily Living Activities in Alzheimer's Disease Patients. *Front Syst Neurosci.* 2021;15:103. doi:10.3389/fnsys.2021.746859

129. Krause MR, Vieira PG, Csorba BA, Pilly PK, Pack CC. Transcranial alternating current stimulation entrains single-neuron activity in the primate brain. *Proc Natl Acad Sci U S A*. 2019. doi:10.1073/pnas.1815958116
130. Benussi A, Cantoni V, Cotelli MS, et al. Exposure to gamma tACS in Alzheimer's disease: A randomized, double-blind, sham-controlled, crossover, pilot study. *Brain Stimul*. 2021. doi:10.1016/j.brs.2021.03.007
131. Bréchet L, Yu W, Biagi MC, et al. Patient-Tailored, Home-Based Non-invasive Brain Stimulation for Memory Deficits in Dementia Due to Alzheimer's Disease. *Front Neurol*. 2021;12:775. doi:10.3389/FNEUR.2021.598135/BIBTEX
132. Reale M, Costantini E. Cholinergic Modulation of the Immune System in Neuroinflammatory Diseases. *Diseases*. 2021;9(2):29. doi:10.3390/DISEASES9020029
133. Stephenson J, Nutma E, van der Valk P, Amor S. Inflammation in CNS neurodegenerative diseases. *Immunology*. 2018;154(2):204. doi:10.1111/IMM.12922
134. Meyer JH, Cervenka S, Kim MJ, Kreisl WC, Henter ID, Innis RB. Neuroinflammation in psychiatric disorders: PET imaging and promising new targets. *The lancet Psychiatry*. 2020;7(12):1064-1074. doi:10.1016/S2215-0366(20)30255-8
135. Lin L, Desai R, Wang X, Lo EH, Xing C. Characteristics of primary rat microglia isolated from mixed cultures using two different methods. *J Neuroinflammation*. 2017;14(1):1-10. doi:10.1186/S12974-017-0877-7/FIGURES/5
136. Saura J, Tusell JM, Serratos J. High-yield isolation of murine microglia by mild trypsinization. *Glia*. 2003;44(3):183-189. doi:10.1002/GLIA.10274
137. Mobini S, Leppik L, Barker JH. Direct current electrical stimulation chamber for treating cells in vitro. *Biotechniques*. 2016;60(2):95-98. doi:10.2144/000114382/ASSET/IMAGES/LARGE/FIGURE2.JPEG
138. Ziabka M, Dziadek M, Pielichowska K. Surface and Structural Properties of Medical Acrylonitrile Butadiene Styrene Modified with Silver Nanoparticles. *Polymers (Basel)*. 2020;12(1). doi:10.3390/POLYM12010197
139. Song B, Gu Y, Pu J, Reid B, Zhao Z, Zhao M. Application of direct current electric fields to cells and tissues in vitro and modulation of wound electric field in vivo. *Nat Protoc* 2007 26. 2007;2(6):1479-1489. doi:10.1038/nprot.2007.205
140. Anderson WB, Huck PM, Dixon DG, Mayfield CI. Endotoxin Inactivation in Water by Using Medium-Pressure UV Lamps. *Appl Environ Microbiol*. 2003;69(5):3002. doi:10.1128/AEM.69.5.3002-3004.2003
141. Miyamoto T, Okano S, Kasai N. Inactivation of Escherichia coli Endotoxin by Soft Hydrothermal Processing. *Appl Environ Microbiol*. 2009;75(15):5058.

doi:10.1128/AEM.00122-09

142. Peng Y, Chu S, Yang Y, Zhang Z, Pang Z, Chen N. Neuroinflammatory In Vitro Cell Culture Models and the Potential Applications for Neurological Disorders. *Front Pharmacol.* 2021;12. doi:10.3389/FPHAR.2021.671734
143. Wen X, Xiao L, Zhong Z, et al. Astaxanthin acts via LRP-1 to inhibit inflammation and reverse lipopolysaccharide-induced M1/M2 polarization of microglial cells. *Oncotarget.* 2017;8(41):69370-69385. doi:10.18632/ONCOTARGET.20628
144. Karunia J, Niaz A, Mandwie M, et al. Pacap and vip modulate lps-induced microglial activation and trigger distinct phenotypic changes in murine bv2 microglial cells. *Int J Mol Sci.* 2021;22(20). doi:10.3390/IJMS222010947/S1
145. Yu HM, Zhao YM, Luo XG, et al. Repeated lipopolysaccharide stimulation induces cellular senescence in BV2 cells. *Neuroimmunomodulation.* 2012;19(2):131-136. doi:10.1159/000330254
146. Dai X jing, Li N, Yu L, et al. Activation of BV2 microglia by lipopolysaccharide triggers an inflammatory reaction in PC12 cell apoptosis through a toll-like receptor 4-dependent pathway. *Cell Stress Chaperones.* 2015;20(2):321. doi:10.1007/S12192-014-0552-1
147. Yan A, Liu Z, Song L, et al. Idebenone alleviates neuroinflammation and modulates microglial polarization in LPS-stimulated BV2 cells and MPTP-induced parkinson's disease mice. *Front Cell Neurosci.* 2019;12:529. doi:10.3389/FNCEL.2018.00529/BIBTEX
148. Gellner AK, Reis J, Fiebich BL, Fritsch B. Electrified microglia: Impact of direct current stimulation on diverse properties of the most versatile brain cell. *Brain Stimul.* 2021;14(5):1248-1258. doi:10.1016/J.BRS.2021.08.007
149. Ruohonen J, neurophysiology JK-C, 2012 undefined. tDCS possibly stimulates glial cells. *Elsevier.* <https://www.sciencedirect.com/science/article/pii/S1388245712002209>. Accessed May 28, 2022.
150. Mishima T, Nagai T, Yahagi K, et al. Transcranial direct current stimulation (tDCS) induces adrenergic receptor-dependent microglial morphological changes in mice. *ncbi.nlm.nih.gov.* <https://www.ncbi.nlm.nih.gov/pmc/articles/pmc6751370/>. Accessed May 28, 2022.
151. Monai H, Ohkura M, Tanaka M, Oe Y, ... AK-N, 2016 undefined. Calcium imaging reveals glial involvement in transcranial direct current stimulation-induced plasticity in mouse brain. *nature.com.* https://www.nature.com/articles/ncomms11100?source=post_page-----. Accessed May 28, 2022.
152. Baba T, Kameda M, Yasuhara T, et al. Electrical Stimulation of the Cerebral Cortex Exerts Antiapoptotic, Angiogenic, and Anti-Inflammatory Effects in Ischemic Stroke Rats Through Phosphoinositide 3-Kinase/Akt Signaling Pathway. 2009. doi:10.1161/STROKEAHA.109.563627

153. Liu XY, Zhou HF, Pan YL, et al. Electro-acupuncture stimulation protects dopaminergic neurons from inflammation-mediated damage in medial forebrain bundle-transected rats. *Exp Neurol*. 2004;189(1):189-196. doi:10.1016/J.EXPNEUROL.2004.05.028
154. Shinoda M, Fujita S, Sugawara S, et al. Suppression of Superficial Microglial Activation by Spinal Cord Stimulation Attenuates Neuropathic Pain Following Sciatic Nerve Injury in Rats. *Int J Mol Sci*. 2020;21(7):2390. doi:10.3390/IJMS21072390
155. Zhou W ting, Ni Y qin, Jin Z bing, et al. Electrical stimulation ameliorates light-induced photoreceptor degeneration in vitro via suppressing the proinflammatory effect of microglia and enhancing the neurotrophic potential of Müller cells. *Exp Neurol*. 2012;238(2):192-208. doi:10.1016/J.EXPNEUROL.2012.08.029
156. Pelletier SJ, Lagace M, St-Amour I, et al. The morphological and molecular changes of brain cells exposed to direct current electric field stimulation. *Int J Neuropsychopharmacol*. 2015. doi:10.1093/ijnp/pyu090
157. Liu Q, Jiao Y, Yang W, et al. Intracranial alternating current stimulation facilitates neurogenesis in a mouse model of Alzheimer's disease. *Alzheimer's Res Ther*. 2020. doi:10.1186/s13195-020-00656-9
158. Rojo LE, Fernández JA, Maccioni AA, Jimenez JM, Maccioni RB. Neuroinflammation: implications for the pathogenesis and molecular diagnosis of Alzheimer's disease. *Arch Med Res*. 2008;39(1):1-16. doi:10.1016/J.ARCMED.2007.10.001
159. Mandrekar-Colucci S, Landreth GE. Microglia and Inflammation in Alzheimer's Disease. *CNS Neurol Disord Drug Targets*. 2010;9(2):156. doi:10.2174/187152710791012071
160. Cojocaru A, Burada E, Bălșeanu AT, et al. Roles of Microglial Ion Channel in Neurodegenerative Diseases. *J Clin Med*. 2021;10(6):1-18. doi:10.3390/JCM10061239
161. Tsuda M, Shigemoto-Mogami Y, Koizumi S, et al. P2X4 receptors induced in spinal microglia gate tactile allodynia after nerve injury. *Nature*. 2003;424(6950):778-783. doi:10.1038/NATURE01786
162. Raouf R, Chabot-Doré AJ, Ase AR, Blais D, Séguéla P. Differential regulation of microglial P2X4 and P2X7 ATP receptors following LPS-induced activation. *Neuropharmacology*. 2007;53(4):496-504. doi:10.1016/J.NEUROPHARM.2007.06.010
163. Godoy PA, Ramírez-Molina O, Fuentealba J. Exploring the Role of P2X Receptors in Alzheimer's Disease. *Front Pharmacol*. 2019;10. doi:10.3389/FPHAR.2019.01330
164. Stebbing MJ, Cottee JM, Rana I. The role of ion channels in microglial activation and proliferation - a complex interplay between ligand-gated ion channels, K⁺ channels, and intracellular Ca²⁺. *Front Immunol*. 2015;6(OCT). doi:10.3389/fimmu.2015.00497
165. Färber K, Kettenmann H. Functional role of calcium signals for microglial function. *Glia*.

- 2006;54(7):656-665. doi:10.1002/GLIA.20412
166. Eder C. Regulation of microglial behavior by ion channel activity. *J Neurosci Res.* 2005;81(3):314-321. doi:10.1002/JNR.20476
 167. Eder C. Ion channels in microglia (brain macrophages). *Am J Physiol.* 1998;275(2). doi:10.1152/AJPCELL.1998.275.2.C327
 168. Espinosa-Parrilla JF, Martínez-Moreno M, Gasull X, Mahy N, Rodríguez MJ. The L-type voltage-gated calcium channel modulates microglial pro-inflammatory activity. *Mol Cell Neurosci.* 2015;64:104-115. doi:10.1016/j.mcn.2014.12.004
 169. Rangaraju S, Gearing M, Jin LW, Levey A. Potassium channel Kv1.3 is highly expressed by microglia in human Alzheimer's disease. *J Alzheimers Dis.* 2015;44(3):797-808. doi:10.3233/JAD-141704
 170. Cameron MA, Al Abed A, Buskila Y, Dokos S, Lovell NH, Morley JW. Biology of Neuroengineering Interfaces: Differential effect of brief electrical stimulation on voltage-gated potassium channels. *J Neurophysiol.* 2017;117(5):2014. doi:10.1152/JN.00915.2016
 171. Laprell L, Schulze C, Brehme ML, Oertner TG. The role of microglia membrane potential in chemotaxis. *J Neuroinflammation.* 2021;18(1):1-10. doi:10.1186/S12974-020-02048-0/FIGURES/3
 172. Biber K, Neumann H, Inoue K, Boddeke HWGM. Neuronal 'On' and 'Off' signals control microglia. *Trends Neurosci.* 2007;30(11):596-602. doi:10.1016/J.TINS.2007.08.007
 173. Goldfarb S, Fainstein N, Ganz T, Vershkov D, Lachish M, Ben-Hur T. Electric neurostimulation regulates microglial activation via retinoic acid receptor α signaling. *Brain Behav Immun.* 2021;96:40-53. doi:10.1016/J.BBI.2021.05.007
 174. Henn A, Lund S, Hedtjörn M, Schrattenholz A, Pörzgen P, Leist M. The suitability of BV2 cells as alternative model system for primary microglia cultures or for animal experiments examining brain inflammation. *ALTEX.* 2009;26(2):83-94. doi:10.14573/ALTEX.2009.2.83
 175. De Groot CJA, Hulshof S, Hoozemans JJM, Veerhuis R. Establishment of microglial cell cultures derived from postmortem human adult brain tissue: immunophenotypic and functional characterization. *Microsc Res Tech.* 2001;54(1):34-39. doi:10.1002/JEMT.1118
 176. Bikson M, Datta A, Elwassif M. Establishing safety limits for transcranial direct current stimulation. *Clin Neurophysiol.* 2009;120(6):1033-1034. doi:10.1016/J.CLINPH.2009.03.018
 177. Iyer MB, Mattu U, Grafman J, Lomarev M, Sato S, Wassermann EM. Safety and cognitive effect of frontal DC brain polarization in healthy individuals. *Neurology.* 2005;64(5):872-875. doi:10.1212/01.WNL.0000152986.07469.E9

178. Chhatbar PY, Chen R, Deardorff R, et al. Safety and tolerability of transcranial direct current stimulation to stroke patients – A phase I current escalation study. *Brain Stimul.* 2017;10(3):553-559. doi:10.1016/J.BRS.2017.02.007

Curriculum Vitae

NAME: Hopf, Alois Conradin
 CONTACT: Palmenstrasse 12, 4055 Basel, Switzerland, phone: +41 (0) 79 602 94 55,
 e-mail: alois.hopf@bottneuro.ch
 CURRENT POSITION: Co-Founder & Chief Scientific Officer (CSO) at Bottneuro AG

EDUCATION/TRAINING:

INSTITUTION AND LOCATION	DEGREE	Completion Date MM/YYYY	FIELD OF STUDY
Freies Gymnasium (FG), Basel, Switzerland	Matura	06/2011	High School
Swiss Federal Institute of Technology (ETH), Zurich, Switzerland	BSc.	09/2015	Biotechnology
Swiss Federal Institute of Technology (ETH), Zurich, Switzerland	MSc.	05/2017	Biotechnology
FELASA, Zurich, Switzerland	LTK 1	04/2018	Laboratory animal science (mice & rats)
University of Basel & University Hospital of Basel, Switzerland	Ph.D.	11/2022	Neurobiology
University Hospital Zurich, Switzerland	GCP 1-3	09/2023	Good Clinical Practice for Sponsor and Investigator

A. Personal Statement

During my at the University Hospital of Basel in the research group of Prof. Raphael Guzman, I investigated the mechanism of action for modulating neuroinflammatory responses by electrical stimuli. My findings led to the incorporation of Bottneuro to bring academic research to direct clinical applications and help patients in need. Following incorporation, I've took over the role as Chief Scientific Officer (CSO) & Co-founder of Bottneuro and now lead the clinical and scientific development. As a scientist I'm convinced that neurodegenerative disorders have to be well understood to bring sustainable improvements to patients. By expanding our knowledge about neurodegenerative diseases, we are able to limit and counteract harmful disease progression. To understand biological systems and to find ways to control and manipulate them for our benefit I studied biotechnology. I graduated from the Swiss Federal Institute of Technology Zurich (M.Sc. ETH) in 2017, where I was taught scientific work on fundamental research.

After my Master graduation at ETH, I joined the University Hospital of Basel to continue my studies and to work in translational neuroscience research. During my Ph.D. I focused on regenerative neuroscience and worked on different projects with various collaborations. Each project during my Ph.D. resulted in either peer-reviewed publications, patents and/or the incorporation of Bottneuro.

As a CSO of Bottneuro my work switched from the laboratory to project administrations, setting up academic and industrial collaborations, budgeting and defining long-term research plans and goals.

Conducting research at the university Hospital of Basel taught me the importance of multi-disciplinary collaborations for successful project termination. A point which was further strengthened during incorporation of Bottneuro and subsequent investment rounds. Therefore, I am aware of the importance of collaborating with the experts in the relevant fields of business, regulations, medicine and science for successful project termination in industry as well as in academia.

B. Positions, Scientific Appointments, and Honors

Positions and Scientific Appointments

2021 – Present	Co-founder & Chief Scientific Officer, Bottneuro AG, Switzerland <ul style="list-style-type: none">• Clinical development• Business development• Product development based on patients' needs• Non-dilutive & dilutive fundraising
2017– 2022	Ph.D. student, Brain Ischemia and Regeneration (Prof. Raphael Guzman), Department of Biomedicine, University of Basel, Switzerland <ul style="list-style-type: none">• Development of acellular conduits for peripheral nerve repair and regeneration• <i>In-vitro</i> neuromodulation targeting microglia activity
2019 – 2022	Member of Ph.D. Club, Department of Biomedicine, University of Basel, Switzerland <ul style="list-style-type: none">• Organization of various social and academic events• Student representative
2017 – 2017	Research associate, Laboratory of Nano Bio Imaging (Prof. Periklis Pantazis), Department of Biosystems Science & Engineering (D-BSSE), Swiss Federal Institute of Technology (ETH), Zurich, Switzerland <ul style="list-style-type: none">• Genome engineering of murine Embryonic Stem cell
2016 – 2017	Master thesis, Cell System Dynamics Research Group (Prof. Timm Schroeder), Department of Biosystems Science & Engineering (D-BSSE), Swiss Federal Institute of Technology (ETH), Zurich, Switzerland <ul style="list-style-type: none">• Immobilization of murine Hematopoietic Stem and Progenitor Cells by monoclonal Antibodies enables High-Throughput live Single-cell Imaging
2015 – 2016	Research project, Plant Biotechnology Group (Prof. Wilhelm Gruissem), Department of Biology (D-BIOL), Swiss Federal Institute of Technology (ETH), Zurich, Switzerland <ul style="list-style-type: none">• Development of drought resistant <i>Manihot esculenta</i>

2015 – 2017

Member of Biotechnology student association, Department of Biosystems Science & Engineering (D-B SSE), Swiss Federal Institute of Technology (ETH), Zurich, Switzerland

- Organization of various social and academic events
- Student representative

C. Contributions to Science

Publications:

1. Dirk Loeffler, Weijia Wang, **Alois Hopf**, Oliver Hilsenbeck, Paul E Bourguine, Fabian Rudolf, Ivan Martín, Timm Schroeder (2018). Mouse and human HSPC immobilization in liquid culture by CD43- or CD44-antibody coating. *Blood*. PMID: 29453290
2. **Alois Hopf**, Dirk J Schaefer, Daniel F Kalbermatten, Raphael Guzman, Srinivas Madduri (2020). Schwann Cell-Like Cells: Origin and Usability for Repair and Regeneration of the Peripheral and Central Nervous System. *Cells*. PMID: 32872454
3. Hervé Nguendon Kenhagho, Ferda Canbaz, **Alois Hopf**, Raphael Guzman, Philippe Cattin, Azhar Zam (2022) Toward optoacoustic sciatic nerve detection using an all-fiber interferometric-based sensor for endoscopic smart laser surgery. *Lasers in Surgery and Medicine*. PMID: 34481417
4. **Alois Hopf**, Dirk J Schaefer, Daniel F Kalbermatten, Raphael Guzman, Srinivas Madduri (2022). Optimized Decellularization Protocol for Large Peripheral Nerve Segments: Towards Personalized Nerve Bioengineering

Patents:

1. Tissue regeneration patch and corresponding fabrication process
Inventors: Bekim Osmani, Raphael Guzman, Tino Töpfer, Bert Müller, Carina Luchsinger Salinas, **Alois Hopf**, Mahyar Joodaki

Submitted to the European Patent Office (07.May 2021), Application No.: EP21172804.3
2. Neural implant based on a cellulose thin film and corresponding fabrication process
Inventors: Bekim Osmani, Raphael Guzman, Tino Töpfer, Bert Müller, Carina Luchsinger Salinas, **Alois Hopf**, Mahyar Joodaki
Submitted to the European Patent Office (07.May 2021), Application No.: EP21172809.2

Incorporations:

1. **Bottneuro AG** – Incorporation date: 20. January 2021
Founders: Bekim Osmani, Tino Töpfer, Bert Müller, Pascal Brenneisen, Rolf Wildermuth, **Alois Hopf**, Raphael Guzman, Cornelia Gut-Villa, Guido Sigron, Magnus Kristiansen